SKB

TECHNICAL REPORT 87-01

Radar measurements performed at the Klipperås study site

Seje Carlsten
Olle Olsson
Stefan Sehlstedt
Leif Stenberg
Swedish Geologicl Co.
Uppsala/Luleå, Sweden

February 1987

SVENSK KÄRNBRÄNSLEHANTERING AB
SWEDISH NUCLEAR FUEL AND WASTE MANAGEMENT CO

BOX 5864 S-102 48 STOCKHOLM
TEL 08-665 28 00 TELEX 13108-SKB

RADAR MEASUREMENTS PERFORMED AT THE KLIPPERÅS STUDY SITE

Seje Carlsten, Olle Olsson, Stefan Sehlstedt,
Leif Stenberg

Swedish Geological Co, Uppsala/Luleå

February 1987

RADAR MEASUREMENTS PERFORMED AT THE KLIPPERÅS STUDY SITE

Seje Carlsten
Olle Olsson
Stefan Sehlstedt
Leif Stenberg

Swedish Geological Co.
Uppsala/Luleå, Sweden

February 1987

ABSTRACT

Single hole radar measurements, with center frequencies of 22 and 60 MHz, have been performed in ten out of fourteen boreholes at the study site Klipperås. VRP (Vertical radar profiles) have also been performed in six of the ten boreholes. All fracture zones previously derived from core maps and logging data were discovered during the analysis of the radar measurements. From the large-scale pattern of the radar maps it can be deduced that most radar reflecting structures are oriented in E-W and have a vertical or subvertical dip. Greenstone constitutes a large part of these structures, which can be considered as extensive structures and do not constitute isolated fragments in the rock mass. A majority of the interpreted radar reflecting structures intersecting the borehole are coupled together with low resistivity. All greenstones and mafic dykes (dolerite and basalt) which are characterized by low resistivity give rise to radar reflections. Wider fracture zones and other units, e.g mafic dykes (dolerite and basalt), with a very low resistivity give a strong loss in radar pulse energy. The predicted orientation of the fracture zones from earlier investigations agrees well with the orientation calculated from radar crossing angles. Different orientations of the fracture zone H1 have been analyzed. With a strike in north-south and a dip of 20° the outcrop of this fracture zone correlates well with a geophysical anomaly obtained along profiles extended outside the investigated area.

SUMMARY

The Swedish Nuclear Fuel and Waste Management Co (SKB) currently performs investigations in crystalline bedrock in Sweden. The purpose is to find a suitable location for a repository for storage of high level radioactive waste. This report comprise borehole radar investigations performed at the Klipperås study site, located approximately 45 km WNW of Kalmar in the southern part of Sweden.

Single hole radar measurements with a center frequency of 22 MHz were performed in ten out of fourteen boreholes. In six boreholes radar measurements with a center frequency of 60 MHz were also performed. Vertical radar profile measurements (VRP) were performed in six of the ten measured boreholes. A total of 7 857 m of single hole radar reflection measurements and 834 m of VRP measurements were made at the study site.

All fracture zones previously derived from core maps and logging data were discovered during the analysis of the radar measurements. The fracture zones can be seen in the radar maps in form of reflections and/or loss of radar pulse energy. From the large scale pattern of the radar maps it can be deduced that most radar reflecting structures are oriented in E-W and have a vertical or subvertical dip. Greenstone constitutes a large part of these structures, which can be considered as extensive structures and do not constitute isolated fragments in the rock mass. Dolerite dykes are oriented in a northerly direction.

A majority of the interpreted radar reflecting structures intersecting the borehole are coupled together with low resistivity. All greenstones and mafic dykes (dolerite and basalt) which are characterized by low resistivity give rise to radar reflections. Most of the porphyries do not have a

contrast in resistivity to the surrounding granite and they gave, as a consequence, no radar reflections. The reflections associated with porphyries are in stead correlated to the greenstones which appear at the margins of the porhyries or to mylonites within the porhyries. Both these features are characterized by contrasting low resistivity. Wider fracture zones and other units, e.g mafic dykes (dolerite and basalt), with a very low resistivity give a strong loss in radar pulse energy.

Fracturing is a common feature associated with the different dykes detected by the radar. There is a possibility that they can be associated with higher hydraulic conductivity than dykes not detected by radar.

In general, the predicted orientation of the fracture zones from earlier investigations agrees well with the orientation calculated from radar crossing angles. Different orientations of the fracture zone H1 have been analyzed. The best correlation with independent information is obtained when the strike direction of fracture zone H1 is between 180°-210° and the dip is 20° to the west. With an orientation of $180^{\circ}/20^{\circ}$, the outcrop of the fracture zone correlates well with a geophysical anomaly obtained along profiles extended outside the investigated area.

It can be concluded that the borehole radar measurements have given a valuable contribution to the evaluation of the geological, geophysical and hydrogeological conditions at the Klipperås study site. The borehole radar measurements have confirmed the tectonical model and have also given complementary information for the construction of a three-dimensional model of the site.

1 INTRODUCTION

Single hole and VRP (Vertical Radar Profile) measurements have been performed at the study site Klipperås during February, March and October 1986. The study site Klipperås is situated in the southern part of Sweden (Figure 2.1). The objective of the radar measurements were to:

- Achieve experience of the borehole radar technique in new geological environments.

- Develop and apply measurement and interpretation methods of borehole radar within a study site with a large number of boreholes.

- Elucidate the ultimate use of the information received by borehole radar measurements in connection with the geological, tectonical and hydrological models of a site investigation area.

- Receive a better database for modelling of the Klipperås area.

The interpretation of radar reflecting structures presented in this report is correlated with conventional geophysical investigations presented in Sehlstedt and Stenberg (1986) and geological investigations presented in Olkiewicz et al (1986). The geophysical logs from the radar measured boreholes are presented in Appendix A.

2 DESCRIPTION OF THE SITE

2.1 Location and topography

The Klipperås study site area is located approximately 45 km west-north-west of Kalmar in the southern part of Sweden, Figure 2.1. The area is situated on a plateau about 180 m above sea level which is more than 100 km^2 in size. The topography is relatively flat, gently dipping about 0.5 percent to the east. Elevation within the area varies between 170 and 200 m above sea level.

The location is forested and includes small peat bogs. The overburden covering the Precambrian bedrock is mainly of moraine origin, 3-5 m thick. Rock exposures occur very rarely, only about 0.5 percent of the area consists of exposed bedrock.

Morphological lineaments are rare due to the flat topography within the area. Thus, ground surface geophysical measurements play a major role for detecting major fracture zones within the area.

The location of the different boreholes within the Klipperås study site is presented in Figure 2.2.

2.2 Geological and tectonical models

The scarcity of outcrops have reduced the surface geological information to a minimum. From the core mapping (Egerth, 1986) the rock type distribution have been calculated (Olkiewicz and Stejskal, 1986), Table 2.1.

The main rock type within the study area is a grey-red to red, coarse to medium grained, granite. A few thin aplites and pegmatites also occur within the granite.

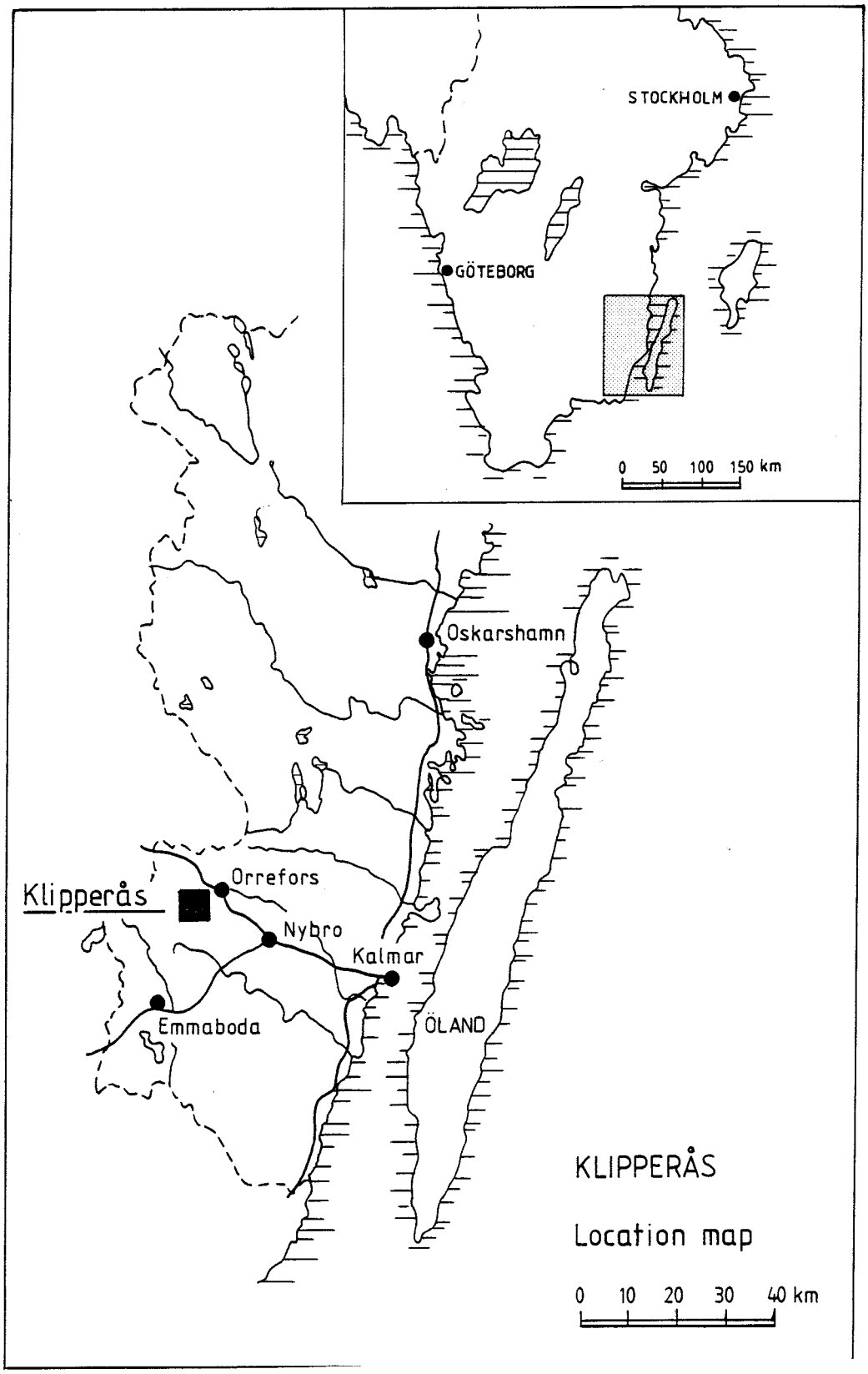

Figure 2.1 Location map of the Klipperås study site.

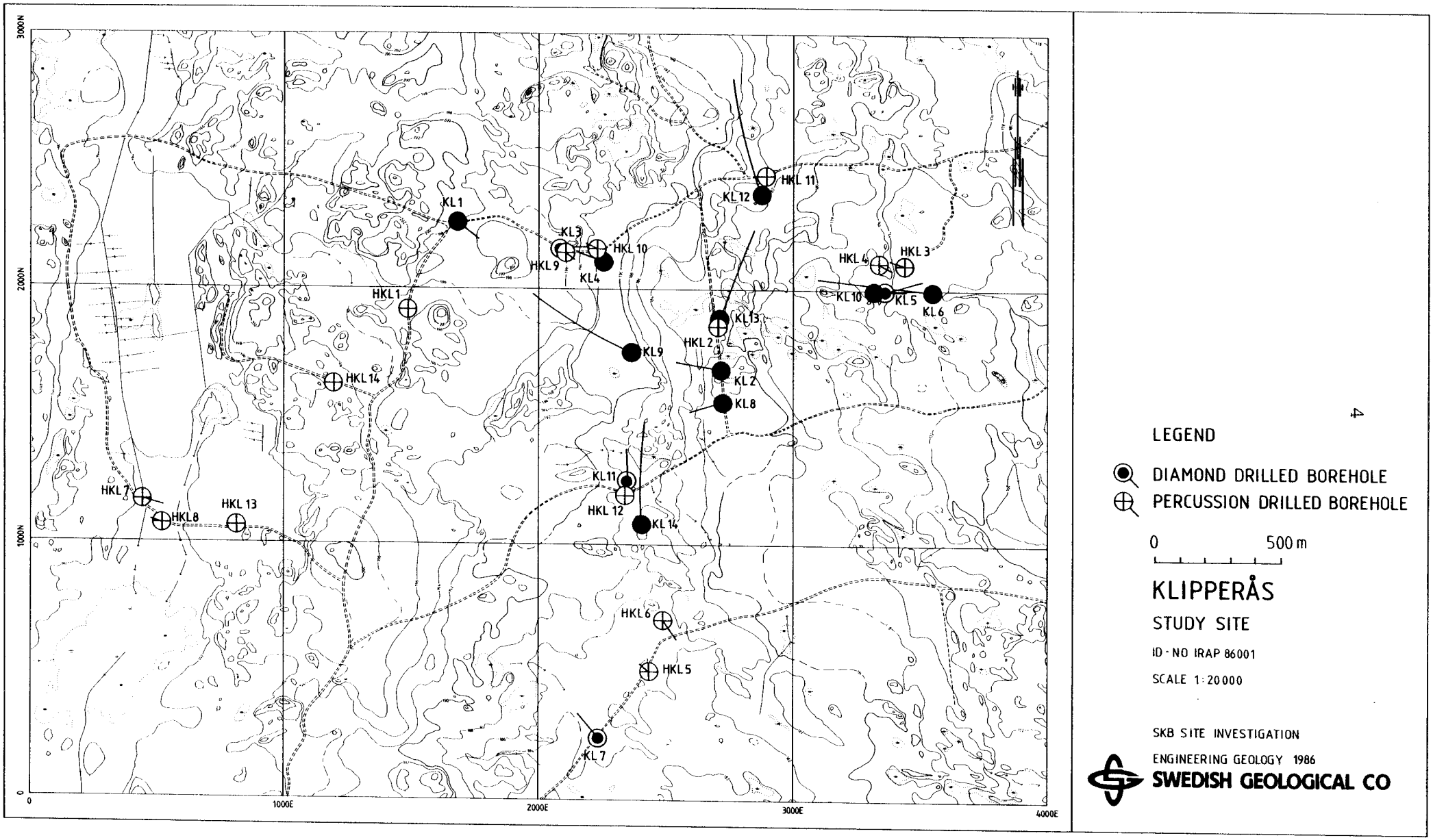

Figure 2.2 The Klipperås study site. Radar measured boreholes are marked with filled circles.

Table 2.1 Rock type distribution from geological core logging.

Granite	85
Greenstone	7
Porphyry dykes	5.5
Mafic dyke (dolerite)	1.4
Mafic dyke (basalt)	0.1
Aplite	1
Total	100.0 %

Some mafic dykes have been observed within the area (Olkiewicz and Stejskal, 1986). The location and extent of these dykes have mainly been interpreted from the ground surface geophysical measurements, Figure 2.3. One of the mafic dykes strikes in NNE-SSW and dips steeply to the east (65-90^{o}). Another mafic dyke strikes in N-S direction and dips steeply to the west (80-90^{o}).

A number of porphyry dykes of acidic to intermediate composition have been observed within the area (Olkiewicz and Stejskal, 1986). From magnetic surface measurements the strike direction was interpreted (Sehlstedt and Stenberg,1986), while the dip was estimated from the geological core logging. In the geological model the strike of the porphyries is WNW-ESE and the dip is steeply to the south (75-90^{o}).

Greenstones have often been observed at the margins of the porphyries with a strike and dip direction parallel to the porphyry dykes. However, greenstones have also been observed elsewhere within the granite.

The extent of the fracture zones was determined by ground geophysical measurements (Sehlstedt and

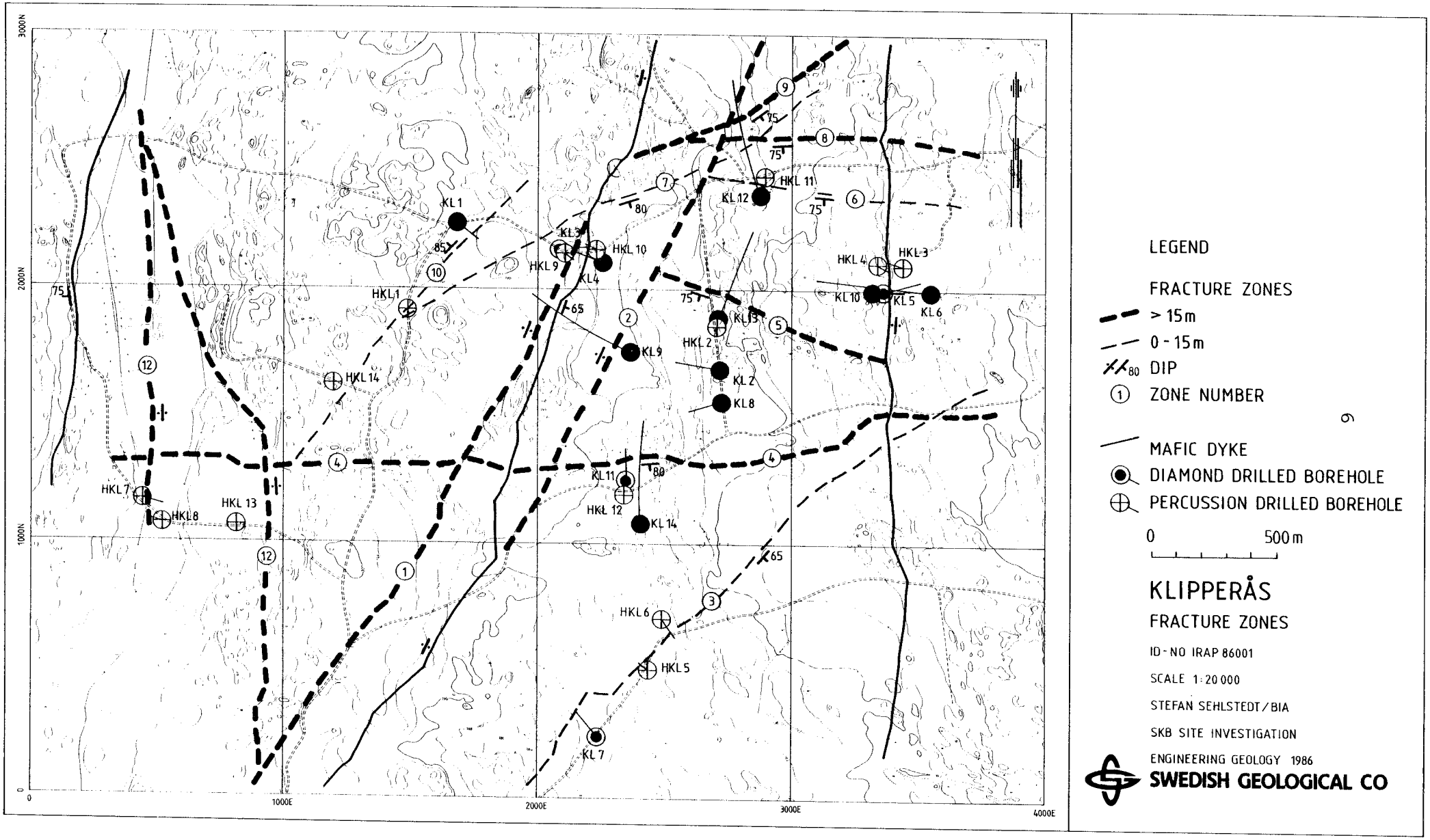

Figure 2.3 Interpretation map showing zones and dykes at the study site Klipperås. Radar measured boreholes are marked with filled circles.

Stenberg, 1986). The indications from the measurements have been checked by core drilling, geological core mapping and geophysical borehole logging. From these investigations the dip of the zones were calculated by simple trigonometry. In Table 2.2 the zones are listed. Each zone is shortly described below.

Zone 1 is strongly indicated at the ground surface. This zone crosses the study site area. It has been intersected by three boreholes, Kl 3, Kl 4 and Kl 9, Table 2.2. The zone was identified in all boreholes by borehole logging and core logging. Trigonometric calculation gave a vertical zone dip in all three boreholes, which confirms the interpretation.

Zone 2 is weakly indicated at ground surface. It is parallel to zone 1 and crosses the study site area. It is believed to have the same dip as zone 1. If this is the case, the zone should be intersected by Kl 9 and Kl 12. Only weak anomalies are found in each borehole and the interpretation is rather uncertain. The interpreted zone sections give a dip that is vertical in Kl 9 and 85°E in Kl 12.

Zone 3 is strongly indicated at ground surface. The zone is intersected only by Kl 7, but is strongly indicated by all logging methods and by an increased fracture frequency. The calculated dip in the intersected section is 65°E.

Zone 4 is strongly indicated at the surface and crosses the site area. The zone is intersected by Kl 11 and Kl 14. It is indicated distinctly by logging and by an increased fracture frequency in both boreholes. The dip is calculated to be vertical in Kl 11 and 80°S in Kl 14.

Zone 5 is shorter than the zones described earlier and is indicated distinctly at the surface. The zone is intersected only by Kl 13. It is indicated distinctly by resistivity logging in the borehole. The location in the borehole is confirmed by magnetic ground surface measurements and susceptibility logging. The dip is calculated to be 75°S.

Zone 6 is rather short and indicated distinctly. It is intersected by Kl 12. The zone is weakly indicated by logging and the interpretation is somewhat uncertain. The calculated dip is 75°S.

Zone 7, 8 and 9 are rather short and distinctly indicated at the surface. The three zones are intersected by Kl 12. From logging, these zones look like one wide, strongly indicated, fracture zone. To explain the surface indications and build an evaluation model, this wide section was divided into three zones. Zones 7 and 9 are almost parallel. They have nearly the same dip, 80°S and 75°S respectively. A vertical dip was calculated for zone 8.

Zone 10 is distinctly indicated at the surface. The zone is intersected by Kl 1. It is clearly indicated by borehole logging. The dip is calculated to be nearly vertical, 85°NW.

Zone Hl was encountered by borehole Kl 2 in the section between 792-804 m. This zone is interpreted as sub-horizontal. The surface investigation methods used are not likely to detect sub-horizontal fracture zones at some depth.

Table 2.2. Fracture zone data.

Zone number	Bore-hole	Zone section	Strike/dip	True width
1	Kl 3	140-195 m	N-S/90°	28 m
1	Kl 4	110-180 m	N20E/90°	36 m
1	Kl 9	615-665 m	N30E/90°	29 m
2	Kl 9	120-160 m	N30E/90°	22 m
2	Kl 12	595-630 m	N15E/85°E	13 m
3	Kl 7	115-130 m	N35E/65°E	12 m
4	Kl 11	108-148 m	N75E/90°	23 m
4	Kl 14	368-410 m	N85E/80°	27 m
5	Kl 13	152-188 m	N80W/75°S	23 m
6	Kl 12	70- 88 m	N75W/75°S	12.5 m
7	Kl 12	288-306 m	N65E/80°S	13.5 m
8	Kl 12	312-347 m	N85W/90°	28 m
9	Kl 12	362-384 m	N60E/75°S	17.5 m
10	Kl 1	280-310 m	N45E/85°NW	10.5 m
H1	Kl 2	792-804 m	Sub-Horizontal	12 m

2.3 Desired radar information

This is a first attempt to use the borehole radar in a large number of holes at a study site. If the measurements are sucessful the results may confirm or develop the predicted geological and tectonical models.

Fracture zones

The most important task of the radar is to check the tectonic model. This is done by comparing the predicted zone orientations and see if they fit with the borehole crossing angles from the radar

measurements. If these data disagree perhaps the model should be modified.

One specific problem is the orientation of the zone H1 in K1 2 at 792-804 m borehole length. The conclusion from former investigations was that the zone probably is subhorizontal. This interpretation is uncertain and of great significance when model calculations are made for the site. It would be valuable if radar measurements would shed some light on this problem.

Lithology

Other tasks of the radar are to confirm the geological model, e.g. the strike and dip of the greenstone and porphyry dykes/ rests described earlier. Perhaps the measurements will indicate if these are isolated rests or continous dykes. Since these rock types seem to cause an anisotropy in the bedrock, they will probably have influence on the water flow through the bedrock.

Some specific geological problems where the radar may provide valuable data:

Is it possible that the porphyries encountered in the bottom of K1 1 are the same as in the bottom of K1 9.

Is the grenstone at 78-92 m in K1 4 the same as in K1 9 at 356-374 m?

A greenstone has been encountered between 219-300 m in K1 6. This greenstone has not been found in the adjacent K1 5. Is it a thin dyke almost parallel to K1 6 or an isolated fragment within the granite?

In K1 6 two porphyry sections occur, 450-520 m and 700-747 m. The sections may be the same dyke crossed twice by the borehole due to the borehole deviation.

In K1 8 at 92-96 m there is a significant resistivity

anomaly. The correlation of this section and a weak ground surface anomaly should be examined. There might also be a connection with the zone H1 in K1 2.

The orientation and character of a prominent resistivity anomaly within a porphyry in K1 9, 764-776 m. The section is mylonitized and contains pyrite.

Check the orientation of a mafic dyke encountered in K1 5 at 12-29 m, in K1 10 at 88-100 m and in K1 6 at 338-371 m.

Hydrogeology

In many of the boreholes long sections of high hydraulic conductivity have been measured (Gentzschein, 1986). Perhaps it is possible to distinguish the extent and character of the structures which cause these high values.

3 DESCRIPTION OF THE RADAR EQUIPMENT

The radar system, RAMAC, used for these measurements has been developed by the Swedish Geological Co. (SGAB) as a part of the International Stripa Project. Continued development of the system has been funded by SKB in order to construct a system adapted for field work on a production basis.

The radar system can be classified as a short pulse system, which means that the length of the pulse transmitted into the rock will be approximately one wavelength. The system works in principle in the following manner: A short current pulse is fed to the transmitter antenna, which generates a radar pulse which propagates through the rock. The pulse is made as short as possible to obtain high resolution. The pulse is received by the same type of antenna, amplified, and registered as a function of time. The receiver may be located in the same borehole as the transmitter or in any other borehole. The borehole radar system can register the distance (travel time) to a reflector, the strength of the reflex, and the attenuation and delay of the direct wave between transmitter and receiver (Olsson, Forslund, Lundmark, Sandberg, and Falk, 1985).

The radar system consists of four different parts;

- a microcomputer with two 5 inch floppy disc units for control of measurement, data storage, data presentation, and signal analysis.

- a control unit for timing control, storage and stacking of a single radar measurement.

- a borehole transmitter for sending out short radar pulses.

- a borehole receiver for detection and digitization of radar pulses.

A summary of the technical specifications of the system is given in Table 3.1.

Table 3.1 Technical specifications for the RAMAC borehole radar system.

General	
Frequency range	20-80 MHz
Total dynamic range	150 dB
Sampling time accuracy	1 ns
Maximum optical fiber length	1000 m
Maximum operating pressure	100 Bar
Outer diameter of transmitter/receiver	48 mm
Transmitter	
Peak power	500 W
Operating time	10 h
Length	4.8 m
Weight	16 kg
Receiver	
Bandwidth	10-200 MHz
A/D converter	16 bit
Least significant bit at antenna terminals	1 uV
Data transmission rate	1.2 MBaud
Operating time	10 h
Length	5.4 m
Weight	18 kg
Control unit	
Microprocessor	RCA 1806
Clock frequency	5 MHz
Pulse repetition frequency	43.1 kHz
Sampling frequency	30-500 MHz
No of samples	256-4096
No of stacks	1-32767
Time window	0-11 us

4 MEASUREMENT PROCEDURES AND DATA PROCESSING.

4.1 Principles of radar measurements

The principle of radar measurements is depicted in Figure 4.1. The distance to a reflecting object is determined by measuring the difference in arrival time between the direct and reflected pulse. As the radar is pushed step by step into the borehole the time difference will vary in a characteristic manner typical of the reflector. The two basic patterns are point reflectors and plane refectors as shown in Figure 4.1. The planar pattern characterizes fracture zones and is found in all radar maps. The planar reflectors works like a mirror and are therefore the most efficient type of reflector and the only one likely to be observed at large ranges. Point like reflectors can for example be generated by fracture zones crossing each other where the axis of the crossing extends in a direction almost perpendicular to the borehole.

Planar fracture zones produce significant reflections of radar pulses. The characteristic pattern produced by planar fracture zones depends on the angle of intersection between the fracture plane and the borehole. Fracture planes oriented almost parallel to the borehole produce reflections parallel to the borehole axis. Fracture planes intersecting the borehole with a large angle produces 'V'- shaped reflections, generated both from the front side and from the back side of the fracture plane. The angle of intersection of the fracture plane to the borehole axis and the point of intersection can be read of from a theoretical calculated nomogram (Figure 5.1 and 5.2). It is sufficient that the fracture plane intersect the extension of the borehole since the visible part of a pattern can often be extended far beyond both ends of the borehole. The intersection with the borehole is often also characterized by the

bulging shape of the primary pulse due to loss in energy of the primary pulse. The energy of the radar pulse is dependent on the electrical properties of the rock surrounding the borehole. Highly fractured zones are characterized by increased porosity and a significant change in resistivity, which effects both the reflection coefficient and the energy of the primary pulse.

In borehole radar measurements dipole antennas are used. Hence, the radar reflections observed are cylindrically symmetric around the borehole. Consequently, complete orientation of a fracture plane can not be determined by measurements in a single borehole. The orientation can however be determined by combining results from several boreholes, assuming that the same fracture zone has been intersected by two or more boreholes. A future possibilty of orientation of a fracture plane from a single borehole is by the developement of directional antennas.

4.2 Measurement history

The radar measurements were performed during three main periods, February, March and October 1986. The first two periods were performed during very cold winter climate and a very humid thaw climate, respectively. The radar equipment worked satisfactorily at both types of climate. To prevent the equipment from damage by moisture and cold, it was necessary to use a heater during the nights. The third main period was performed at a drier and warmer but still rather chilly climate. During all three main periods the radar equipment was transported to Klipperås from Uppsala, and vice versa, by car. The measurements were performed with the car as mobile measure station. Electricity for the equipment was received from a mobile generator.

A total of 7 857 m of single hole measurements and 834 m of VRP measurements were performed.

4.3 Reflection measurements

In a single hole reflection measurement transmitter and receiver are put into the same hole and the distance between the probes is kept constant. The transmitter-receiver array is moved stepwise in the hole and measurements are made with 1 m increments. In the 22 MHz measurements performed at Klipperås the probes were separated by 10 m of glass fiber rods, which gives a separation of 15 m between the midpoints of the antennas (Figure 4.2). In the 60 MHz measurements the probes were separated by 4 m of glassfiber rods which gives a separation of 9 m between the midpoints of the antennas.

The measurement procedure is relatively simple. After initialization of a data disc and selection of variable parameters the borehole probes are put into the borehole and the measurement is started. When the measurement of a trace is completed the computer unit gives an audio signal to indicate that it is time for the operator to move the probes to the next measuring position. The probes were lowered down into the holes by an electrical cable winch driven by a mobile generator. The measurement at each position takes about 30-60 s depending on the number of stacks and samples. This corresponds to about 50-100 m of measured borehole per hour in one meter steps.

Reflection measurements were performed in the ten boreholes Kl 1, Kl 2, Kl 4, Kl 6, Kl 8, Kl 9, Kl 10, Kl 12, Kl 13 and Kl 14 (Table 4.1), with a center frequency of approximately 22 MHz. A sampling frequency of 245.1 MHz was used and 512 samples registered for each trace. This corresponds to a

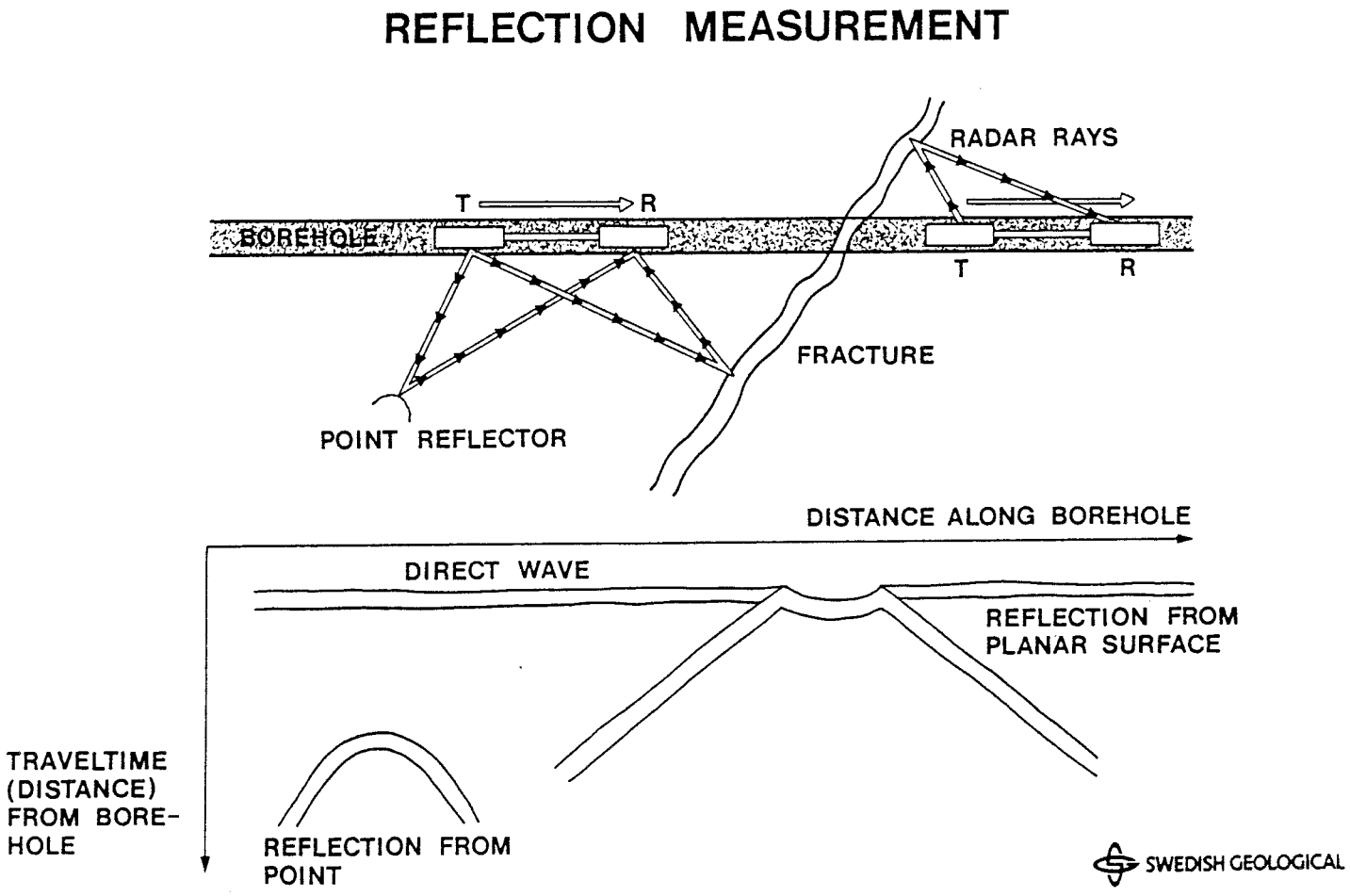

Fig 4.1 Principle of the borehole reflection radar and the patterns generated by plane and point reflectors.

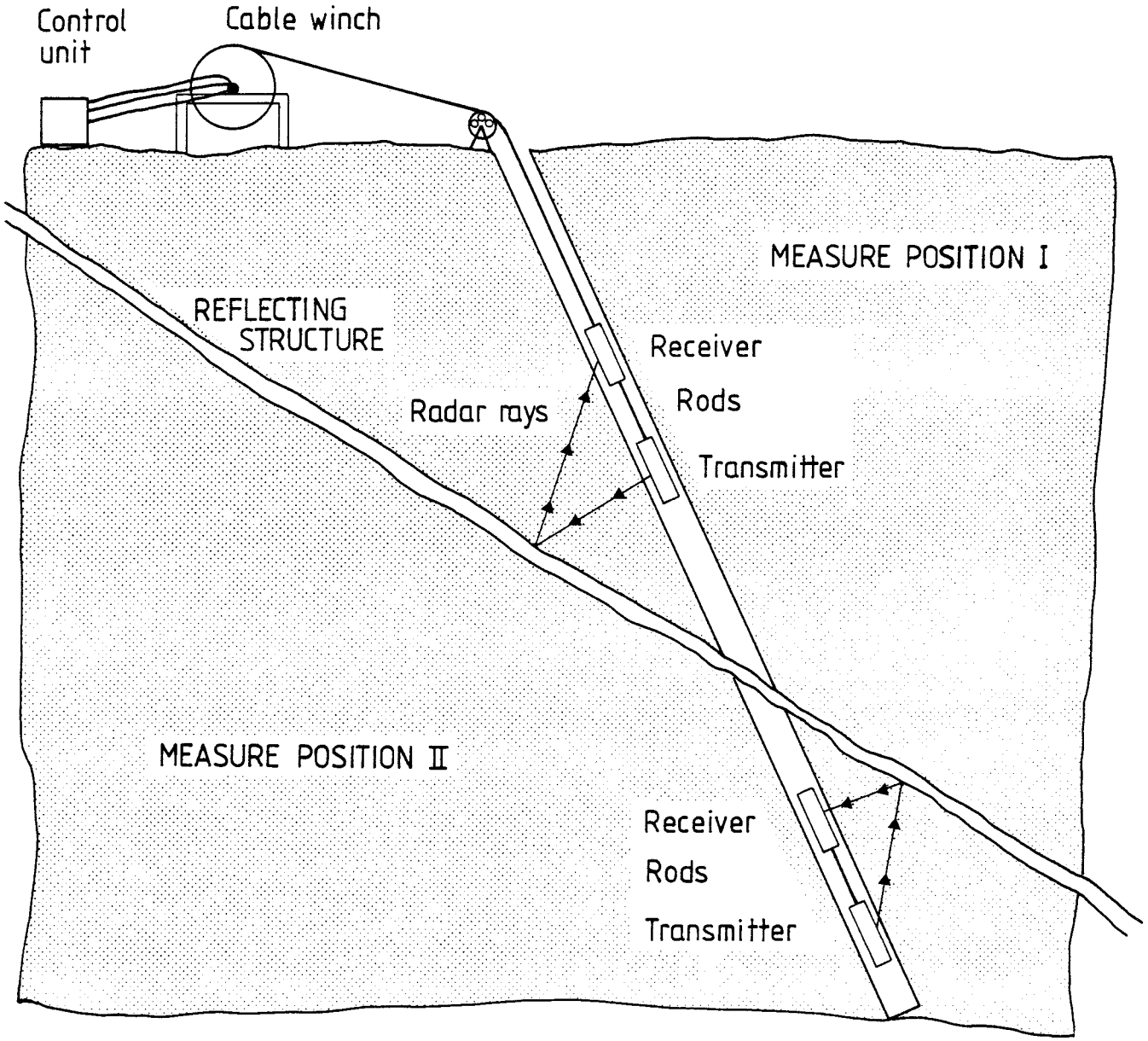

Figure 4.2 Principle of single hole reflection measurement.

Table 4.1 Borehole depths and radar measured intervals (22 MHz).

	Depth (m)	Completed	Measured interval (m)	VRP	Comments
Kl 1	564	x	34 - 500	x	
Kl 2	958	x	55 - 900		
Kl 4	200	x	10 - 176	x	
Kl 6	808	x	10 - 782	x	
Kl 8	266	x	5 - 240	x	
Kl 9	801	x	7 - 780	x	
Kl 10	202	x	10 - 175	x	
Kl 12	730	x	8 - 705		
Kl 13	700		7 - 150		Blocked at 175m
Kl 14	705	x	7 - 678		

Table 4.2 Borehole depths and radar measured intervals (60 MHz).

	Depth	Completed	Measured interval (m)	Comments
Kl 1	564	x	35-544	
Kl 2	958	x	55-938	
Kl 6	808		10-357	Blocked at 370m
Kl 8	266	x	10-248	
Kl 9	801	x	7-780	
Kl 10	202	x	7-180	

registered time window of roughly 2 us. Each trace was stacked 256 times to improve the signal to noise ratio.

Reflection measurements were also performed in six of the ten boreholes using a center frequency of approximately 60 MHz, namely in Kl 1, Kl 2, Kl 6, Kl 8, Kl 9 and Kl 10 (Table 4.2). The objective of using a higher frequency was to obtain more detailed information from the section close to the borehole. The 60 MHz measurement gives more information close to the borehole but instead the propagation is much lesser and thereby is the information from greater distance limited. The boreholes chosen for 60 MHz measurement are characterized by having structures close to or parallel to the borehole.

4.4 VRP measurements

The objective of the VRP measurements was to determine the velocity of the radar rays in the rock mass, and to gain information about geological structures, horizontal or dipping, at shallow depth in the boreholes. The maps from the VRP measurements are presented in Appendix C.

The VRP (Vertical Radar Profile) measurements were performed with the transmitter placed on the surface at a fixed distance from the borehole, and the receiver were lowered into the borehole in one meter increments. At the VRP measurements in vertical or subvertical boreholes the transmitter was placed at four perpendicular directions around the borehole, each at a distance of 30 m from the borehole. In dipping holes the transmitter was placed at the surface above the borehole in the drilling direction at a distance of 40 m from the start of the borehole (Figure 4.3). Thus, four radar maps were obtained from each vertical borehole and one radar map from each dipping hole. In the VRP measurements the receiver was lowered down until the distance between transmitter and receiver was too large for the transmitted pulse to reach the receiver.

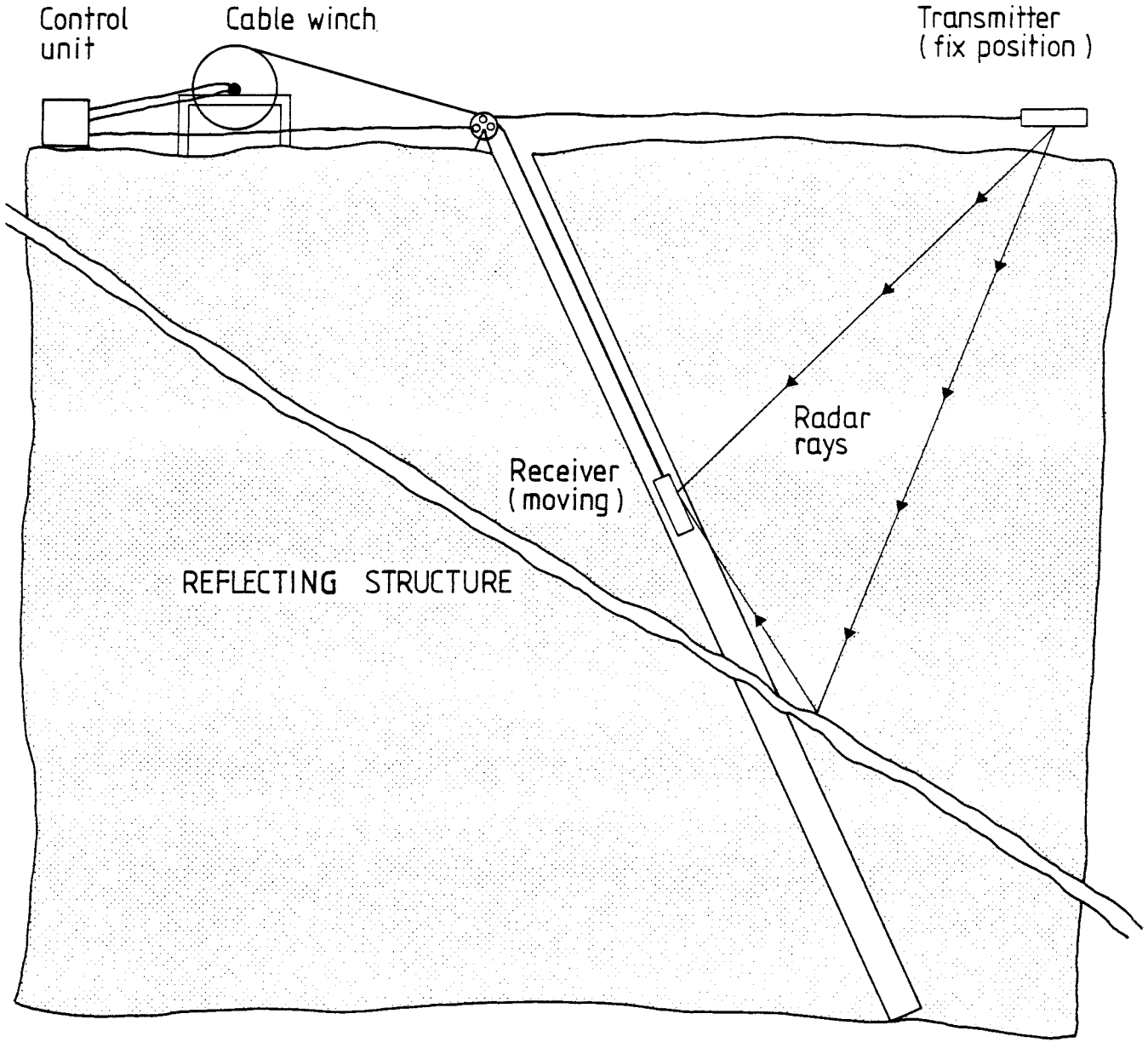

Figure 4.3 Principle of vertical radar profile (VRP) measurement.

The measurements were made with a sampling frequency of 245.1 MHz and 512 samples were recorded for each trace. At Klipperås a total of 9 VRP measurements were performed in 6 boreholes, namely Kl 1 (4 profiles), Kl 4, Kl 6, Kl 8, Kl 9 and Kl 10 (Table 4.1).

4.5 Radar velocity determination

The velocity of the radar waves at the Klipperås site has been determined from the VRP measurements. As the receiver is lowered down the hole the distance between the transmitter and the receiver will change. The radar velocity is easily determined from a plot of the travel time of the radar pulse versus the distance between transmitter and receiver. It should be noted that the accuracy in borehole coordinates will determine the accuracy in velocity. In general borehole coordinates obtained from borehole deviation surveys provide sufficient accuracy.

The radar velocity at the Klipperås site has been estimated to 125 m/us.

The radar velocity is an essential parameter for the interpretation of the radar data. It is necessary for converting travel times to distances and for calculation of the nomograms which are used for obtaining the intersection angles between boreholes and fracture zones.

4.6 Signal filtering

The raw data registrations contain some spurious signals which should be removed in order to obtain high quality displays of the radar data. The raw data from Klipperås have been treated in the following way;

First a DC-level offset is removed from the rawdata (RD-DC). The result of this compensation is that the radar map is given the same background level even if variations in temperature, battery power etc. has affected the DC-level during the measurement time. The RD-DC data is then transformed to the frequency domain by a Fast Fourier Transformation (FFT).

A correlation function is generated and transformed to the frequency domain by a FFT. The correlation function used for the Klipperås data is a sine wave oscillation modulated by a Gauss curve, H(t), where

$$H(t)=A \sin(2\Pi t) \exp(-((t-t_o)/w)^2/2).$$

For the Klipperås data the following values were used: f = 22 MHz, t_o = 35 ns and w = 17 ns.

The correlation with the measured data is performed in the frequency domain and the result is transformed to the time domain by an inverse FFT. The correlated radar data is then plotted as a radar map.

The correlated radar maps are shown in the Appendix B.

5 INTERPRETATION PROCEDURE

The basis for the interpretation of the radar reflecting structures are radar maps. The most significant reflectors have been identified and plotted on the radar maps for each of the 10 boreholes. The radar maps are presented in Appendix B. Nomograms to determine the angle of the reflector relative to borehole and point of intersection have been used for 22 and 60 MHz, respectively (Figures 5.1 and 5.2). The best fit between radar reflecting structures and geology is achieved when using the first solid black line, representing arrival time of the direct pulse, as zero level for the nomogram. Each reflecting structure has been given a unique number for each borehole and listed in a set of tables together with the point of intersection, angle relative to borehole, corresponding geological character and comments (e.g. response of conventional geophysical logs). However, when it can be concluded with certainty that the same reflection is presented in both 22 MHz and 60 MHz, it has been given the same number in both maps. The abbreviations u.s. and l.s. in the tables denotes upper and lower surface respectively.

Loss of radar pulse energy occur in several sections in the boreholes. This phenomena indicates that the rock in this section is fractured or has high porosity.

For the interpretation between radar reflecting structures intersecting the borehole and suitable geological structures, the information from both conventional geophysical logs (Sehlstedt and Stenberg, 1986) and geological investigations was used (Olkiewicz et al, 1986).

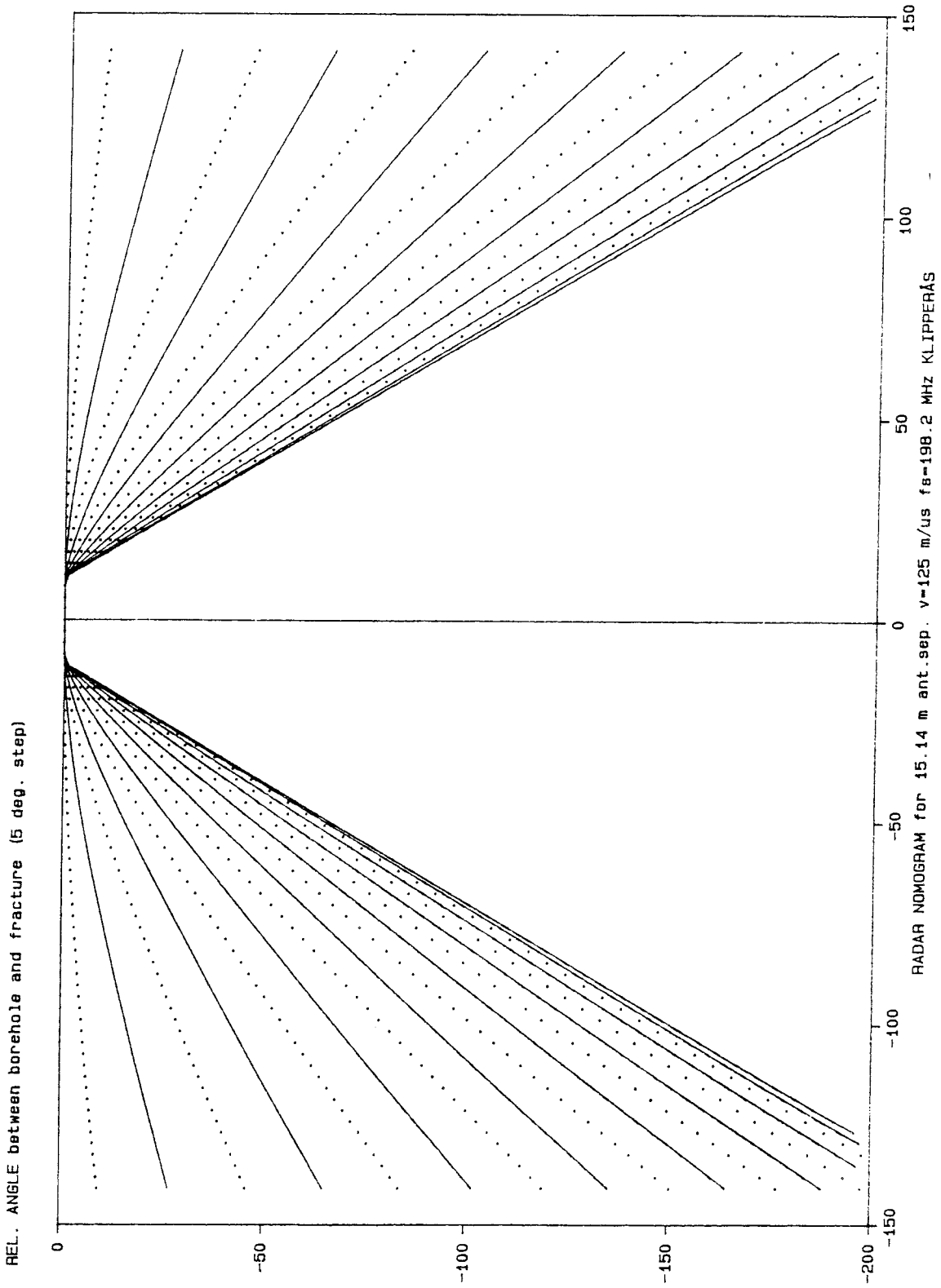

Figure 5.1 Nomogram used for interpretation of intersection and angle of radar reflecting structures from the boreholes in Klipperås, 22 MHz.

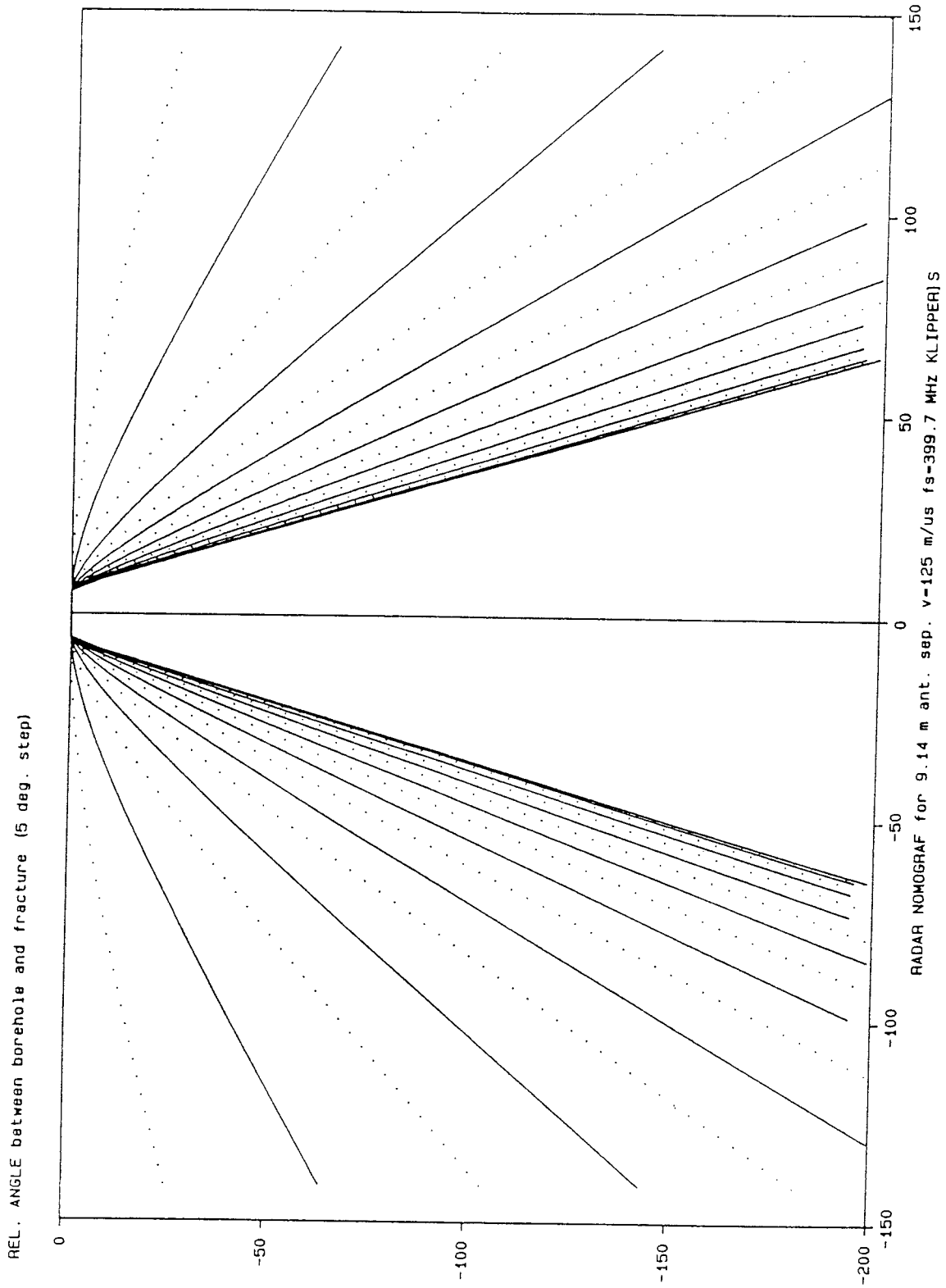

Figure 5.2 Nomogram used for interpretation of intersection and angle of radar reflecting structures from the boreholes in Klipperås, 60 MHz.

In some cases the interpreted intersection and the core-mapped structure can differ by a couple of meters. These cases are marked in the tables by giving the core-mapped depth in brackets. The cause of the discrepancy can be difficulties in defining the intersection of structures, especially if the structures have a small angle to the borehole. It can also depend on fracturing close to, or at the contact between different rock types. Another possibility is if the velocity calibration is not exact, which influences the determination of the intersection of structures with small angle to the borehole axis. An error in the velocity determination will also result in that structures with a steep angle to the borehole axis will receive a large error in the intersection angle.

Occasionally there is a difference in the depth of intersection for the same structure between 22 MHz and 60 MHz radar maps. This can be caused either by a difference in the velocity determination between the two frequencies, or that the arrangement of the probes and rods in the 60 MHz equipment makes it 6 m shorter than the 22 MHz equipment.

The ground surface is visible in all radar maps in the form of a distinct radar reflection which starts at the zero level in the radar maps. The angle of the surface reflection is dependent on the inclination of the borehole. The surface reflections have not been drawn on the radar maps.

6 REFLECTORS OBSERVED

6.1 Borehole Kl 1

The borehole Kl 1 is inclined 80° from horizontal plane and directed S 46 E. The bedrock is dominated by granite which constitutes 74 % of the borehole length. The granite in this borehole is intensely penetrated by a network of hairline cracks sealed by epidote and sericite. Greenstone constitutes 15 % of the bedrock, porphyry 10 % and finally aplite 1 %.

The borehole was radar measured with both 22 MHz and 60 MHz equipment (Figures B.1 - B.2).

The number of interpreted radar reflecting structures intersecting the borehole in the 22 MHz measurement is 15. Greenstone constitutes 6 of these, aplite 3, porphyry 2 and other structures 4. The number of reflectors not intersecting the borehole is 7 (Table 6.1).

The most prominent radar reflecting structures in the 22 MHz radar map from the borehole are no. 1 (greenstone, low resist.), no. 3 (fracture zone 10, low resist.), no. 4 (porphyry) and no. 6 (high fracture frequency, low resist.). These prominent reflectors can be traced over 200 m along the borehole and at a distance of 75 m outside the borehole. Most reflectors in this borehole have an acute angle to the borehole which indicates that the structures interpreted from this near vertical borehole are vertical or subvertical. The reflected structures also exhibit a somewhat undulating character. The other interpreted reflectors are mainly short compared to the prominent reflectors.

Loss of pulse energy occurs between 77-91 m (fractured) and 309-328 m (Zone 10).

The number of interpreted radar reflecting structures intersecting the borehole in the 60 MHz measurement is 22. Greenstone constitutes 10 of these, aplite 1 and other structures 11 (Table 6.2).

The most prominent structures in the 60 MHz radar map are no. 3, 4, 5 and 38. No. 3 and 4 are described above, while no.5 is an aplite and no.38 is a fractured granite. Also, several structures can be seen close to the borehole.

A comparison between the two different radar maps shows that 6 of the interpreted reflectors in both radar maps, are the same or originate from the same object. These are no. 3, 4, 5, 7, 12 and 13. A loss of pulse energy between 310-326 m is more pronounced in the 60 MHz map than in the 22 MHz. This is the part just beneath the interpreted zone 10 between 280-310 m,(Olkiewicz and Stejskal, 1986), thereby indicating the probability of expanding the zone.

Table 6.1 Radar reflecting structures identified from the borehole Kl 1 (22 MHz).

Radar reflecting structures intersecting the borehole.

Position (m)	Reflector	Angle Upper/Lower	Geological structure	Comments
94 m	2	40/	Greenstone(86)	
128 m	6	/35	Fractured	Resist.anom.
194 m	1	/25	Greenstone l.s.	Somewhat low resistivity
217 m	5	18/	Aplite(218)	Gamma anom.
219 m	8	27/	(222)	
238 m	15	25/	Greenstone l.s. (236)	Somewhat low resistivity.
294 m	10	/45	Zone 10	Change of resist. within zone.
310 m	3	25/	Zone 10 l.s. fractured.(305)	Resist.anom.
315 m	7	13/	Greenstone u.s. (316)	Resist.anom. Gamma anom.
326 m	9	35/	Greenstone l.s. (325)	Resist.anom.
345 m	13	/18	Aplite(344)	
375 m	11	30/		Rapid decrease in

				resist.
393 m	12	28/	Greenstone(391)	Resist.anom.
456 m	4	25/	Porphyry l.s.(460)	
515 m	14	35/	Contact(518) porphyry/aplite	Magnet.anom. Gamma anom.

Radar reflecting structures not intersecting the borehole

Depth interval along hole (m)	Distance from borehole (m)	Reflector	Inter-section with extension (m)	Angle Upp/Low	Comments
40-145	35-40	19		0-5	Undulating
60-100	40-50	16		/25	Short
110-150	70-80	17		/30	Short
120-150	85-105	18		/25	
160-210	30-35	20		0-5	Short, undul.
310-380	30	21		0-5	Short, undul.
335-420	60-90	22	577	25/	Straight, broken, long

Table 6.2 Radar reflecting structures identified from the borehole Kl 1, (60 MHz).

Radar reflecting structures intersecting the borehole.

Position (m)	Reflector	Angle Upp/Low	Geological structure	Comments
60	31	/18	Fractured	
166	32	20/	Greenstone u.s.	Somewhat low resistivity
185	35	/15	Greenstone l.s.	Gamma anom.
189	33	30/	Fractured	Gamma anom.
203	34	30/	Fractured l.s.	
217	5	/18	Aplite	Strong gamma an
247	36	23/	Within fractured section	Somewhat low res. Sonic an. Gamma an.
252	37	10/	Fractured	-
280	38	/30	Greenstone, fractured Zone 10	Gamma anom.
295	39	13/	Crushed within fractured section Zone 10	Low res. Strong sonic an.
306	7	20/	Greenstone,	Low res.

			fractured within fractured section Zone 10	Strong sonic an Gamma an.
310	3	28/28	Zone 10, fractured	Low res. Sonic an. Gamma anom.
326	40	/14	Greenstone l.s. fractured	Somewhat low res. Gamma anom
349	13	/20	Greenstone (346)	Gamma anom.
354	41	/10	Fractured	Somewhat low res.
396	12	30/	Fractured	-
457	4	30/	Fractured within porphyre	-
479	42	28/	Greenstone within porphyry	
498	43	35/	Fractured within porphyry	Somewhat low res.
545	44	35/	Greenstone	Somewhat low res. Gamma anom
560	45	45/	Contact green-stone/porphyry fractured	

6.2 Borehole Kl 2

The borehole Kl 2 is inclined 78° from horizontal plane and directed N 82 W. The bedrock is dominated by granite which constitutes 86 % of the borehole length. Greenstone constitutes 10 % of the bedrock, mafic dyke (dolerite) 1 %, aplite 0.1 % and unknown rock 3 %.

The borehole was radar measured with both 22 MHz and 60 MHz equipment (Figures B.3 - B.7).

The sections between 0-450 m, 450-700 m and 700-900 m were measured at separate occasions with the 22 MHz equipment. Between these occasions was the radar equipment partly exchanged, and the fitness between the separate maps is therefore not perfect. The radar plots from the first two occasions are separated in the figures by a white section, and the third is presented in a separate figure.

The number of interpreted radar reflecting structures intersecting the borehole in the 22 MHz measurement is 28. Greenstone constitutes 16 of these, mafic (dolerite) 2 and other structures 10. The number of reflectors not intersecting the borehole is 5 (Table 6.3).

The most prominent radar reflecting structures in the 22 MHz radar map from the borehole are no. 5 (greenstone, low resist.) no. 7 (parallel to the borehole), no. 9 (interpreted as greenstone, low resist., Unit B), no. 19 (greenstone, low resist., Unit A), no. 23 (greenstone, Unit B) and no.24 (fractured zone Hl). All these reflectors are subparallel to the borehole or intersect at an acute angle except no. 23 and 24 which both intersect at an angle of 58°. The reflectors subparallel to the borehole can be traced over a length of 400 m along the borehole and at a distance of 75 m outside the

borehole. These reflectors exhibit a somewhat bulging or undulating structure. In some cases, for example no. 7 and 9, they seem to converge or split. Reflectors no.23 and 24 are straight and intersect the borehole at a diverging angle. Together with no.25 and 27 they indicate the extension of zone H1. However, the radar map also indicate a somewhat shallower beginning of the upper parts of the zone H1, namely about 780 m. The other reflectors intersecting the borehole are not as prominent. They are short and often seem to cease against, or be cut by, the elongated subparallel reflectors.

Loss of pulse energy occurs between 758-769 m (Unit B) and 778-796 m (Zone H1).

The number of interpreted radar reflecting structures intersecting the borehole in the 60 MHz measurement is 54. Greenstone constitutes 26 of these, mafic (dolerite) 3 and other structures 25 (Table 6.4).

The most prominent structures in the 60 MHz radar map are no. 5, 7, 8, 16, 19, 23, 24, 29, 37, 66 and 67. They consist of no.8 (greenstone), no.16 (fractured section), no.29 (within fracture zone H1),no.37 (within fracture zone H1), no.66 (fractured section), no.67 (fractured part within greenstone), while the remaining are described above. The number of reflectors not intersecting the borehole is 9.

A comparison between the two different radar maps shows that 27 of the interpreted reflectors are the same or originate from the same object. Both radar maps exhibit a similar pattern of fracture zone H1, with loss of pulse energy in two sections between 760-810 m. The 60 MHz map exhibits a more detailed pattern of the area close to the borehole.

Table 6.3 Radar reflecting structures identified from the borehole Kl 2 (22 MHz).

Radar reflecting structures not intersecting the borehole.

Position (m)	Reflector	Angle Upp/Low	Geological structure	Comments
124	1	20/	Greenstone u.s	Low resist. Contact fractured granite /greenstone
132	13	/15	Greenstone l.s	Low resist (133) Gamma (133) Fract.freq. decrease.
140	12	/35	(Greenstone l.s)?	-
177	14	/20	Greenstone?	Somewhat low resist.
280	15	40/	Greenstone(285)	Somewhat low resist.
318	4	/25	? (315-316)	crushed, core loss
359	2	14/	Greenstone(364) Crushed zones(363)	Low resist.
359	18	/14		Same as 2
365	17	/55	Greenstone	Low resist. Gamma anom.

370	3	50/	Greenstone(371)	Somewhat low resist.
422	16	25/	Somewhat fractured section	
440	(20	10°)		
480	6	/5-10	Greenstone same as no.5	Low resist. (490)
484	5	10/	Greenstone(491)	Low resist. (490)
588	19	15/	Greenstone u.s Unit A	Same greenstone as 22 Low resist. Gamma anom. Sonic anom. Magnetic an.
609	22	/15	Within greenstone Unit A	
665	21	15/	Greenstone(674)	Low resist. Gamma anom.
685	28	/13	Greenstone l.s.	Resist.anom.
765	23	58/	Dolerite or greenstone, parallel to zone H1 Unit B	Low resist Gamma anom. Magnetic anom
772	9	10-15/	Greenstone Unit B	Low resist. (771-773)

780	24	58/	Fracture zone H1	Somewhat low resist. Small sonic Gamma anom.
780	25	/58		Same as 24
791	29	/23	Fractured l.s. Greenstone u.s. Zone H1	Resist.anom. Sonic anom.
801	27	70/	Greenstone within zone H1	Strong res. Strong sonic Gamma anom.
818	26	35/		
839	30	/25	Idiomorphic calcite cryst. in a single fracture	
859	31	/25	Fractured	
941	32	30/	Dolerite	Sonic anom.

Radar reflecting structures not intersecting the borehole

Depth interval along hole (m)	Dist. from bore-hole (m)	Reflection	Angle Upp/Low	Inter-section with extension (m)	Comments
60-105	25-35	10	13		Stop against no.7
80-550	15-50	7	0-5		Undulating more or less parall. to the borehole
80-170	20-60	11	15		Stop against no.7
530-610	15-30	20			Stop against no.19
790-860	65-105	33	40/	960	Straight

Table 6.4 Radar reflecting structures identified from the borehole Kl 2, (60 MHz).

Radar reflecting structures intersecting the borehole.

Position (m)	Reflector	Angle Upp/Low	Geological structure	Comments
63	6	/50	Fractured granite	Resistivity and sonic anomaly
70	53	/28	Fractured granite (69)	Resistivity and sonic anomaly
99	61	18/	Greenstone u.s. (99-113)	Lower res.
106	4	20/18	Greenstone fractured part	Lower res.
113	62	20/15	Greenstone l.s. (99-113)	Lower res.
123	1	25/	Fractured and clay altered contact between granite/greenstone	Sharp res. and sonic spike
128	63	25/	Some fractured part within greenstone (123-132)	Somewhat lower res.
132	13	/18	Greenstone l.s. (123-132)	Somewhat lower res.
154	64	/15	Fractured granite (154)	

168	65	/15	Crushed zone (168,5)	Minor res. and sonic indication
285	15	40/40	Fractured greenstone u.s.	Minor res. indication
341	12	/15	Greenstone u.s. (341-345)	Lower res.
345	8	/10	Greenstone l.s.	Resistivity and sonic anomaly
363	2	18/	Crushed zone (363)	Resistivity and sonic anomaly
364	17	10/10	Greenstone u.s. (364-366)	Resistivity anomaly
371	3	10/10	Greenstone u.s. (371)	Minor res. and anomaly
402	66	10/8	Fracture zone (401-402)	Minor res. and sonic anomaly
418	16	10/5	Fracture zone (418)	Minor res. and sonic anomaly
491	5	8/7	Greenstone (491-492) Somewhat fractured	Resistivity and sonic anomaly
503	20	10/	Greenstone (503-504)	
587	19	18/	Fractured contact granite/greenstone u.s. (587-619)	Resistivity and sonic anomaly higher velocity

			Unit A	
594	67	18/	Fractured part within green-stone (587-619) Unit A	Resistivity and sonic anomaly higher velocity
606	22	/18	Fractured part within green-stone (587-619) Unit A	Resistivity and sonic anomaly higher velocity
614	68	/18	Fractured part within green-stone (587-619) Unit A	Resistivity and sonic anomaly higher velocity
620	53	/18	Fractured granite 1 m below contact greenstone/granite	Sonic anomaly lower velocity
635	54	10/	Fractured green-stone	Resistivity anomaly
640	55	10/	Fractured green-stone	Resistivity anomaly
674	21	13/12	Fractured green-stone u.s.	Resistivity anomaly
677	69	15/15	Fractured contact granite (green-stone u.s.	Resistivity anomaly
687	28	/13	Greenstone l.s.	Resistivity contrast low/high

734	70	15/	Fractured granite	Sonic anomaly
769	23	60/	Greenstone or dolerite u.s., Unit B	Sharp res. and sonic anomaly
772	9	15/15	Greenstone or dolerite, within Unit B	Sharp res. and sonic anomaly
778	24	60/	Fractured granite Zone H1	Minor res. and sonic anomaly
793	29	/20	Fracture zone H1 u.s.	Sharp res. and sonic anomaly
796	36	/60	Fracture zone H1 (within)	Sharp res. and sonic anomaly
798	37	/20	Fracture zone H1 (within)	Sharp res. and sonic anomaly
800	38	/45	Fracture zone H1 (within)	Sharp res. and sonic anomaly
804	39	/10	Fracture zone H1 l.s.	Sharp contrast in res. and sonic travel-time
857	31	/30	Weathered and clayaltered crushed fractured zone	Sharp res. and sonic anomaly
889	41	/20	Dolerite l.s. (888,5) fracture zone (890)	Somewhat lower res.

943	32	10/	Dolerite u.s. (943-953) fractured	Sharp contrast in magnetic susceptibility res. not logged
952	43	/20	Dolerite l.s fractured and chrushed (952,5)	See 42

Radar reflecting structures not intersecting the borehole

Position (m)	Reflector	Distance from borehole (m)	Angle Upp/Low	Intersection with borehole (m)	Comments
60-150	44	15-25	/10		Undulating stop against no. 45
60-480	7	20-60	/5		Undulating
60-140	10	22-45	18/	210-215	Straight stop against no. 44
250-285	47	25	0		Straight
730-750	9	13	0		Straight
810-820	49	15	0		Same as 48?
900-930	50	14	0		Same as 48?
890-920	51	20-28	20/	970-975	Stop against 39?
850-900	52	32-45	20/	995-1000	Stop against 37?

6.3 Borehole Kl 4

The borehole Kl 4 is inclined 59° from horizontal plane and directed N 71 W. The bedrock is dominated by granite which constitutes 71 % of the borehole length. Greenstone constitutes 15 % of the bedrock, mafic (dolerite) 7 % and porphyry 7 %.

The number of interpreted radar reflecting structures intersecting the borehole is 4. Greenstone constitutes 1, mafic (dolerite) 2 and 1 is a fracture zone within the mafic (dolerite). The number of radar reflectors not intersecting the borehole is 4 (Table 6.5).

All reflecting structures in the radar map from the borehole show about the same prominent character and elongation and most of them are straight (Figure B.8). They can be traced 30-40 m along the borehole and at a distance of 40 m outside the borehole. Between the reflectors no. 2 and no. 4 there is a decrease in arrival time of the direct radar pulse (Unit A). This is clearly shown by the bulging shape of the black line representing arrival time of direct pulse along the borehole. These two reflectors are interpreted as a highly fractured dolerite (78-91 m) with altered fractures and infilling of chlorite and illite. The geophysical logs exhibit a strong decrease in resistivity. The dolerite has a northerly strike and dips towards SE.

Loss of pulse energy occurs between 71-98 m (Unit A), 118-135 m (Zone 1) and 167-175 m (fractured porphyry).

The radar map of the borehole exhibits fewer subparallel reflectors than other boreholes in the same direction and inclination. However, it should be kept in mind that the borehole is rather short compared to the other boreholes.

Table 6.5 Radar reflecting structures identified from the borehole Kl 4 (22 MHz).

Radar reflecting structures intersecting the borehole.

Position (m)	Reflector	Angle Upp./Low.	Geological structure	Comments
78	2	50/	Dolerite u.s. Unit A	Strong decr. resist. Gamma anom. Same dolerite as no.4
83	1	23/	Fracture zone within dolerite Unit A	High fracture freq. within the dolerite Low resist. Spike-like
91	4	/50	Dolerite l.s.(91) Unit A	Same dolerite as no.2 Strong decr. resist. Gamma anom.
123	5	/27	Greenstone u.s. fractured Zone 1	Fractured granite between two greenstones. Strong decr. resist. Gamma anom.

Radar reflecting structures not intersecting the borehole.

Depth interval along hole (m)	Dist. from bore-hole- (m)	Reflector	Angle Upp/Low	Inters. with extension of hole (m)	Comments
20-70	5-30	3			At surface, close to the borehole
140-185	20-45	6	30	228	
140-185	18-30	7	30	220	
160-185	45-55	8	30	277	

6.4 Borehole Kl 6

The borehole Kl 6 is inclined 56° from horizontal plane and directed N 84 W. The bedrock is dominated by granite which constitutes 71 % of the borehole length. Greenstone constitutes 15 % of the bedrock, porphyry 11.5 %, mafic (basalt) 2 % and aplite 0.5 %.

The borehole was radar measured with both 22 MHz and 60 MHz equipment (Figures B.9 - B.11). It was discovered during the 60 MHz measurement that the borehole had been blocked at about 370 m since the performance of the 22 MHz measurement.

The number of interpreted radar reflecting structures intersecting the borehole in the 22 MHz measurement is 18. Greenstone constitutes 8 of these, aplite 1, mafic (basalt) 2 and other structures 7. The number of radar reflectors not intersecting the borehole is 13, most of them are elongated subparallel structures (Table 6.6).

The most prominent radar reflecting structures in the 22 MHz radar map from the borehole are those subparallel to the borehole or intersecting at a small angle. They can be traced 200-300 m along the borehole and at a distance of 120 m outside the borehole. They do not exhibit a straight line but a somewhat wavy or bulging structure. In some cases they seem to converge or be cut by other structures. Two other prominent reflectors are no.9 and no.30, none of them intersect the borehole. Between the reflectors no.2 and no.3 there is a marked loss of radar pulse energy. This is shown by the bulging shape of the black line representing arrival time of the direct pulse along the borehole. The reflectors represent upper and lower side of a basaltic dyke, included in Unit B, (338-372 m). The dyke is intensely fractured and the geophysical logs exhibit strong decrease in

resistivity. The dyke is interpreted as vertical and striking N-S.

Loss of radar pulse energy occurs between 340-374 m (Unit B), 403-427 m (Unit C) and 506-530 m (Unit C).

The number of interpreted radar reflecting structures intersecting the borehole in the 60 MHz measurement is 21. Greenstone constitutes 4 of these, aplite 1, mafic (basalt) 3 and other structures 13. The number of reflectors not intersecting the borehole is 2 (Table 6.7).

The most prominent structures in the 60 MHz radar map are no. 1, 37, 38, 43 and 46. No.1 is described above and no.43 is a part of no.1. Th remaining structures are no.37 (crushed within greenstone, Unit A), no.38 (fractured within greenstone, Unit A) and no.46 (not intersecting).

A comparison between the two different radar maps show that 5 of the interpreted reflectors are the same or originate from the same object, namely 1, 2, 11, 13, and 18. The wealth of detail close to the borehole is larger in the 60 MHz map. The marked loss of radar pulse energy between 348-363 m can only be seen in its beginning in the 60 MHz map, but the character is the same.

Table 6.6 Radar reflecting structures identified from the borehole Kl 6 (22 MHz).

Radar reflecting structures intersecting the borehole.

Position (m)	Reflector	Angle Upp./Low.	Geological structure	Comments
12	13	/30	Aplite (15)	Not logged
34	17	/23	Fracture zone (Aplite 39)	
145	14	28/	Greenstone u.s. (146)	Low resist. Gamma anom.
157	1	/10	Greenstone l.s. clay (151,5), fractured	Low resist Gamma anom.
213	18	5-10/	Greenstone u.s. (219) crushed zone Unit A	Low res. Gamma anom.
245	12	/37	Greenstone u.s.	Low resist. Gamma anom.
255	11	50/	Crushed zones within greenstone Unit A	Strong change in resist.
348	2	30/	Basaltic dyke Unit B, u.s.	Strong decr. resist. Gamma anom.
363	3	/29	Basaltic dyke	Strong decr.

			Unit B, l.s.	resist. Gamma anom.
395	19	/17	Chlorite fracture 1 mm	
415	20	/33	Greenstone u.s. (413)	Low res. (412) Gamma (412)
471	21	28/	Greenstone u.s. (473) Unit C	Somewhat low res. (473)
477	7	/5-10	Crushed zones within porphyry Unit C	Somewhat low res. Strong sonic
487	5	/35	Greenstone u.s. fractured Unit C	Gamma anom.
525	4	20/	Greenstone l.s. fractured Unit C	Low resist.
568	6	20/	Fractured zone altered Unit D	Somewhat low res. Sonic anom.
665	8	20/	No signs in the core	Very small sonic (667)
696	10	28/	Crushed zone, altered	Low resist

Radar reflecting structures not intersecting the borehole.

Depth interval along hole (m)	Distance from bore-hole (m)	Reflector	Angle Upp/Low	Inter-section with extension (m)	Comments
20-330	50-60	25	0-10/		Parallel to borehole, elong.
30-120	35-40	27	0-10		Parallel to borehole, undul.
80-350	35-75	32	0-25		Seems to converge with no.4. Very long
110-160	100-120	28	25/		Straight
	40-60	29	/10		Elong.,-undulat.
120-210	105-130	33	/25		Undulating
150-250	20-25	26	0-5		Parallel to borehole
450-480	65-95	24	70/		Straight
465-565	50-65	34	10/		Broken
500-785	10-110	9	15-25/	801	Undulating, elong

535-785	30-60	23	/10		Elongated
560-720	75-80	31	0-5		Short
680-785	10-40	30	/15-25	810	Parallel to no.9

Table 6.7 Radar reflecting structures identified from the borehole K1 6, (60 MHz).

Radar reflecting structures intersecting the borehole.

Position (m)	Reflector	Angle Upp/Low	Geological structure	Comments
13	13	/33	Fractured aplite	Low res. Sonic an. gamma
62	30	/55	Fractured	
84	31	/50	Fractured	S.L. res.
99	32	/50	Fractured	
104	33	30/40	?	
106	34	50/	Core loss 5cm	
129	35	20/	Fractured (133)	
145	1	/10	Greenstone u.s.	Low resist sonic an strong gamma
154	43	10/	Greenstone l.s.	Low resist sonic an strong gamma
177	36	/33	Fractured	
219	18	8/	Greenstone u.s. Unit A	Low res. strong gamma strong sonic
248	38	/40	Fractured within	Low res. strong

			greenstone Unit A	Strong sonic Strong gamma
255	37	30/	Crushed, fractured within greenstone Unit A	Res peak, strong gamma strong sonic
257	11	60/	Fractured, partly crushed within greenstone Unit A	Res. peak strong gamma strong sonic
275	39	30/	?	
340	2	35/	Basaltic dyke Unit B	Low res. Sonic an Gamma an
351	40	45/	Basaltic dyke Unit B	Low res. Sonic an Gamma an
367	42	40/	Basaltic dyke, crushed, fractured Unit B	Res. peak Strong sonic
385	41	40/	Open fracture	Somewhat low res. Sonic an
414	43	8/	Greenstone, fractured	Low res. Strong gamma

Radar reflecting structures not intersecting the borehole

Position (m)	Reflector	Distance from borehole (m)	Angle Upp/Low	Inter-section with extension (m)	Comments
20-200	25	38-45			Parallel, undulating
150-300	27	18-25			Straight

6.5 Borehole Kl 8

The borehole Kl 8 is inclined 58° below horizontal plane and directed S 78 W. The bedrock is totally dominated by granite which constitutes 100 % of the borehole length.

The borehole was radar measured with both 22 MHz and 60 MHz equipment (Figures B.12 - B.13).

The number of interpreted radar reflecting structures intersecting the borehole in the 22 MHz measurement is 5. All of them are interpreted as other structures than different rock types. The number of reflectors not intersecting the borehole is 9 (Table 6.8)

The most prominent radar reflecting structures in the 22 MHz radar map are those which run subparallel to the borehole. These structures can be traced over 200 m along the borehole and to a distance of 100 m outside the borehole. However, the radar map does not clearly show if the steeper structures continue across the reflector no.4, which runs parallel along the borehole at a distance of 10-15 m outside the borehole.

The number of interpreted radar reflecting structures intersecting the borehole in the 60 MHz measurement is 6. All of them originate from other structures than different rock types. The number of reflectors not intersecting the borehole is 4(Table 6.9).

The most prominent structures in the 60 MHz radar map are no.1 (highly fractured and crushed, Unit B), no.4 (not intersecting) and no.19 (core loss, Unit B).

A comparison between the two different radar maps shows that 3 of the interpreted reflectors are the same, or originate from the same object, namely 1, 3

and 4. Several structures can be observed between the borehole and reflector no.4 in the 60 MHz map, which was not possible in the 22 MHz map.

Table 6.8 Radar reflecting structures identified from the borehole Kl 8 (22 MHz).

Radar reflecting structures intersecting the borehole

Position (m)	Reflector	Angle Upp./Low.	Geological stucture	Comments
86	1	/38	Highly fract. and crushed (91-95) Unit B	Core loss 0,4 m (94) Strong decr. resist. Self pot.an.
108	11	48/	Somewhat fract.	
143	12	38/	Clayfilled fracture 1 mm(145,5)	Waterloss (141)
207	9	28/		
256	3	35/		Waterloss (254)

Radar reflecting structures not intersecting the borehole.

Depth interval along hole (m)	Distance from borehole (m)	Reflector	Angle Upp/Low	Inter-section with extension (m)	Comments
15-180	40-55	6	5-10		More or less parallel to boreh.
15-250	15-20	4	0-10		Undulating more or less parallel to boreh.
35-150	25-35	5	5		Undulating more or less parallel to boreh.
40-250	65-105	7	15-20		Undulating
120-250	70-75	8	5-15		Undulating
120-250	85-90	13	5/		Parallel to boreh.
150-250	30-35	15	0-5		Undulating
175-250	25-60	14	30/	298	Straight
180-250	60-70	10	15-20		Undulating

Table 6.9 Radar reflecting structures identified from the borehole K1 8, (60 MHz).

Radar reflecting structures intersecting the borehole.

Position (m)	Reflector	Angle Upp/Low	Geological structure	Comments
91	1	/50	Mylonite, crushed, fractured Unit B	Strong res. Strong sonic
94	19	70/	Coreloss Unit B	Strong res. Strong sonic
114	16	13/	Core loss ?	
153	17	45/	?	
172	18	/40	?	
250	3	50/	Fractures	Small sonic

Radar reflecting structures not intersecting the borehole

Position (m)	Reflector	Distance from borehole (m)	Angle Upp/Low	Inter-section with extension (m)	Comments
10-250	4	15-20			Undulating
35-100	5	30-35			Bend shape
180-255	14	20-60	25-30	300	Straight
190-255	20	20-60	25-30	308	Straight

6.6 Borehole Kl 9

The borehole Kl 9 is inclined 56° below horizontal plane and directed N 60 W. The bedrock is dominated by granite which constitutes 81 % of the borehole length. Greenstone constitutes 7 % of the bedrock, porphyry 10 %, mafic (dolerite) 2 % and aplite 0.2 %.

The borehole was radar measured with both 22 MHz and 60 MHz equipment (Figures B.14 - B.18).

The sections between 0-455 and 370-780 m was measured with 22 MHz at two different occasions, and the equipment was partly exchanged between them. The two different occasions are presented in two separate figures, because the fitness between them is not perfect.

The number of interpreted radar reflecting structures intersecting the borehole in the 22 MHz measurement is 32. Greenstone constitutes 14 of these, mafic (dolerite) 3 and other structures 15. The number of radar reflectors not intersecting the borehole is 7 (Table 6.10).

The most prominent radar reflecting structures in the 22 MHz radar map from the borehole are no.1 (fractured section incl. greenstone, low resist.), no.5 (greenstone, low resist.), no.6 (greenstone, somewhat low resist.), no.7 (greenstone, low resist.), no.8 (greenstone, low resist.), no.9 (dolerite, low resist., Unit A), no.11 (greenstone, low resist.), no.13 (dolerite, low resist., Unit A), no.27 (fractured greenstone), no.32 (fractured greenstone) and no.38 (not intersecting). They all intersect the borehole, except no.38, and all of them, except three, are interpreted as greenstone. The reflectors are rather straight and can be traced over 100 m along the borehole and up to 80 m outside the borehole. There is

a marked loss of radar pulse energy between the reflectors no.8 and no.9. This is clearly indicated by the bulging shape of the black line representing arrival time of the direct pulse. The section between these reflectors (Unit A, 356-374 m) contains a fractured dolerite and a greenstone. The dolerite dyke has a NNE strike and dips towards E. The geophysical logs exhibit strong decrease in resistivity in this section.

Loss of radar pulse energy occurs between 138-161 m (Zone 2), 257-273 m (somewhat fractured), 347-377 m (Unit A) and 755-768 m (Unit B).

The number of interpreted radar reflecting structures intersecting the borehole in the 60 MHz measurement is 25. Greenstone constitutes 13 of these, dolerite 2, porphyry 1 and other structures 9 (Table 6.11).

The most prominent structures in the 60 MHz radar map are no.5, 6, 7, 9, 11, 13, 26, 34, 45, 46, and 54. No. 5-13 are described above. The other prominent structures are no.26 (greenstone), 34 (porphyry, Unit B), 45 (strong resistivity change and sonic), 46 (contact porphyry/greenstone) and 54 (greenstone).

A comparison between the two different radar maps shows that 13 of the interpreted reflectors are the same or originate from the same object, namely no. 1, 5, 6, 7, 9, 11, 13, 16, 22, 25, 26, 30 and 34. Several reflectors close to the borehole can also be seen in the 60 MHz map. Besides the section between 355-377 m with loss of radar pulse energy, which can be seen in both radar maps, exhibit the 60 MHz map also two other similar sections. These are found between 142-160 m (within zone 2, 120-160 m) and 766-776 m (Unit B, 764-776 m).

Table 6.10 Radar reflecting structures identified from the borehole Kl 9

Radar reflecting structures intersecting the borehole.

Position (m)	Reflector	Angle Upp/Low	Geological structure	Comments
32	15	/40	Altered fracture zone(31-33)	Somewhat low resist. Sonic anom.
122	4	/25	Crushed and altered section upper parts Zone 2	Low resist. Sonic anom.
149	2	30/	Altered breccia, clay, incl. a crushed zone Zone 2	Strong decr. resistivity
149	3	/28		Same as no.2
179	1	10/	Fractured and altered section incl.greenstone	Low resist.
179	16	/ 10		Same as no.1
262	5	23/	Greenstone u.s. (265)	Low resist. Gamma anom. Sonic anom.
263	7	/24		Same as no.5
307	6	20/	Greenstone l.s.	Somewhat low

			(303)	resist. Somewhat low sonic
313	18	/23	Greenstone u.s. (317)	Somewhat low resist (317) Gamma anom.
328	11	/10	Greenstone l.s. (323)	Low resist. (320)
333	14	22/		
355	8	30/	Greenstone l.s.	Low resist.
357	13	55/	Dolerite u.s. Unit A	Low resist.
362	36	90/	Unit A	Low resist.
374	9	60/	Dolerite l.s. (373) fractured Unit A	Low resist. (355-373)
394	17	/33	Greenstone (393)	Somewhat low resist.
478	23	20/	Fractured	Somewhat low resist.
480	12	14/	Altered fractures (481-482)	
522	24	30/		Small sonic Somewhat low resist.
555	25	/40	Greenstone, fractured	Sonic anom. Somewhat low resist.

589	26	20/	Fractured (592-594)	
598	27	40/	Greenstone, fractured	Somewhat low resist. Gamma anom.
618	28	45/	Greenstone l.s. fractured Zone 1	Gamma anom.
625	29	/35	Fractured, crushed, altered Zone 1	Sonic anom. Gamma anom.
638	30	50/	Greenstone Zone 1	Gamma anom.
674	31	/38	Greenstone u.s. (678)	
713	32	33/	Greenstone, fractured	
727	35	28/	Dolerite	
742	33	30/	Within porph., fractured (740)	
772	34	30/	Within porph., fractured Unit B	Low resist.
790	40	15/	Greenstone, fractured	Somewhat low resist.

Radar reflecting structures not intersecting the borehole.

Depth interval along hole (m)	Distance from borehole (m)	Reflector	Angle Upp/Low	Inter-section with extension (m)	Comments
40-115	25-35	21	5/		
275-350	35-40	22	8/		
370-435	35-55	19	30/	503	
380-430	50-55	20	/10		
670-777	40-120	38	60/	817	Straight
680-777	100-125	39	20/	1040	Straight
700-777	25-50	37	20/	853	Straight

Table 6.11 Radar reflecting structures identified from the borehole Kl 9, (60 MHz).

Radar reflecting structures intersecting the borehole.

Position (m)	Reflector	Angle Upp/Low	Geological structure	Comments
42	45	50/		Strong res. Strong sonic
42	45	/60		
179	1	10-15/	Greenstone	
179	16	/10-15		
269	5	23/	Contact greenstone/porphyry	Res. anom. Sonic
269	7	/23		Same as no.5
276	22	/20		Same intersection as no.5 and 7.
296	46	30/	Lower contact porphyry/greenstone	
309	6	28/	Greenstone	Res. anom. Sonic anom.
339	11	/13	?	
358	13	70/	Dolerite u.s. Unit A	Strong res. an.
372	9	/30	Dolerite	Strong res. an.

Unit A

400	48	/40	?	Within res. an.
449	49	/20	?	
498	50	15/	?	
498	51	30/	?	
530	52	30/	Greenstone u.s.	
557	25	/30	Greenstone	
593	26	55/55	Greenstone	
638	30	40/40	Fractured section within greenstone Zone 1	
646	55	/20	Greenstone l.s. (650) Zone 1	Low res.
682	53	30/	Greenstone l.s.	Somewhat low res.
682	54	/30	Greenstone l.s.	
757	56	25/	Within porphyry	
776	34	35/	Porphyry l.s. (780) Unit B	

6.7 Borehole Kl 10

The borehole Kl 10 is inclined 49° from horizontal plane and directed N 90 E. The bedrock is dominated by granite which constitutes 79 % of the borehole length. Greenstone constitutes 2 % of the bedrock, porphyry 8 %, mafic (basalt) 6 % and aplite 5 %.

The borehole was radar measured with both 22 MHz and 60 MHz equipment (Figures B.19 - B.20).

The number of interpreted radar reflecting structures intersecting the borehole in the 22 MHz measurement is 9. Greenstone constitutes 3 of these, porphyry 1, mafic (basalt) 1, aplite 1 and other structures 3. The number of radar reflectors not intersecting the borehole is 9 (Table 6.12).

The most prominent radar reflecting structures in the 22 MHz radar map are no.3 (greenstone, low resist.), no.4 (greenstone, low resist.), no.6 (not intresecting), no.7 (not intersecting), no.9 (aplite, low resist.), no.11 (clayfilled shear zone, low resist.), no.13 (not intersecting) and no.15 (contact mafic/porphyry, low resist.). The reflected structures exhibit both straight and undulating character. They can be traced over 100 m along the borehole and up to 60 or even 100 m outside the borehole.

The 22 MHz radar map exhibits a marked loss of radar pulse energy between 82-106 m, which is very close to reflector no.14 and no.2 (89-97 m). This is indicated by the bulging shape of the black line representing arrival time of the direct radar pulse. The section contains a fractured mafic dyke (Unit A, 88-100 m). The geophysical logs exhibit strong decrease in resistivity in this section.

The number of interpreted radar reflecting structures

intersecting the borehole in the 60 MHz measurement is 15. Greenstone constitutes 3 of these, porphyry 2, mafic 4 and other structures 6. The number of reflectors not intersecting the borehole is 5 (Table 6.13).

The most prominent structures in the 60 MHz radar map are no.6, 9, 10, 11, 13 and 21. No.6-13 are described above, while no.21 is a fractured section within the granite. Between 89-97 m occurs a loss of primary radar pulse (Unit A, 88-100 m).

A comparison between the two radar maps shows that 8 of the interpreted reflectors are the same or originate from the same object, namely no.2, 4, 6, 9, 10, 11, 13 and 14. Most of them are described above except no.2 (crushed and altered mafic dyke, Unit A), 10 (shear zone with clay) and 14 (contact porphyry/mafic dyke, Unit A). The characteristic loss at Unit A is found in both radar maps. The section 46-57 m in the 60 MHz map also exhibits a loss of radar pulse energy, but not as distinct as at Unit A. This section is close to a fractured and altered part. Between 117-128 m also occurs a loss of radar pulse energy. This section corresponds to a fractured and altered section including a greenstone, (reflector no.21, 28, 25 and 22).

Table 6.12 Radar reflecting structures identified from the borehole Kl 10 (22 MHz).

Radar reflecting structures intersecting the borehole.

Position (m)	Reflector	Angle Upp/Low	Geological structure	Comments
11	10	/28	Shear zone(15.5)	Low resist. Sonic anom.
46	11	/40	Shear zone with clay	Low resist. Sonic anom.
76	9	/35	Aplite l.s. fractured	Low resist. Small sonic anom.
78	1	25/	Greenstone contact with porphyry	
88	14	40/	Contact porphyry/ mafic dyke (basalt) Unit A	Strong decr. resist. Sonic anom.
97	2	/40	Crushed and altered zone within mafic dyke (basalt) Unit A	Low resist. Gamma anom. Magnetic -"-
103	4	/25	Greenstone (104) u.s.	Low resist.
112	15	28/	Contact mafic dyke/	Strong decr.

			porphyry	resist. Sonic anom.
123	3	45/	Greenstone l.s.	Low resist. Gamma anom.

Radar reflecting structures not intersecting the borehole.

Depth interval along hole (m)	Distance from borehole (m)	Reflector	Angle Upp/Low	Inter-section with extension (m)	Comments
20- 50	45-60	16	35		Probably stopped by no.3
20- 85	50-60	7	10-15		Undulating contin. of 6
40- 80	100-105	18	/15		Short
60- 80	90	17	/15		Short
65-180	23-60	13	20-30	235	
100-120	15-30	12	40		Probably dislocat. by no.3
105-180	5-40	6	20	195	Undulating
120-170	53-70	8	30	270	
155-180	25-40	5	30		Probably dislocat by no.6

Table 6.13 Radar reflecting structures identified from the borehole Kl 10, (60 MHz).

Radar reflecting structures intersecting the borehole.

Position (m)	Reflector	Angle Upp/Low	Geological structure	Comments
15	10	/35	Shear zone (15,5) with clay	Sonic spike
46	11	30/45	Shear zone with clay/l.s.	Sonic and res. anom. u.s.
76	9	35/38	Fractured and altered contact porphyry/aplite	Sonic and res. anom. u.s.
88	14	50/	Contact porphyry/ mafic dyke u.s. (basalt) Unit A	Sonic and res. anom.
95	20	/50	Weathered contact mafic dyke/ porphyry l.s. Unit A	Sonic and res. anom.
100	2	/40	Crushed and altered mafic dyke, (basalt) Unit A	Sonic and res., spike
105	4	/25	Greenstone (104-105)	Resistivity spike
115	21	30/	Fractured zone within granite	Resistivity and sonic spike

(113)

120	28	/40	Greenstone u.s.	Resistivity and sonic
122	25	50/	Greenstone (121-124) somewhat altered	Resistivity and sonic anomaly
128	22	/22	Fractured and altered granite	Somewhat increased sonic traveltime
173	24	30/	Fractured granite	Somewhat increased sonic traveltime

Radar reflecting structures not intersecting the borehole.

Position (m)	Reflector	Distance from borehole (m)	Angle Upp/Low	Inter-section with extension (m)	Comments
105-187	23	10-40	20/	210	Undulating
145-187	26	10-40	50/	196	Straight
105-187	6	12-50	20/	243	Undulating
120-187	13	25-55	22/	252	Undulating
110-150	27	28-45	27/	212	Straight

6.8 Borehole Kl 12

The borehole Kl 12 is inclined 50° below horizontal plane and directed N 14 W. The bedrock is dominated by granite which constitutes 85 % of the borehole length. Greenstone constitutes 8 % of the bedrock, porphyry 6 % and aplite 1 %.

The number of interpreted radar reflecting structures intersecting the borehole is 30 (Figures B.21 - B.22). Greenstone constitutes 16 of these, porphyry 4, aplite 1 and other structures 9. The number of radar reflectors not intersecting the borehole is 6 (Table 6.14).

The most prominent reflecting structures in the radar maps from the borehole are no.5 (greenstone), no.7 (contact greenstone/porphyry, somewhat low resist.), no.9 (contact greenstone/porphyry, low resist., Zone 7), no.10 (contact porphyry/greenstone, low resist., Zone 7), no.18 (greenstone), no.21 (greenstone) and no.23 (greenstone, Zone 2) All of them are interpreted as greenstone or associated with greenstone and all of them are straight and intersecting the borehole at an angle between 40-60°. Most of the reflectors interpreted from the borehole are more or less parallel to each other, thereby giving the radar map a characteristic pattern.

Loss of radar pulse energy occurs between 157-174 m (fractured), 323-338 m (Zone 8), 371-381 m (Zone 9), 610-624 m (Zone 2), 655-672 m (greenstone) and 686-700 m (greenstone).

Table 6.14 Radar reflecting structures identified from the borehole K1 12 (22 MHz).

Radar reflecting sructures intersecting the borehole.

Position (m)	Reflector	Angle Upp/Low	Geological structure	Comments
72	1	30/	Porphyry u.s. (74) Zone 6	Somewhat low res.
82	2	40/	Fracture zone within porphyry Zone 6	
87	3	/43	Mylonite within porphyry Zone 6	Low resist.
145	6	/35	Greenstone u.s (147)	Somewhat low resist.
150	4	35/	Greenstone u.s.	Somewhat low res. Gamma
168	5	40/	Greenstone u.s. (165,5)	
219	7	50/	Contact green-stone/porphyry	Somewhat low resist.
219	8	/50		Same as no.7
275	12	/45	Pegmatite (279)	Somewhat low res.
284	9	45/	Contact green-	Low resist.

			stone/porphyry (281) Zone 7	Gamma anom.
298	10	55/	Contact porphyry/greenstone Zone 7	Low resist. Gamma
299	11	/70	Breccia Zone 7	Low resist.
331	29	40/	Greenstone u.s Zone 8	Gamma anom. Magnetic an.
377	36	35/	Fractured, crushed,altered brecciated Zone 9	Low resist. Sonic anom.
390	13	40/	Thin mylonite (393)	Low resist. (288-384) Sonic anom.
390	14	25/		
404	15	50/	Greenstone(401)	Somewhat low resist.
430	16	45/	Greenstone u.s. (433)	Gamma anom.
440	18	/40	Greenstone l.s. (437)	
499	17	55/	Altered fractures within compact granite	
524	21	/50	Greenstone l.s.	

530	19	45/	Greenstone l.s. (524)	
547	20	45/		
565	22	/40	Altered fracture set	
609	23	60/	Greenstone (606) Zone 2	
623	24	50/	Greenstone l.s. (622) Zone 2	Low resist. Gamma anom.
662	25	55/	Greenstone u.s.	
670	27	/70	Greenstone l.s. (672)	
686	26	60/	Greenstone u.s. (689)	Low resist. Gamma anom
712	30	30/	Greenstone l.s. fractured	Somewhat low resist.

Radar reflecting structures not intersecting the borehole.

Depth interval along hole (m)	Distance from borehole (m)	Reflector	Angle Upp/Low	Inter-section with extension (m)	Comments
650-710	15-50	28	43/	731	
685-710	35-60	31	70/	753	Straight
690-710	45-65	32	70/	770	Straight
120-180	85-115	33	35/		Straight
165-195	70-100	34	/55		Straight, short
240-290	60-90	35	/50		Straight

6.9 Borehole Kl 13

The borehole Kl 13 is inclined 60° from horizontal plane and directed N 20 E. The bedrock is dominated by granite which constitutes 90 % of the borehole length. Greenstone constitutes 6 % and porphyry 4 %. However, it should be noted that these percentages are given for the total length of the borehole. Kl 13 is blocked at 175 m and is consequently radar measured only down to 150 m.

The number of interpreted radar reflecting structures intersecting the borehole is 10 (Figure B.23). Greenstone constitutes 7 of these and other structures 3. The number of radar reflectors not intersecting the borehole is only 1 (Table B.15).

The most prominent radar reflecting structures in the radar map from the borehole are no.1 (greenstone, low resist.), no.2 (greenstone, low resist.), no.3 (greenstone, low resist.), no.6 (Zone 5, low resist.), no.8 (greenstone, low resist., Zone 5) and no.10 (not intersecting). Most of them are interpreted as greenstone. However, no.6 is interpreted as the crushed and fractured zone 5.

Loss of radar pulse energy occurs between 78-92 m (fractured greenstone).

The radar reflecting structures in the borehole are oriented more or less parallel to each other, thereby giving the radar map a characteristic pattern.

Table 6.15 Radar reflecting structures identified from the borehole Kl 13 (22 MHz).

Radar reflecting structures intersecting the borehole.

Position (m)	Reflector	Angle Upp/Low	Geological structure	Comments
28	9	/50	Altered fracture zone	Low resist. Sonic anom.
62	11	50/	Narrow altered fracture zone 7 mm EP	Somewhat low res. Somewhat low son
79	1	40/	Greenstone u.s. (81) fractured	Low resist. Gamma anom.
92	4	/45	Greenstone l.s. (90) fractured	Low resist. Gamma anom.
98	2	30-40/	Greenstone (95) fractured	Low resist.
115	5	/50	Greenstone u.s. fractured	Same as no.3
118	3	40-50/	Greenstone l.s. fractured	Low resist. Gamma anom.
166	8	35-50/	Greenstone Zone 5	Low resist. Gamma anom.
180	6	35/	Crushed, fractured and altered Zone 5	Strong res. anom. Sonic anom.
250	7	45-50/	Three greenstones (251-256)	Somewhat low res.

Radar reflecting structures not intersecting the borehole.

Depth interval along hole (m)	Distance from borehole (m)	Reflector	Angle Upp/Low	Inter-section with extension (m)	Comments
50-130	40-80	10	40/		Undulating

6.10 Borehole Kl 14

The borehole Kl 14 is inclined 55° from horizontal plane and directed N 2 W. The bedrock is dominated by granite which constitutes 80 % of the borehole length. Greenstone constitutes 4 %, mafic (dolerite) 7 %, porphyry 10 % and aplite 0.1 %.

The number of interpreted radar reflecting structures intersecting the borehole is 40 (Figures B.24 - B.25). Greenstone constitutes 18 of these, mafic (dolerite) 8, porphyry 2, aplite 3 and other structures 9. The number of interpreted radar reflections not intersecting the borehole is 5 (Table 6.16).

The most prominent radar reflecting structures in the radar map from the borehole are no.1 (dolerite, somewhat low resist.), no.3 (greenstone, low resist., Zone 4), no.6 (porphyry, low resist.) no.13 (greenstone, somewhat low resist.), no.16 (clayfilled fracture zone, low resist.), no.25 (greenstone, low resist.), no.27 (greenstone, low resist.), no.29 (strongly deformed granite, low resist., Zone 4) and no.43 (not intersecting). All prominent reflectors are more or less parallel to each other and they are intersecting the borehole at angles in the interval 37-60°. All the interpreted radar reflectors in the borehole are more or less parallel to each other, thereby giving the radar map a characteristic pattern.

Loss of radar pulse energy occurs between 258-275 m (crushed and fractured greenstone), 367-381 m (Zone 4) and 511-527 m (somewhat fractured dolerite).

Table 6.16 Radar reflecting structures identified from borehole Kl 14 (22 MHz).

Radar reflecting structures intersecting the borehole.

Position (m)	Reflector	Angle Upp/Low	Geological structure	Comments
27	16	/37	Fracture zone, narrow clay-filled (Illite)	Low resist.
90	37	35/	Greenstone (88) fractured	Low resist.
116	32	33/		
126	33	35/	Greenstone (128) brecciated	Same as no.18
126	18	/35	Greenstone (128) brecciated	Low resist.
133	17	45/	Greenstone (130) brecciated	
167	20	/35		Same as no.19
170	19	33/	Dolerite u.s. (169) fractured	Low resist. Gamma anom.
198	22	35/		Same as no.21
200	21	/35	Dolerite l.s.	Somewhat low res. Gamma anom.

227	23	35/		
244	24	33/	Greenstone within porphyry, fractured sect.	Low resist. Magnet. an. Gamma anom.
244	44	/33		Same as no.24
264	27	/38	Greenstone u.s. Fractured, altered	Low resist. Gamma anom. Sonic anom.
273	34	40/	Greenstone l.s. (271) contact to porphyry	Res anom. Magn. an. Sonic anom.
296	26	/40	Fracture zone within porphyry	
301	25	45/	Greenstone u.s, to porphyry(305)	Low resist. Gamma anom. Magnet
301	38	/45		Same as no.25
366	30	45/	Greenstone u.s. (368) fractured Zone 4	Low resist. Gamma anom.
377	28	45/	Greenstone l.s. fractured section Zone 4	Low resist. Gamma anom. Sonic anom.
381	35	/40		Same as no.29

383	29	50/	Strongly deformed granite, clayfilled fractures, altered, cavities (379) Zone 4	Low resist.
409	3	45/	Greenstone l.s. (408) fractured, altered Zone 4	Low res. Magnetic an.
409	45	/45		Same as no.3
421	31	40/	Greenstone (420) crushed fractured altered	Low resist. Gamma anom. Sonic anom.
444	4	/30	Greenstone l.s (442) fractured, altered u.s.(446) Unit A	Somewhat low res.
488	5	60/	Aplite (490)	Somewhat low magn.
510	2	/33		
516	1	50/	Dolerite (520)	Somewhat low res. Magn. anom. Gamma anom.
525	15	/55	Greenstone l.s. (527)	Somewhat low res. Magnet. an. Gamma anom.
543	6	60/	Porphyry u.s.	Low resist.

			(548)	Somewhat low magn.
560	7	60/		
567	9	/60	Dolerite u.s. (571)	Low resist. Gamma anom.
577	8	80/	Dolerite l.s. (575)	Low resist. Gamma anom.
629	36	28/	Pegmatite	Same as no.10
631	10	55/	Pegmatite (633)	
637	11	55/	Dolerite	Somewhat low res.
645	14	/40	Fracture zone altered (648)	Low resist.
651	12	50/	Greenstone (656) crushed, altered	Low resist. (653) Magn. (651) Sonic anom. (651)
672	13	50/	Greenstone (680) fractured	Somewhat low res. Gamma anom.

Radar reflecting structures not intersecting the borehole

Depth interval along hole (m)	Distance from borehole (m)	Reflector	Angle Upp/Low	Inter-section with extension (m)	Comments
15-160	10-45	39	/35		At surface, close to borehole
300-375	100-130	40			Point reflector
440-500	60-90	41	35/		Straight
450-505	80-105	42	/30		Straight
580-680	65-125	43	30-40/	806	Elongated, undulating

7 UPDATING OF GEOLOGICAL MODEL OF THE KLIPPERÅS SITE

7.1 General

One of the tasks for the radar measurements in Klipperås study site was to confirm the geological model, e.g. the strike and dip of the greenstones and porphyry dykes. This is described in section 7.2 below and in more detail in chapter 8. Some specific geological problems are discussed in section 7.5 and also in chapter 8.

The most important task of the radar was to check the tectonic model, i.e the location and orientation of fracture zones intersected by the different boreholes. This is discussed in section 7.3. One specific problem was the orientation of the fracture zone H1 intersected by borehole K1 2. This zone was intersected at only one location and an outcrop of the zone has not been identified. The zone was thus interpreted to be subhorizontal. The discussion of the orientation of this zone as it is observed by radar investigations is discussed in detail in section 7.4.

The analysis of the orientation of fracture zones was performed by a computer program which calculates the possible orientations and positions derived from the angle of intersection or two points of intersection in different boreholes. The orientation of the plane may be described by plotting its normal in a stereographic Wulff diagram, Figure 7.1. The vector Ob′ in the figure represents the normal to the fracture plane. The normal is plotted in the lower hemisphere observed from a point P vertical above the origo, O, of the hemisphere. The point b′ is projected to the unit circle in point b.

In the analysis the dip and deviation of the different boreholes are taken into account. The dip and deviation of the borehole is represented by the centre

of the circle obtained when plotting the possible orientation of a plane with a given radar angle to the borehole axis. A complete orientation of a fracture plane can not be obtained, due to the fact that the radar gives a cylindrically symmetric picture around the borehole. If a fracture zone is intersected by two or more boreholes, the orientation of the fracture plane can be examined by combining results from the boreholes. The orientation of the plane is obtained, where two or more circles from different boreholes cross or are close to each other. This point represents the normal to the fracture plane.

The result can be confirmed by plotting the orientation of a fracture plane from the intersection points in the different boreholes. This is performed by taking the location in the boreholes where the fracture plane intersects the boreholes and rotate a plane with this positions fixed. The normal to the possible planes obtained in this way should cross the point where the circles crosses each other.

7.2 General structural information

From the large scale pattern of the radar maps of the boreholes it can be deduced that most radar reflecting structures are oriented in a E-W direction and with a vertical or subvertical dip. This is supported by comparing radar maps from boreholes directed to north with radar maps from boreholes directed to east or west. There is a significant difference in the appereance on the different radar maps. This difference in the large scale pattern reflects the anisotropy of the bedrock on a large scale.

Inclined boreholes directed towards north (Kl 12, Kl 13, and Kl 14, see Figure 2.2) exhibit a very characteristic pattern of almost exclusively parallel structures intersecting the boreholes. The angle of

intersection of the radar angles with the borehole axis is larger than for the boreholes directed to the east or west. Structures more or less parallel to the boreholes are unusual.

Inclined boreholes directed towards east or west (Kl 4, Kl 6, Kl 8, Kl 9 and Kl 10) exhibit another characteristic pattern on the radar maps. Radar reflecting structures with a small angle of intersection and several parallel structures outside the borehole is a dominating feature in these holes. This contributes to the suggestion of vertical east-west striking zones and dykes in the area.

The subvertical boreholes (Kl 1 and Kl 2) also support the suggestion of vertical east-west striking zones and dykes. These two boreholes also penetrate the structures at a small angle. In borehole Kl 2 semi-parallel structures can be followed almost along the entire length of the borehole up to a distance of 100 m from the borehole. Most of these structures have been identified as greenstones (Table 6.3).

From earlier investigations (Olkiewicz et al., 1986 and Sehlstedt et al. 1986) the strike and dip of the greenstones and also the porphyries have been interpreted to WNW-ESE and steeply to the south (75-90^{o}), respectively. In general, the large scale pattern from the radar maps support the geological model with respect to the orientation of the greenstones and porphyries within the area. The orientation of mafic dikes (dolerite and basalt dykes) are discussed in more detail in section 7.5 and in chapter 8.

The radar investigations performed in the boreholes with different directions show that a majority of the structures causing reflections are straight and elongated in one predominating direction. This would imply a relatively simple geological model of

structures striking in east-west. This anisotropy will probably have a great effect also on the water movements within the bedrock. The hydrogeological anisotropy depends also on the three dimensional pressure distribution in the rock volume. This has not been investigated within the area and warrants further studies.

7.3 Orientation of fracture zones

Zone 1 is intersected by boreholes Kl 3, Kl 4 and Kl 9, see Table 2.2. The strike and dip of the fracture zone was by earlier investigations calculated to N30E and 90^{o}, respectively. The normal to a plane with this orientation is plotted in a Wulff net in Figure 7.2. The boreholes Kl 4 and Kl 9 were investigated with radar measurements. The intersection of the fracture zone with boreholes Kl 4 and Kl 9 was interpreted at 110-180 m and 615-665 m borehole length respectively, Table 2.2. The normals to the possible planes intersecting the boreholes with the corresponding radar angles from these sections are plotted in the same Wulff net. The radar angle from borehole Kl 4 was 27^{o} (no.5), and in borehole Kl 9 the radar angles were obtained in the interval 35^{o}-50^{o} (no. 28, 29, 30) for the corresponding sections. The radar angles obtained in the two boreholes fit very well to the predicted orientation for fracture zone 1.

Zone 2 is intersected by boreholes Kl 9 and Kl 12, see Table 2.2. The strike and dip of the fracture zone was by earlier investigations calculated to N30E and 90^{o}, respectively. The normal to a plane with this orientation is plotted in a Wulff net in Figure 7.3. The boreholes Kl 9 and Kl 12 were investigated with radar measurements. The intersection of the fracture zone with boreholes Kl 9 and Kl 12 was interpreted at 120-160 m and 595-630 m borehole length respectively,

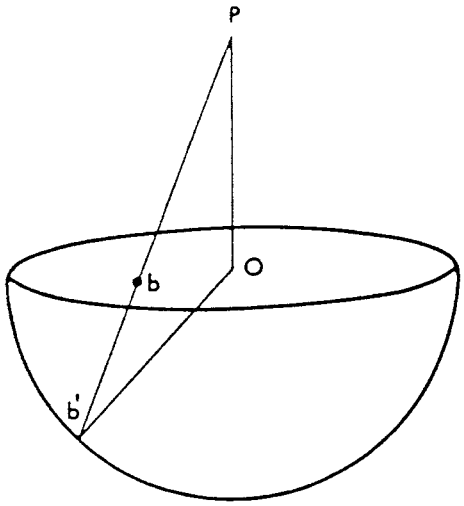

Figure 7.1 The Wulff projection b of the normal Ob' to a fracture plane onto the unit circle.

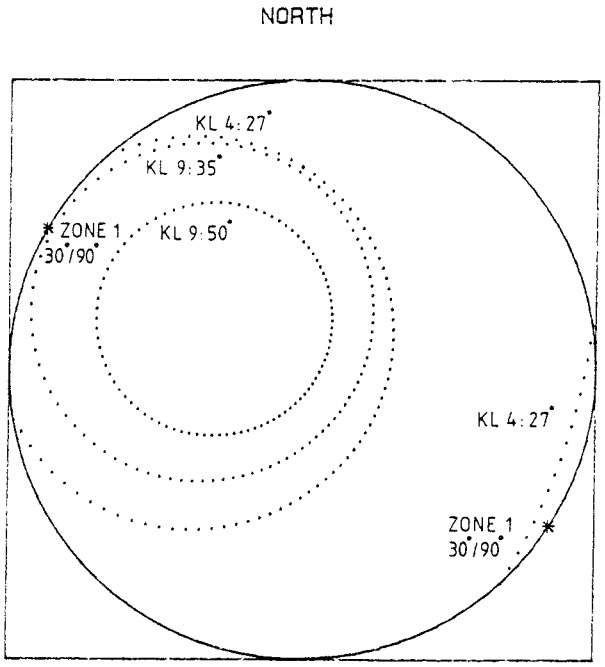

Figure 7.2 Orientation of fracture zone 1 and obtained radar angles in boreholes Kl 4 and Kl 9 plotted in a Wulff net.

Table 2.2. The normals to the possible planes intersecting the boreholes with the corresponding radar angles from these sections are plotted in the same Wulff net. The radar angle from borehole Kl 9 was 25°-30° (no.2,3,4), and in borehole Kl 12 the radar angles were obtained to 50°-60° (no. 23, 24) for the corresponding sections. The radar angles obtained in borehole Kl 9 fit very well to the predicted orientation for fracture zone 2. The radar angles obtained in borehole Kl 12 do not fit the proposed orientation for fracture zone 2 intersecting the borehole within this section. However, the radar angles obtained in borehole Kl 12 at these locations are most probably due to greenstones. The radar angles obtained here fits to the orientation of the greenstones with strike in west-north-west and dip 70°-80° to south.

Zone 3 was only intersected by borehole Kl 7. This borehole was not investigated with borehole radar measurements. The orientation of this fracture zone presented in Table 2.2, are interpreted from other investigations.

Zone 4 is intersected by boreholes Kl 11 and Kl 14, see Table 2.2. The strike and dip of the fracture zone was by earlier investigations calculated to N85E and 80° to south, respectively. The normal to a plane with this orientation is plotted in a Wulff net in Figure 7.4. Only borehole Kl 14 was investigated with radar measurements. The intersection of the fracture zone with borehole Kl 14 was interpreted at 368-410 m borehole length, Table 2.2. The normals to the possible planes intersecting the borehole with the corresponding radar angles from this section are plotted in the same Wulff net. The radar angles from borehole Kl 14 was 40°-50° (no. 3, 28, 29, 30, 35, 45) for the corresponding section. The radar angles obtained in borehole Kl 14 fit very well to the predicted orientation for fracture zone 4.

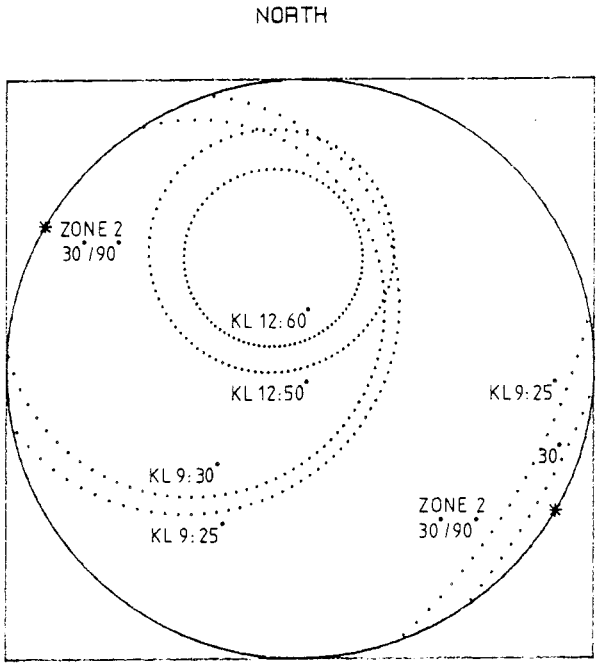

Figure 7.3 Orientation of fracture zone 2 and obtained radar angles in boreholes Kl 9 and Kl 12 plotted in a Wulff net.

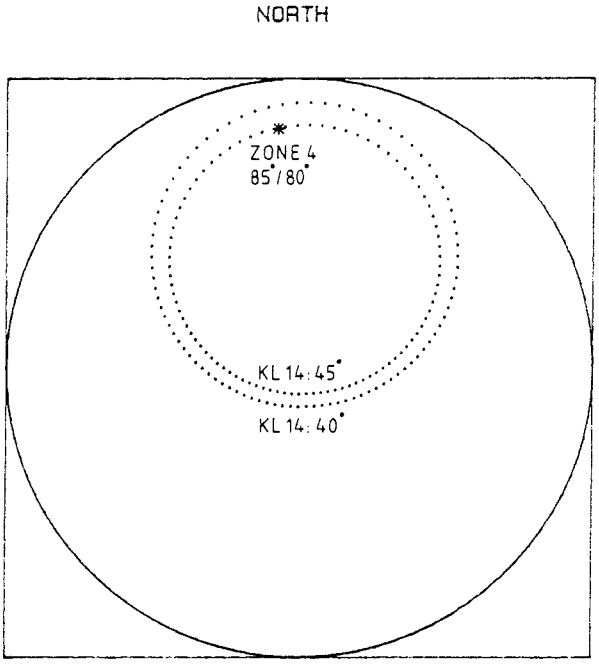

Figure 7.4 Orientation of fracture zone 4 and obtained radar angles in borehole Kl 14 plotted in a Wulff net.

Zone 5 is intersected by borehole Kl 13, see Table 2.2. The strike and dip of the fracture zone was by earlier investigations calculated to N80W and 75° to south respectively. The normal to a plane with this orientation is plotted in a Wulff net in Figure 7.5. The intersection of the fracture zone with borehole Kl 13 was interpreted at 152-188 m borehole length, Table 2.2. The normals to the possible planes intersecting the borehole with the corresponding radar angles from this section are plotted in the same Wulff net. The radar angles from borehole Kl 13 were 35°-50° (no. 6 and 8) for the corresponding section. The radar angles obtained in the borehole fit very well to the predicted orientation for fracture zone 5.

Zone 6 is intersected by borehole Kl 12, see Table 2.2. The strike and dip of the fracture zone was by earlier investigations calculated to N75W and 75° to south respectively. The normal to a plane with this orientation is plotted in a Wulff net in Figure 7.6. The intersection of the fracture zone with borehole Kl 12 was interpreted at 70-88 m borehole length, Table 2.2. The normals to the possible planes intersecting the borehole with the corresponding radar angles from this section are plotted in the same Wulff net. The radar angles from borehole Kl 12 were 30°-43° (no. 9,10,11) for the corresponding section. The radar angle of 43° (not plotted) fit best to the predicted orientation for fracture zone 6.

Zone 7 is intersected by borehole Kl 12, see Table 2.2. The strike and dip of the fracture zone was by earlier investigations calculated to N65E and 80° to south, respectively. The normal to a plane with this orientation is plotted in a Wulff net in Figure 7.7. The intersection of the fracture zone with borehole Kl 12 was interpreted at 288-306 m borehole length, Table 2.2. The normals to the possible planes intersecting the borehole with the corresponding radar

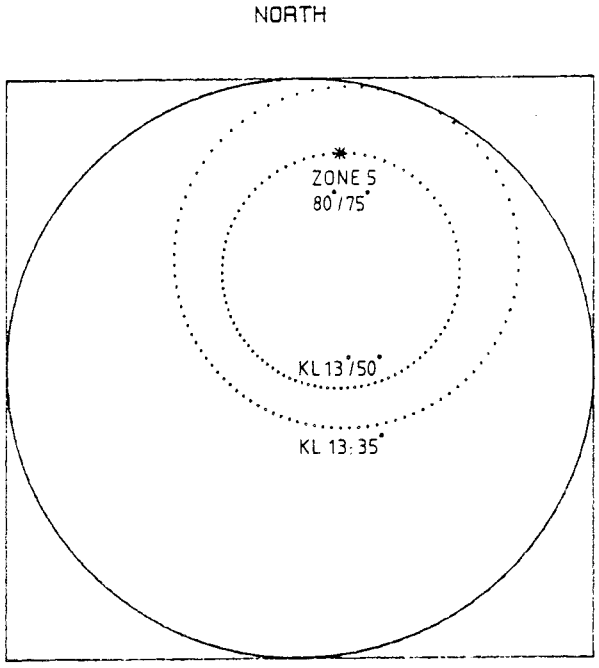

Figure 7.5 Orientation of fracture zone 5 and obtained radar angles in borehole Kl 13 plotted in a Wulff net.

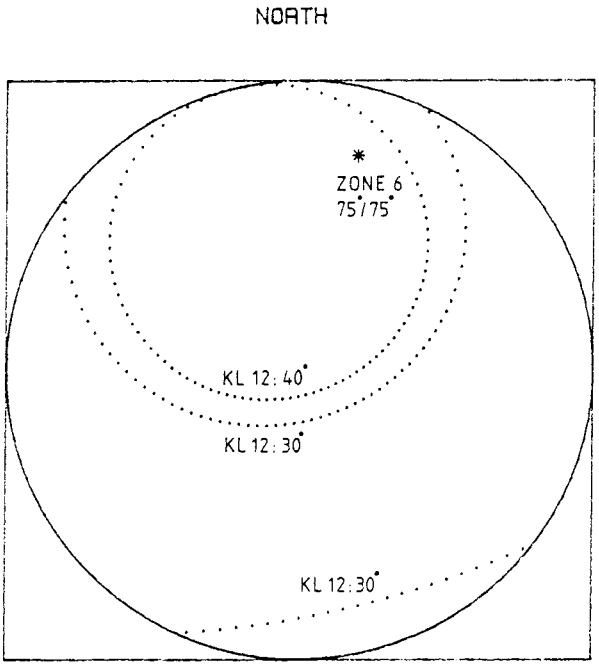

Figure 7.6 Orientation of fracture zone 6 and obtained radar angles in borehole Kl 12 plotted in a Wulff net.

angles from this section are plotted in the same Wulff net. The radar angles from borehole Kl 12 were 45^{o}-70^{o} (no. 9, 10, 11) for the corresponding section. The radar angles obtained in the borehole fit very well to the predicted orientation for fracture zone 7.

Zone 8 is intersected by borehole Kl 12, see Table 2.2. The strike and dip of the fracture zone was by earlier investigations calculated to N85W and 90^{o}, respectively. The normal to a plane with this orientation is plotted in a Wulff net in Figure 7.8. The intersection of the fracture zone with borehole Kl 12 was interpreted at 312-347 m borehole length, Table 2.2. The normals to the possible planes intersecting the borehole with the corresponding radar angle from this section are plotted in the same Wulff net. The radar angle from borehole Kl 12 was 40^{o} (no. 29) for the corresponding section. The radar angle obtained fit very well to the predicted orientation for fracture zone 8.

Zone 9 is intersected by borehole Kl 12, see Table 2.2. The strike and dip of the fracture zone was by earlier investigations calculated to N60E and 75^{o} to south, respectively. The normal to a plane with this orientation is plotted in a Wulff net in Figure 7.9. The intersection of the fracture zone with borehole Kl 12 was interpreted at 362-384 m borehole length, Table 2.2. The normals to the possible planes intersecting the borehole with the corresponding radar angle from this section are plotted in the same Wulff net. The radar angle from borehole Kl 12 was 35^{o} (no. 36) for the corresponding section. The radar angle obtained do not fit the predicted orientation for fracture zone 9. Based on the radar angle obtained this fracture zone should be vertical with the same strike. Another possible solution is that fracture zone 9 is parallel to fracture zone 8, i.e. with a strike in N85W. Fracture zone 8 and 9 are by

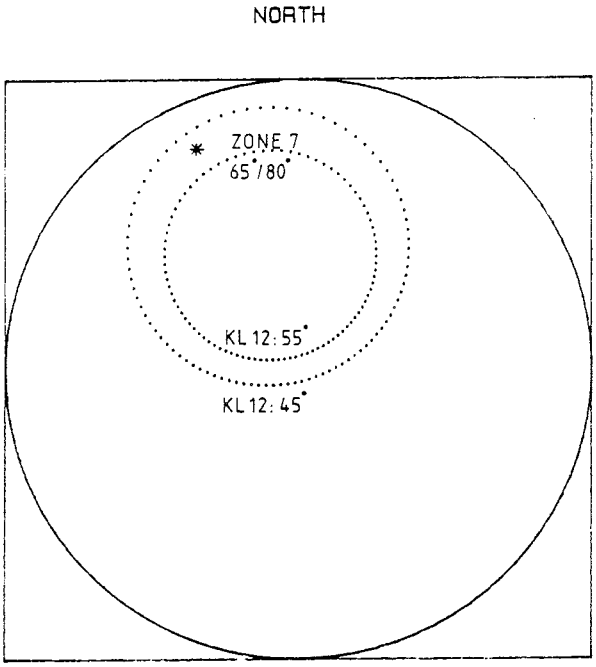

Figure 7.7 Orientation of fracture zone 7 and obtained radar angles in borehole Kl 12 plotted in a Wulff net.

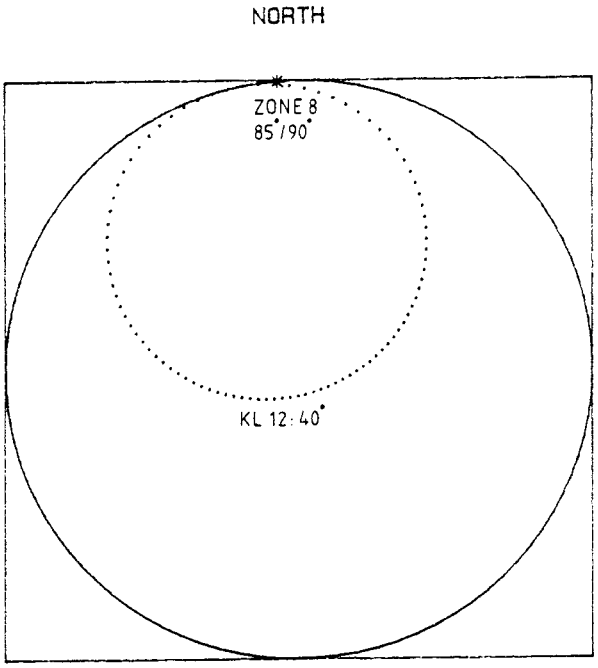

Figure 7.8 Orientation of fracture zone 8 and obtained radar angles in borehole Kl 12 plotted in a Wulff net.

geophysical logging identified as one wide fracture zone. It is only by correlation with surface geophysical data, the zones have been separated into two different fracture zones.

Zone 10 is intersected by borehole Kl 1, see Table 2.2. The strike and dip of the fracture zone was by earlier investigations calculated to N45E and 85° to north-west, respectively. The normal to a plane with this orientation is plotted in a Wulff net in Figure 7.10. The intersection of the fracture zone with borehole Kl 1 was interpreted at 280-310 m borehole length respectively, Table 2.2. The normals to the possible planes intersecting the boreholes with the corresponding radar angles from these sections are plotted in the same Wulff net. The radar angles from borehole Kl 1 were 25°-45° (no. 3, 10) for the corresponding sections. The radar angle of 25° fit best to the predicted orientation for fracture zone 10.

7.4 Orientation of fracture zone Hl

One of the major problems concerning the evaluation of the tectonic model for study site Klipperås was the orientation and extent of fracture zone Hl encountered in borehole Kl 2 at 792-804 m borehole length. There are two possibilities for the orientation of the fracture zone, according to the radar angles obtained in the borehole within this section. Two sets of radar angles to the borehole axis have been obtained from the 22 MHz radar map, one set between 10°-20° (radar angles no. 9 and 29) and another set between 58°-70° (radar angles no. 23, 24, 25 and 27). It is more likely that the last set of angles represent zone Hl since the angle of intersection is differing from the more common ones for greenstones in the area.

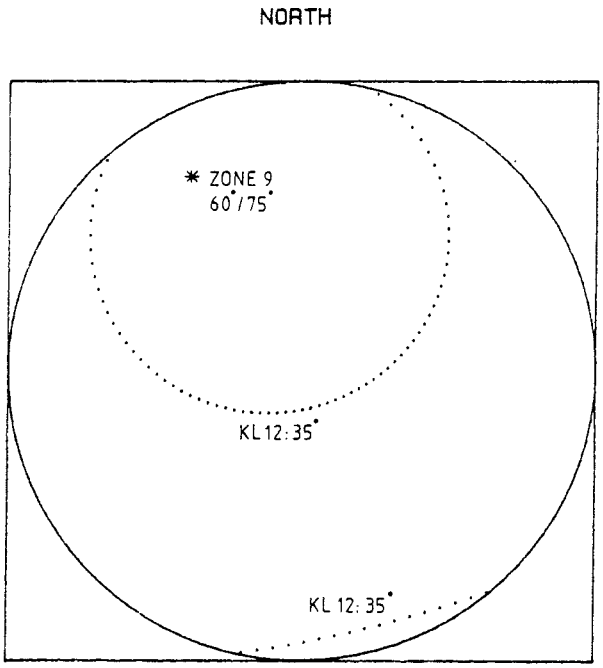

Figure 7.9 Orientation of fracture zone 9 and obtained radar angles in borehole Kl 12 plotted in a Wulff net.

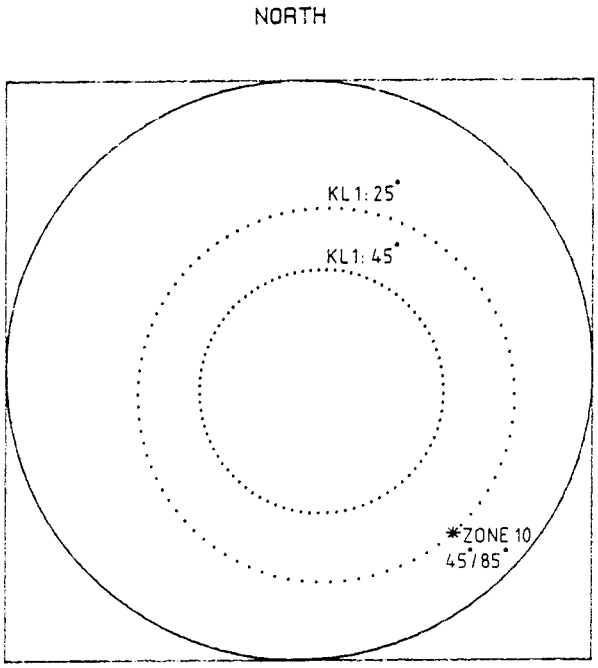

Figure 7.10 Orientation of fracture zone 10 and obtained radar angles in borehole Kl 1 plotted in a Wulff net.

The sets of radar angles which are between 10^{o}-20^{o} to the borehole axis seem to run more or less parallel along the borehole. It is very likely that the structure giving these angles can be interpreted as an undulating greenstone, because it is oriented in a similar way as the other interpreted greenstones in the area, namely WNW-ESE and steeply dip to the south (75-90^{o}).

The radar angles 58^{o}-70^{o} to the borehole axis would imply a dip of the fracture zone H1 of 10^{o}-40^{o} to the horizontal plane depending on the strike direction. A Wulff projection of the normals to zone H1 with a radar angle of 60^{o} around borehole K1 2 is presented in Figure 7.11.

Six possible orientations of the fracture zone, listed in Table 7.1, have been analyzed, by comparison with information from surface geophysical measurements and borehole loggings (Sehlstedt and Stenberg, 1986).

The best correlation with independent information is obtained when the strike direction of fracture zone H1 is between 180^{o}-210^{o} and the dip is 20^{o} to the west. With an orientation of $180^{o}/20^{o}$, the outcrop of the fracture zone correlates well with a geophysical anomaly obtained along profiles extended outside the investigated area. However, the intersection of zone H1 with borehole K1 6 are best defined within the section 552-569 m, called unit D (Sehlstedt and Stenberg, 1986). This unit has a character on the geophysical logs which are similar to that obtained in borehole K1 2 for the defined zone H1. However, from the hydrogeological point of view there is a difference between zone H1 in borehole K1 2 and unit D in borehole K1 6 (Gentzschein, 1986). In borehole K1 2 there is a piezometric underpressure within zone H1 and in borehole K1 6 a piezometric overpressure within unit D. This would imply an outflow of water from borehole

Table 7.1 Possible orientations of fracture zone H1 with a given radar angle of 60 in borehole K1 2 at 796 m. The correlation with other information are marked in comments column as positive (+) or negative (-).

Nr	Strike (°)	Dip (°)	Outcropping coordinate at surface	Intersection with different boreholes	Comments
1	270	30	360N		(-)
				K1 14: 868 m	(+)
2	180	20	4640E		(+)
				K1 6: 655 m	(-)
3	90	30	3060N		(-)
				K1 6: 698 m	(+)
				K1 9: 770 m	(+)
				K1 12: 354 m	(+)
				K1 13: 612 m	(+)
				K1 1: 526 m	(-)
4	0	40	1624E		(-)
				K1 9: 507 m	(-)
				K1 14: 818 m	(+)
				K1 1: 66 m	(+)
5	30	40	1000N/1065E		(-)
			2000N/1646E		(-)
				K1 9: 485 m	(+)
				K112: 643 m	(+)
6	210	20	1000N/4550E		(+)
			2000N/5120E		(+)
				K1 6: 795 m	(+)

Kl 2 into zone Hl and an inflow of water from unit D into borehole Kl 6. Another possibility is that zone Hl intersects borehole Kl 6 just below the bottom of the borehole. This is supported by the occurence of two marked parallel radar reflectors (no. 9 and 30) which can be followed to a distance of 10-110 m outside the borehole. These two reflectors are interpreted to intersect borehole Kl 6 at 801 m and 810 m respectively. The structures are not straight along the visible interval along the borehole. The two structures can be divided into three parts, close to the borehole the angle is 15^{o} and further out the angle is 25^{o} to the borehole axis. The angle between the reflector and the borehole axis increases to 40^{o} at a greater distance from the borehole.

In Figure 7.12 these three angles (15^{o}, 25^{o} and 40^{o}) are plotted in a Wulff net, together with the radar angle obtained in borehole Kl 2 for the zone Hl. There is a good fit between the radar angles obtained in borehole Kl 2 and the angles of 40^{o} obtained in borehole Kl 6 at a greater distance from the borehole. This suggests that the dip of zone Hl is in general 20^{o} to the horizontal. The strike of the fracture zone Hl is 180^{o}, compare with Table 7.1 and Figure 7.11. The outcrop coordinates fit with two alternatives listed in Table 7.1. At these coordinates geophysical anomalies have been obtained along profiles extended outside the investigated area. The geophysical surface anomaly is better defined in the north-south direction, thus implying a strike for fracture zone Hl to 180^{o}.

7.5 Some specific geological problems

A significant geophysical indication was encountered between 92-96 m in borehole Kl 8. The correlation between this indication and a weak geophysical ground surface anomaly was to be examined. A possible

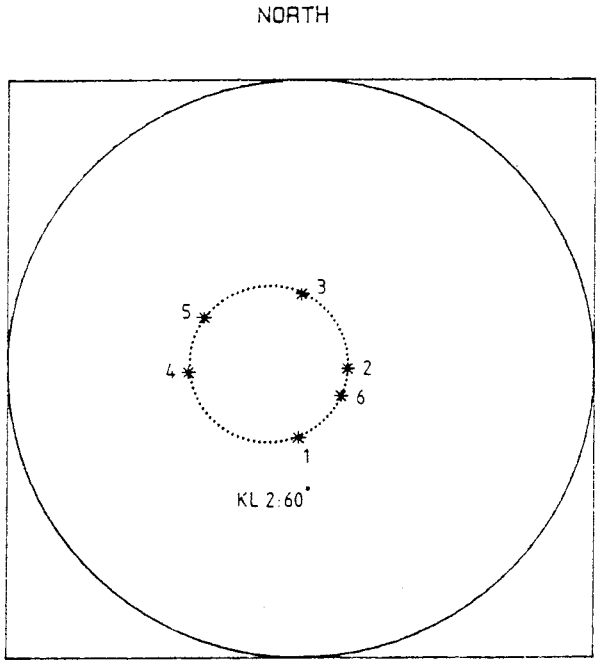

Figure 7.11 A Wulff net plot of the possible orientation of fracture zone H1 with a given angle of 60° to the borehole axis for borehole K1 2.

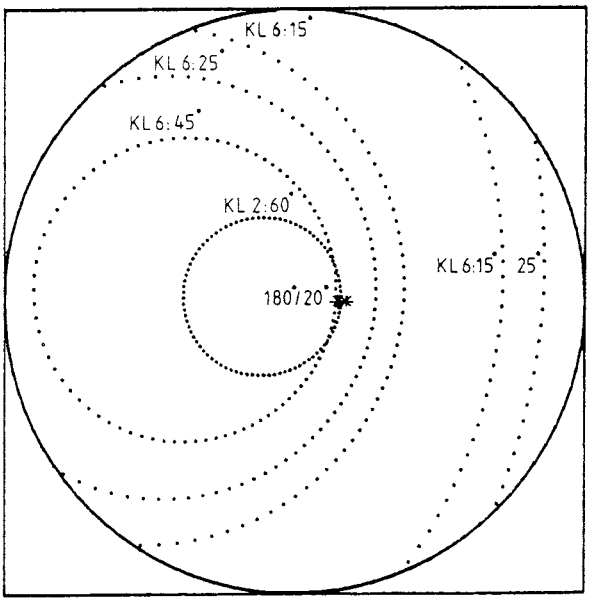

Figure 7.12 A Wulff net plot of the possible orientations of fracture zone H1 with a given angle of 60° to the borehole axis for borehole K1 2 and angles of 15°, 25° and 40° for borehole K1 6.

connection with zone H1 in borehole K1 2 should also be analyzed. The radar reflecting structure no.1 in borehole K1 8 gives an angle of 38° and 50° to the borehole axis on 22 and 60 MHz, respectively. The normals of possible planes intersecting the borehole with the two radar angles are plotted in a Wulff net in Figure 7.13. The normals of planes intersecting borehole K1 2 at 798 m with radar angles 10° and 20° are also plotted in the net. A fracture zone oriented parallel to the geophysical ground surface anomaly and with an intersection with boreholes K1 8 and K1 2 at 91 m and 798 m respectively gives the strike and dip of the fracture zone to 166°/83° west. The normal of a fracture zone with this orientation is also plotted in the Wulff net as a comparison. The radar angles in borehole KL 8 show that a fracture zone with this orientation is not possible.

The radar map in borehole K1 8 shows also that the stucture has a limited extent in the rock mass, and it can be followed to a distance of 45 m outside the borehole. At this distance it seems to fade away or cease against another structure.

Dolerites encountered in boreholes K1 4 and K1 9 were suggested to be the same in both boreholes. This is supported by putting the angles relative to borehole of radar reflecting structures from K1 4 (no.2; 50° and no.4; 50°) and K1 9 (no.9; 60° and no.13; 55°) into the three-dimensional micro-computerized program. The normals of the possible planes intersecting the boreholes with the given radar angles are plotted in a Wulff net in Figure 7.14. The normal of the interpreted orientation of the dolerite from earlier investigations with strike 25° and dip 65° to east is plotted in the same figure for comparison. The orientation of the dolerite dyke is supported by the radar angles obtained for both boreholes.

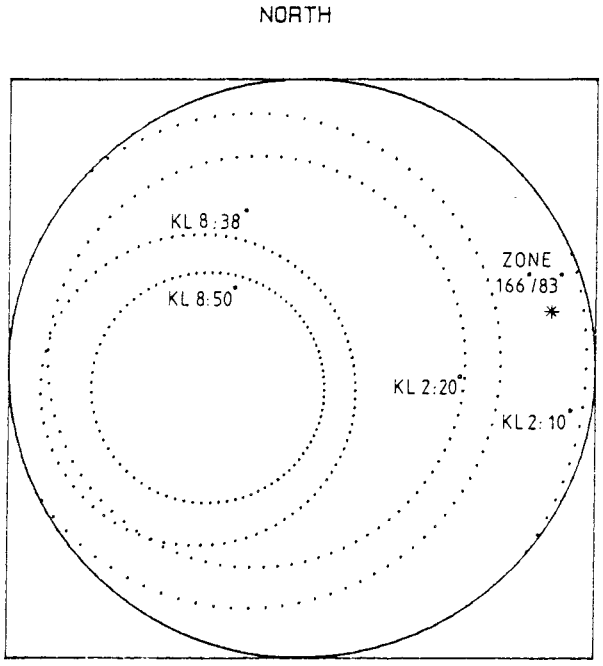

Figure 7.13 A Wulff net plot of the possible orientations of a significant fracture zone intersected by borehole Kl 8 with given radar angles in boreholes Kl 8 and Kl 2.

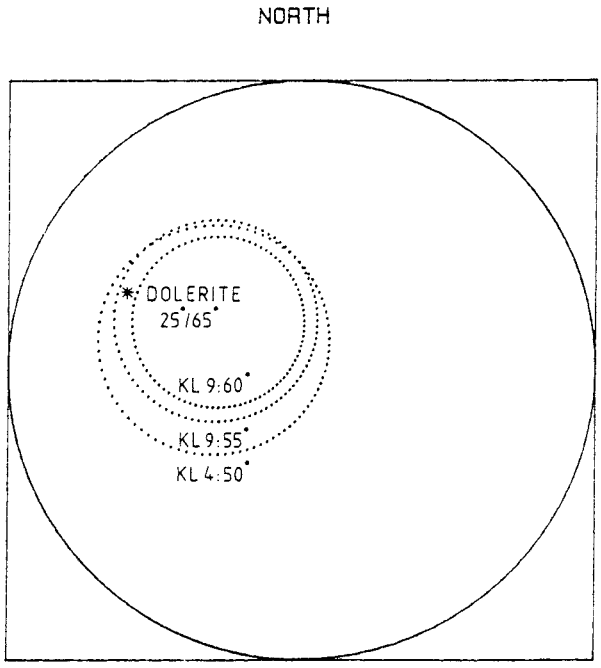

Figure 7.14 A Wulff net plot of the possible orientations of a dolerite intersected by boreholes Kl 4 and Kl 9 for observed radar angles in the boreholes.

A mafic dyke was encountered between 12-29 m in Kl 5, 88-100 m in Kl 10 and 338-371 m in Kl 6. The suggestion was that it is the same dyke in all three boreholes. Borehole Kl 5 was not investigated by radar. A Wulff net plot of the normals of possible orientations for the mafic dyke for the corresponding radar reflecting structures in Kl 6 (no.2; 30° and no.3; 29°) and in Kl 10 (no.14; 40° and no.2; 40°) are presented in Figure 7.15. The orientation of the mafic dyke, with strike 180° and dip 90°, interpreted from earlier investigations is also plotted in the net. The radar angles obtained correlate well with the earlier interpreted orientation of the mafic dyke. A calculated intersection in Kl 5 with the computer program is in good agreement with the actual intersection. The suggested interpretation, that it is the same dyke, is supported by the radar investigations. Also, on the radar maps from the two boreholes it can be seen that the behaviour of the direct radar pulse is the same. There is a marked loss in the radar pulse energy on both radar maps, indicated by the bulging shape of the solid black line.

A greenstone encountered between 219-300 m in Kl 6 is interpreted from the radar map to be almost parallel to the borehole. The greenstone is represented by radar reflecting structure no.18 (5-10°). According to the radar investigation the greenstone is a dike oriented parallel to the borehole. Hence, the greenstone is not an isolated fragment within the granite.

In the same borehole Kl 6 porphyries were encountered between 450-520 m and 700-747 m and it was, during the evaluation work, an alternative suggestion that the porphyry is parallel to the borehole and thereby penetrated at two different depths, due to the deviation of the borehole. However, the radar map shows that the reflecting structures no.4, no.5, no.7

and no.10 do not coincide with each other. It should be noted that two of the structures represent greenstone (no.4 and no.5) which are associated with the margins of the porphyry, while the other two (no.7 and no.10) represent fracture zones within the porphyry. All four structures intersect the borehole at an acute angle (5-35^{o}). It is unlikely that it is the same porphyry encountered at both intersections in the borehole Kl 6.

The porphyries encountered at the bottom of borehole Kl 1, between 449 and 561 m, have been suggested to be the same as those at the bottom of Kl 9, between 731 m and 780 m. A Wulff net plot of the corresponding radar angles in borehole Kl 1 (no 4; 25^{o} and no 14; 35^{o}) and in borehole Kl 9 (no 33; 30^{o}) are presented in Figure 7.16. In general, the porphyry dykes in the area strike in 110^{o} and dip 75^{o} to south (Olkiewicz et al., 1986). This orientation is also presented in the figure. Assuming a strike of 110^{o}, the pophyries should dip 60^{o} to south for the given radar angles, if the porphyries in boreholes Kl 1 and Kl 9 should be the same. The suggestion from the radar measurements is that the possibility still exists that it is the same porphyries encountered in both boreholes.

The orientation of a prominent resistivity anomaly within a porphyry at the borehole length 764-776 m in borehole Kl 9, unit B, were to be analysed. According to the radar angles observed in borehole Kl 9 (no 34; 30^{o} and no 33; 30^{o}), the orientation of unit B is parallel to the general orientation of the porphyries in the area.

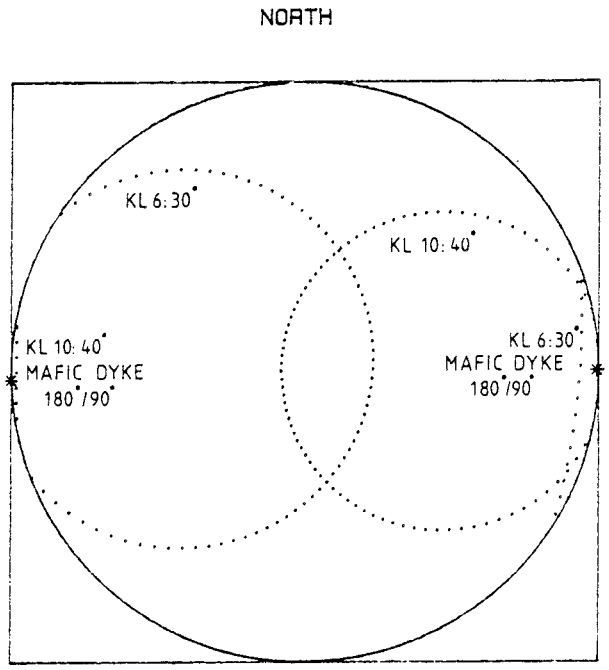

Figure 7.15 A Wulff net plot of the possible orientations of a mafic dyke intersected by boreholes Kl 6 and Kl 10 with observed radar angles in the boreholes.

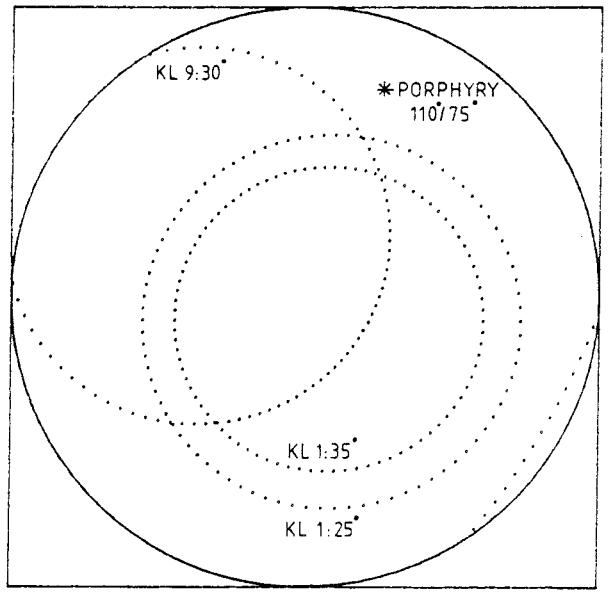

Figure 7.16 A Wulff net plot of the possible orientations of porphyries intersected by the boreholes Kl 1 and Kl 9 with observed radar angles in the boreholes.

8 CORRELATION OF RADAR REFLECTORS WITH GEOLOGY

A number of 191 reflectors intersecting the boreholes have been interpreted from the 22 MHz radar maps (Table 8.1). Of these reflectors 32 constitute upper or lower reflection from the same reflecting object. A number of 66 reflectors which do not intersect the boreholes have also been interpreted. A total of 257 reflectors have been interpreted from the 22 MHz measurement in the boreholes in Klipperås.

Table 8.1 Interpreted radar reflecting structures from the boreholes in Klipperås (22 MHz).

Borehole	No. of all intersecting structures	No. of double intersecting structures	No. of not intersecting structures
Kl 1	15		7
Kl 2	28	6	5
Kl 4	4		4
Kl 6	18		13
Kl 8	5		9
Kl 9	32	6	7
Kl 10	9		9
Kl 12	30	2	6
Kl 13	10	2	1
Kl 14	40	16	5
Sum	191	32	66

Table 8.2 Number of mapped rock types in the boreholes in Klipperås except the hostrock granite (Egerth, 1986).

Borehole	Greenstone	Pegmatite + Aplite	Porphyry	Mafic dyke
Kl 1	33	6	11	
Kl 2	19	1		2
Kl 4	11	3	2	1
Kl 6	16	2	7	8
Kl 8				
Kl 9	28	6	2	3
Kl 10	3	2	3	1
Kl 12	23	10	7	
Kl 13*	5			
Kl 14	17	3	4	7
Sum	155	33	36	22

* Only down to 175 m, because of blocked hole.

In Table 8.2 is the number of different coremapped rock types in the radar measured boreholes presented, except the hostrock granite. The total number of different mapped rock types from the core logging is 246. The thickness of the different rock types has not been taken into consideration. Greenstone constitutes 63 % of these, pegmatite/aplite 13 %, porphyry 15 % and mafic dyke 9 %.

In Table 8.3 is the number of intersecting radar reflecting structures from the 22 MHz measurement and their corresponding characteristic geological structure presented. Observe, in order to prevent overrepresentation in case of double reflectors from the same object, only one of the reflectors is included in Table 8.3. The total number of

Table 8.3 Number of interpreted radar reflecting structures from the 22 MHz measurement corresponding to geological structures, excluding double (upper and lower) reflections at the same point of intersection.

Bore-hole	Greenstone	Pegm. +Aplite	Porphyry	Mafic dyke	Other*
Kl 1	6	3	2		4
Kl 2	14			2	9
Kl 4	1			2	1
Kl 6	8	1		2	7
Kl 8					5
Kl 9	13			3	13
Kl 10	3	1	1	1	3
Kl 12	16	1	3		9
Kl 13	6				3
Kl 14	14	2	2	6	8
Sum	81	8	8	16	62

* including structures such as fracture zones, shear zones, mylonite, altered fractures, clayfilled fractures etc.

interpreted radar reflecting structures is 175, excluding one of each double reflection. Of these 112 are connected with different rock types. It should be noted that fracturing is a very common feature associated with contacts between different rock types, thereby strengthening the radar reflection. Greenstone constitutes 47 % of these, pegmatite/aplite 5 %, porphyry 5 %, mafic dyke 9 % and finally other structures 34 %.

A comparison between Table 8.2 and Table 8.3 shows that the borehole radar detect 52 % of mapped greenstone, 24 % of pegmatite/aplite, 22 % of

porphyry and finally 73 % of mafic dyke. Greenstone is the most abundant rock type in the granite and it is also a rock type that can be very easily detected by borehole radar in this environment. Porphyry and pegmatite/aplite are rather common rock types but they are not so easy to detect by the radar as the other rock types. However, mafic dyke is the most unusual of the rock types, but most of them are detected by the borehole radar.

Of the interpreted radar reflectors intersecting the boreholes (excluding double reflectors) 65 % can be related to different rock types. 35 % of the intersecting reflectors are thereby related to geological structures in the rock such as fracture zones, clayfilled fractures, shear zones, altered fractures, mylonites etc. Several of them are associated with different fracture zones or units. Many of the radar interpreted structures are not very marked in the core and might be included in the rock mass.

All geologically and geophysically interpreted zones or features associated with them are detected by the radar (Table 8.4). A detailed investigation is presented in chapter 7.3.

The 60 MHz radar maps exhibit a similar pattern in the distribution between the different structures. However, there is a higher number of "other structures" i.e. fractured, crushed, altered, isolated fractures etc. Many of them are insignificant features. The 60 MHz maps give a more detailed picture of the area close to the borehole, but the range is not as good as in the 22 MHz maps.

The reflectors in the 22 MHz radar maps also exhibit a large scale pattern. This pattern gives a picture of the anisotropy in the rock volume about 100 m around the extension of each borehole.

Table 8.4 Geologically and geophysically interpreted zones and their occurence in the 22 MHz radar maps.

Zone	Intersected by borehole	Interpreted by radar in borehole	Represented in the 22 MHz radar map by reflection no.
1	Kl 3,	Not radar measured borehole	
	Kl 4,	Kl 4	5
	Kl 9	Kl 9	28, 29, 30
2	Kl 9	Kl 9	4, 2, 3
	Kl 12	Kl 12	12, 23, 24
3	Kl 7	Not radar measured borehole	
4	Kl 11	Not radar measured borehole	
	Kl 14	Kl 14	30, 28, 35, 29, 3, 45
5	Kl 13	Kl 13	8, 6
6	Kl 12	Kl 12	1, 2, 3
7	Kl 12	Kl 12	9, 10, 11
8	Kl 12	Kl 12	29
9	Kl 12	Kl 12	36
10	Kl 1	Kl 1	10, 3
11	-		
12	-		
H1	Kl 2	Kl 2	23, 24, 25, 27

The direction and dip of the different boreholes are presented in Table 8.5 and their position in Figure 2.1. Dipping boreholes directed northwards (Kl 12, Kl 13 and Kl 14 in Table 8.5) exhibit an almost uniform pattern of parallel radar reflecting structures. Structures more or less parallel to the boreholes are unusual. The mean angle of intersecting radar reflecting structures in these boreholes is 48^{o} (Table 8.6). Kl 13 and Kl 14 are inclined 55^{o} below horizontal plane and deviates to 50^{o} in the end, while kl 12 is inclined 50^{o} in the beginning and deviates to 45^{o} in the end. The mean angle of intersecting structures in Kl 12 is somewhat higher than in the other two, a fact which supports a suggestion of the occurence of vertical east-west striking structures in the rock mass. Dipping boreholes directed east- or westward (Kl 4, Kl 6, Kl 8, Kl 9, and Kl 10 in Table 8.5) exhibit a pattern of radar reflecting structures parallel or subparallel to the boreholes. The mean angle of intersecting radar reflecting structures in these boreholes is 32^{o}, compared to 48^{o} in the nortwards directed boreholes. This indicates that the main structures of the rock are more or less perpendicularly penetrated by northwards directed boreholes, while east- or westward directed boreholes are parallel to or penetrates the main structures at a small angle. The pattern from the radar maps indicate that the main structures of the rock are directed more or less east-west and that it is unlikely that they are dipping towards north. The vertical or subvertical boreholes (Kl 1 and Kl 2 in Table 8.5) also exhibit a pattern of parallel or subparallel reflectors. The mean angle of intersecting radar reflecting structures in these boreholes is 25^{o}, i.e. the boreholes penetrate the structures at a small angle. This indicates that the dip of the main structures of the rock is more or less vertical. The undulating character of many of the parallel structures can be interpreted as if the structures are folded. The

Table 8.5 Direction and inclination of the radar investigated boreholes in Klipperås.

Borehole	Direction	Declination (360^{o} system)	Inclination
Kl 1	S 46 E	134	80^{o}
Kl 2	N 82 W	278	78^{o}
Kl 4	N 71 W	289	59^{o}
Kl 6	N 84 W	276	56^{o}
Kl 8	S 78 W	258	58^{o}
Kl 9	N 60 W	300	56^{o}
Kl 10	N 90 E	90	49^{o}
Kl 12	N 14 W	346	50^{o}
Kl 13	N 22 E	22	55^{o}
Kl 14	N 2 E	2	55^{o}

fold-axis in this area should be almost vertical.

The discussion carried on above is supported by Wulff-net plot of the normals to an unoriented zone in each borehole, representing the mean angle of radar reflections from the 22 MHz maps.

Figure 8.1 shows a plot in Wulff-net of all mean angles of radar reflections from each borehole, and a plot of all mean angles of radar interpreted greenstones in the boreholes except Kl 8 where greenstone not occur. The greenstone plot exhibit one point where six of the circles crosscut. This point represents an orientation of WNW/50-70^{o}SW. Three of the circles diverge from the other six. These three circles have in common that they represent boreholes directed towards N or NE, thereby intersecting the greenstones at a very steep angle. Interpretation of steep structures allows large variations in the determination of the angle by the nomogram, while the angle variation is small for structures with an acute

NORTH

a/

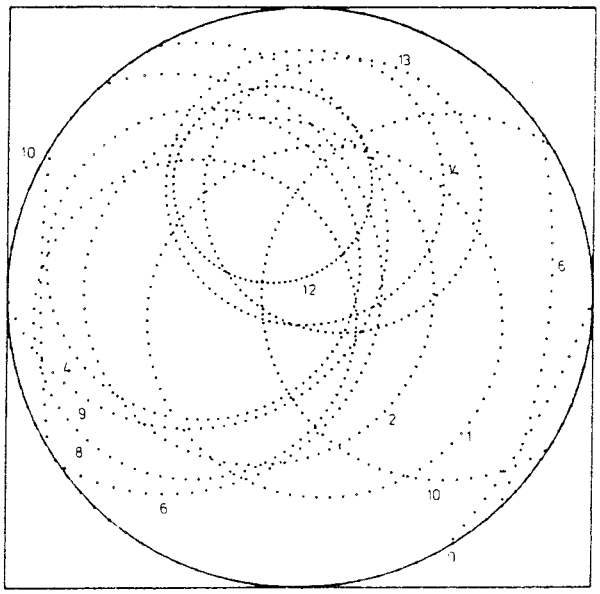

b/

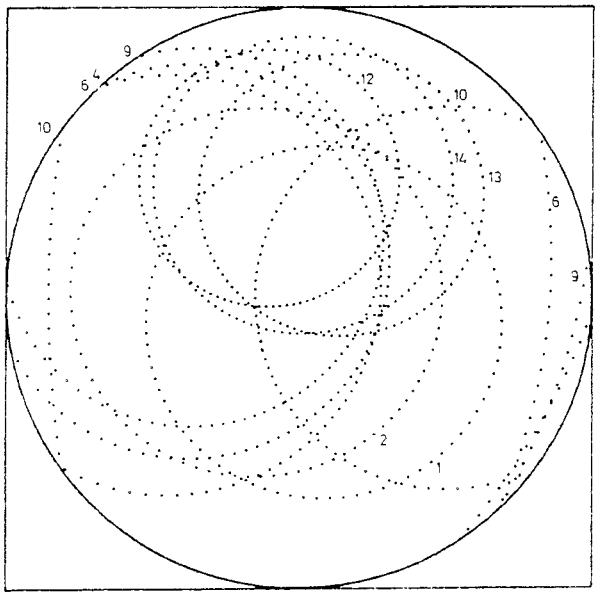

Figure 8.1 Intersecting reflections from 22 MHz radar maps plotted in a Wulff net. All radar investigated boreholes.

a/ Mean angle of all reflections for each radar investigated borehole.

b/ Mean angle of all reflections associated with greenstone for each radar investigated borehole, except K1 8.

Table 8.6 Mean angle of all intersecting radar reflecting structures from the boreholes in Klipperås.

Borehole	Mean angle of intersecting structures	Number of intersecting structures
Kl 1	28°	15
Kl 2	29°	28
Kl 4	38°	4
Kl 6	25°	18
Kl 8	37°	5
Kl 9	29°	31
Kl 10	34°	9
Kl 12	57°	29
Kl 13	44°	10
Kl 14	44°	40

angle to the borehole. Furthermore the calculation of velocity determination might be somewhat incorrect, which also leads to larger variations with steep angles. The plot with all reflections also exhibits a point where most of the circles crosscut each other, but the different crosscuttings are more scattered in this plot. This can partly be explained by the presence of mafic dykes and fracture zones, oriented in a N-NE direction, as previously discussed in chapter 7.

In Figure 8.2 is the angles of all intersecting radar structures grouped together and presented in form of a histogram for each borehole. The histogram for each borehole exhibits a more or less pronounced single peak except for Kl 2 and Kl 4 which have two separated peaks. The single peaks are in rather good agreement with the calculated mean angles of the

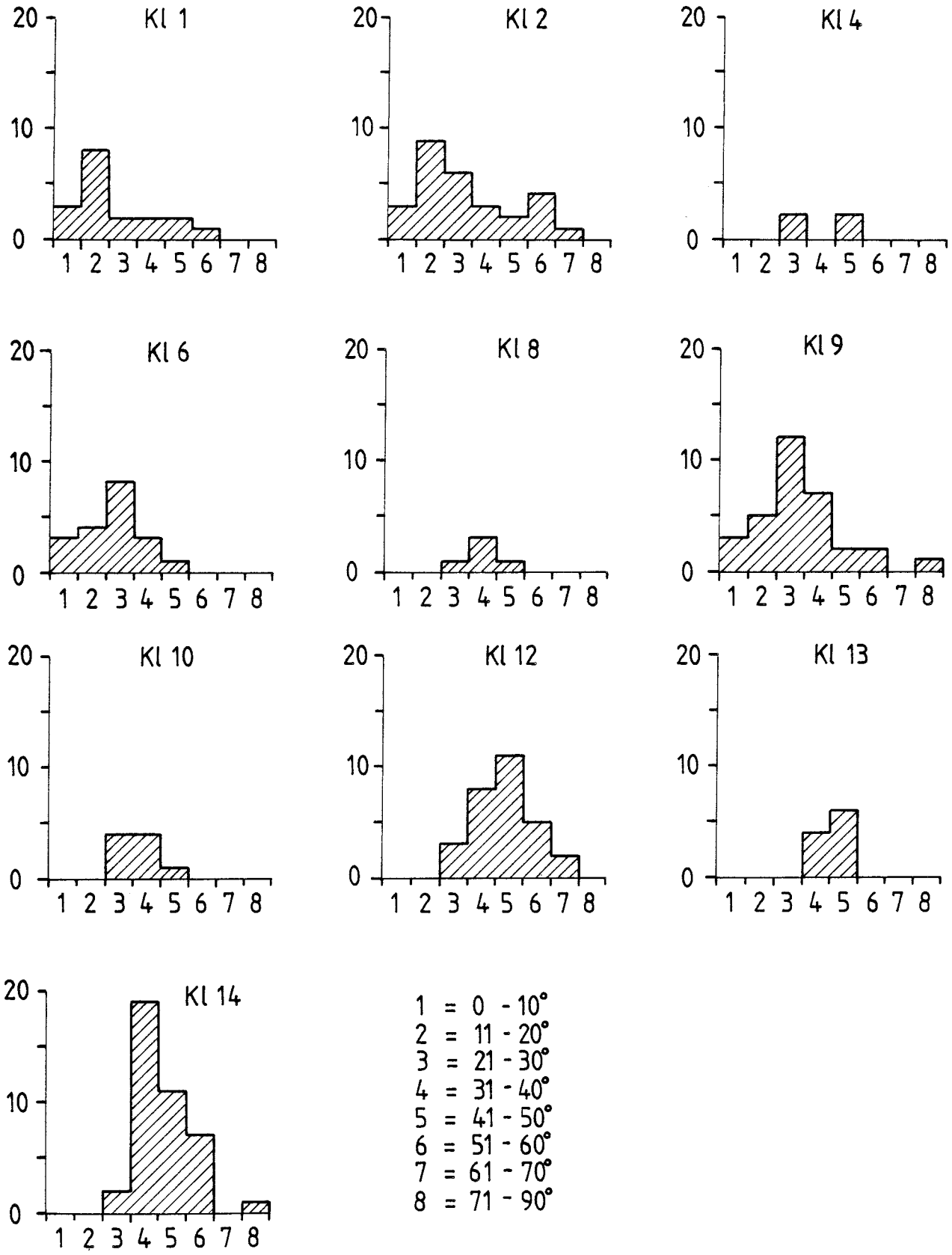

Figure 8.2 Histogram for angles of all intersecting radar structures presented for each borehole, 22 MHz.

boreholes (Table 8.6). Kl 4 contains only four structures, a fact which makes the result statistically uncertain. Other boreholes with a small number of structures do occur, but they do not constitute exceptions from the general trend, like Kl 4. However, Kl 2 penetrates several structures including fracture zone Hl. Fracture zone Hl is an exception in the investigated boreholes by being a rather flat lying zone with a dip of about 20-45°. Kl 2 is otherwise characterized by structures subparallel to the borehole.

However, there is still a possibility of the existence of other horizontal structures in the area. The dipping boreholes exhibit some radar reflecting structures intersecting at an angle between 50-70°, which could be suitable candidates for horizontal structures. Some of them can be excluded because they are connected with interpreted features in another boreholes or surface geophysics, and some can be excluded due to deviation of the boreholes. Furthermore the radar maps from the subvertical boreholes exhibit only one intersecting radar reflecting structure with an angle above 58°. This is a greenstone within the fracture zone Hl in Kl 2. It should be noted that structures perpendicular to the borehole only exhibit weak reflections, if any reflection at all. Taken together, these facts indicate that horizontal structures in the area is not a common feature, but can not be excluded as single features.

The detailed investigation of the radar maps shows that the greenstones can be considered as extensive structures and usually constitute the most continuous radar reflecting structures. It can be ascertained that the greenstones do not constitute isolated fragments in the rock mass. Also, they exhibit a somewhat undulating structure which might be caused by slight folding where the fold-axis is subvertical.

Encountered mafic dykes show that they exhibit a varying performance in the radar maps. They usually exhibit a marked loss of arrival time of the direct radar pulse travelling along the borehole, indicated by the bulging shape of the solid black line, and they also exhibit a loss of reflections in a band outside the borehole. The loss of radar pulse energy can be caused by intense fracturing of the mafic dykes, and the phenomena can be seen, for example, in the boreholes Kl 4, Kl 6, Kl 9 and Kl 14. From the radar maps it can also be seen that the reflecting structures of mafic dykes are straight and not so extensive as those interpreted as greenstone. Mafic dykes differ from greenstone and porphyry by being oriented in a northerly direction.

The characteristic loss of radar pulse energy is a feature which seems to be coupled together to fracturing or rock type differences in the borehole. In Table 8.7 is all encountered loss of radar pulse energy from the 22 MHz maps presented. A great majority of them correspond to different interpreted zones or units in the boreholes. Some of them only correspond to fracturing, different rocktype or a combination of both, but these are all characterized by being weak or medium strong. It should be noted from this fact, that the loss of primary pulse energy is also an important tool for interpretation of important structures in the boreholes, a tool to be used together with radar reflections.

Table 8.7 Sections in the boreholes where loss of radar pulse energy occur, and corresponding structures (22 MHz).

Borehole	Section (m)	Character	Structure
Kl 1	77- 91	Weak	Fractured
	309-328	Weak	Zone 10 (280-310 m) + greenstones, fractur.
Kl 2	758-769	Strong	Unit B (768-774 m)
	778-796	Strong	Zone H1 (792-804 m)
Kl 4	71- 98	Strong	Unit A (87-91 m)
	118-135	Medium	Zone 1 (110-180 m)
	167-175	Weak	Porphyry, fractured
Kl 6	340-374	Strong	Unit B (338-372 m)
	403-427	Weak	Unit C (424-531 m)
	506-530	Weak	Unit C (424-531 m)
Kl 9	138-161	Weak	Zone 2 (120-160 m)
	257-273	Weak	Somewhat fractured
	347-377	Strong	Unit A (356-374 m)
	755-768	Strong	Unit B (764-776 m)
Kl 10	82-106	Strong	Unit A (88-100 m)
Kl 12	157-174	Weak	Fractured
	323-338	Medium	Zone 8 (312-347 m)
	371-381	Weak	Zone 9 (368-384 m)
	610-624	Weak	Zone 2 (595-630 m)
	655-672	Weak	Greenstone
	686-700	Weak	Greenstone
Kl 13	78- 92	Medium	Greenstone, fractured
Kl 14	258-275	Medium	Greenstone, crushed
	367-381	Medium	Zone 4 (368-410 m)
	511-527	Medium	Dolerite, fractured

9 DISCUSSION

There are several different geophysical methods for indication of inhomogeneities in the rock mass such as fracture zones or dykes. Of these methods the borehole radar is the only method that besides the position, also indicates the extension of zones and dykes outside the borehole. However, the determination of position in the borehole is not as exact as other geophysical methods, but in return it shows that structures actually have an extension outside the borehole, and do not constitute limited phenomena in connection with the borehole. Investigations performed with other methods have only assumed that the structures have an extension in the rock mass. The radar gives a geometrical image of the area surrounding the borehole. The range of the radar in the investigated rock is 100-120 m from the borehole.

The radar system has prooven to be operationally efficient for this type of survey. It is easy to load the equipment into a suitable ordinary van for transport to an investigation site. The radar equipment can be power supplied by a mobile generator and it is not especially sensitive for different climates. The most sensitive unit in the equipment is the control box which should not be exposed to large temperature variations during measurement. It is rather simple to put the equipment together and put it into a borehole and start the measurement. Measurement with the borehole radar is also a rapid method where a quantitative result can be obtained directly on the screen during measurement. A radar map is obtained after a relatively quick processing of radar data.

Ten boreholes in Klipperås have been investigated by borehole radar. From the radar maps it is possible to obtain a detailed picture of single zones and dykes and their orientation and extension, as well as a general picture of the anisotropy of the total rock

mass. Also, several structures can be seen outside the borehole which do not intersect or should intersect the extension of the borehole.

The anisotropy of the rock mass is clearly seen on the radar maps from the different boreholes depending on the direction and inclination of the borehole. Inclined boreholes directed towards north exhibit a very characteristic pattern of almost exclusively parallel structures intersecting more or less perpendicular to the boreholes. Inclined boreholes directed towards east or west exhibit another characteristic pattern of the radar maps. Radar reflecting structures with an acute angle of intersection and several parallel structures outside the borehole is a dominating feature in these holes. This contributes to the suggestion of vertical east-west striking zones and dykes in the area. The subvertical boreholes also support the suggestion of vertical east-west striking zones and dykes.

However, there is still a possibility of the existence of horizontal structures in the area. It should be noted that structures perpendicular to the borehole only exhibit weak reflections, if any reflection at all. Taken together these facts indicate that horizontal structures in the area is not a common feature, but can not be excluded as single features. One example of this is the zone H1 in K1 2 which seems to be more or less horizontal.

The detailed investigation of the radar maps shows that the greenstones can be considered as extensive structures and usually constitute the longest radar reflecting structures. They also exhibit a somewhat undulating structure which might be caused by slight folding where the fold-axis is subvertical. Detailed investigations of encountered dolerite and ultramafic dykes show that they usually exhibit a marked loss of the direct radar pulse energy.

Once the location of a fracture zone has been established from the radar maps it is possible to compare it in detail with the results of geophysical logging and core mapping. As expected there is a strong correlation with low resistivity or high porosity, criteria traditionally used to identify fracture zones by geophysical logging, as well as the fracture density obtained by visual inspection of the core. In Appendix A the result from the loggings are presented for the radar measured boreholes (from Sehlstedt and Stenberg, 1986). A majority of the interpreted radar reflecting structures intersecting the borehole are coupled together with low resistivity. This is of course expected, since the propagation and reflection of a radar pulse is directly related to the electrical properties of the medium. In fact, the radar reflections are probably caused by rapid variations in the resistivity. It should be noted that all greenstones and mafic dykes (dolerite and basalt) which are characterized by low resistivity also give rise to radar reflections. Most of the porphyries do not have a contrast in resistivity to the surrounding granite. As expected it was difficult to observe radar reflections from the porphyries. In fact, the reflections observed are correlated to the greenstones which appear at the margin of the porhyries or to mylonites within the porhyries. Both these features are characterized by contrasting low resistivity. Wider fracture zones and other units, e.g mafic dykes (dolerite and basalt), with a very low resistivity give a strong loss in radar pulse energy.

Fracturing is a common feature associated with the different dykes detected by the radar. There is a possibility that they can be associated with higher hydraulic conductivity than dykes not detected by radar. Additional work concerning hydraulic conductivity of the dykes will be required for a

complete understanding.

In general, the predicted orientation of the fracture zones from earlier investigations agree well with the orientation calculated from radar crossing angles. For one fracture zone, i.e. fracture zone 9, the predicted orientation disagrees with the radar angles obtained in borehole Kl 12. According to the radar measurement the orientation of this zone is most probably parallel to fracture zone 8. The radar angle for fracture zone 2 intersecting the borehole Kl 12 disagrees also with the predicted orientation. However, the radar angles obtained in borehole Kl 12 at these locations are most probably due to greenstones. The radar angles obtained here fits to the orientation of the greenstones with strike in west-north-west.

One of the major problems concerning the evaluation of the tectonic model for study site Klipperås was the orientation and extent of fracture zone Hl encountered in borehole Kl 2 at 792-804 m borehole length. According to the radar investigation different orientations of the fracture zone Hl have been analyzed. The best correlation with independent information is obtained when the strike direction of fracture zone Hl is between 180°-210° and the dip is 20° to the west. With an orientation of $180^{\circ}/20^{\circ}$, the outcrop of the fracture zone correlates well with a geophysical anomaly obtained along profiles extended outside the investigated area.

The radar investigations performed in the boreholes with different directions show that a majority of the structures causing reflections are straight and elongated in one predominating direction. This would imply a relative simple geological model of structures striking in east-west. This anisotropy will probably have a great effect also on the water movements within the bedrock. The hydraulic anisotropy depends also on the three-dimensional pressure distribution in the

rock volume. This has not been investigated within the area and warrants further studies.

In whole, the borehole radar has been a useful instrument for detection and characterization of zones and dykes in this geological environment. It has also been found to be useful for obtaining a general picture of the anisotropy of the rock mass and the geometry of the dykes and zones in the surroundings of the boreholes. It can be concluded that the borehole radar measurements have given a valuable contribution to the evaluation of the geological, geophysical and hydrogeological conditions at the Klipperås study site. In some aspects the earlier investigations gave an incomplete picture of the tectonic model of the site. The borehole radar measurements have confirmed the tectonic model and have also given complementary information for the construction of a three-dimensional model of the site.

REFERENCES

Carlsten, S., Magnusson, K-Å., Ahlbom, K., 1986. Reconnaissance study of a fracture zone at Ävrö. AR 86-15, SKB, Stockholm, Sweden.

Egerth, T., 1986. Compilation of geological and technical borehole data from the Klipperås study site. AR 86-10, SKB, Stockholm, Sweden.

Gentzschein, B., 1986. Hydrogeological investigations at the Klipperås study site. TR 86-08, SKB, Stockholm, Sweden.

Olkiewicz, A., Stejskal, V., 1986. Geological and tectonic description of the Klipperås study site. TR 86-06, SKB, Stockholm, Sweden.

Olsson, O., Sandberg, E., Nilsson, B., 1983. The use of Borehole radar for the detection of fractures in crystalline rock. Stripa Project, IR-83-06, SKBF/KBS, Stockholm, Sweden.

Olsson, O., Sandberg, E., 1984. Preliminary design of a new borehole radar system. Stripa project, IR 84-04, SKBF/KBS, Stockholm, Sweden.

Sehlstedt, S., Stenberg, L., 1986. Geophysical investigations at the Klipperås study site. TR 86-07, Stockholm, Sweden.

APPENDIX A

Geophysical logs from the radar investigated boreholes.

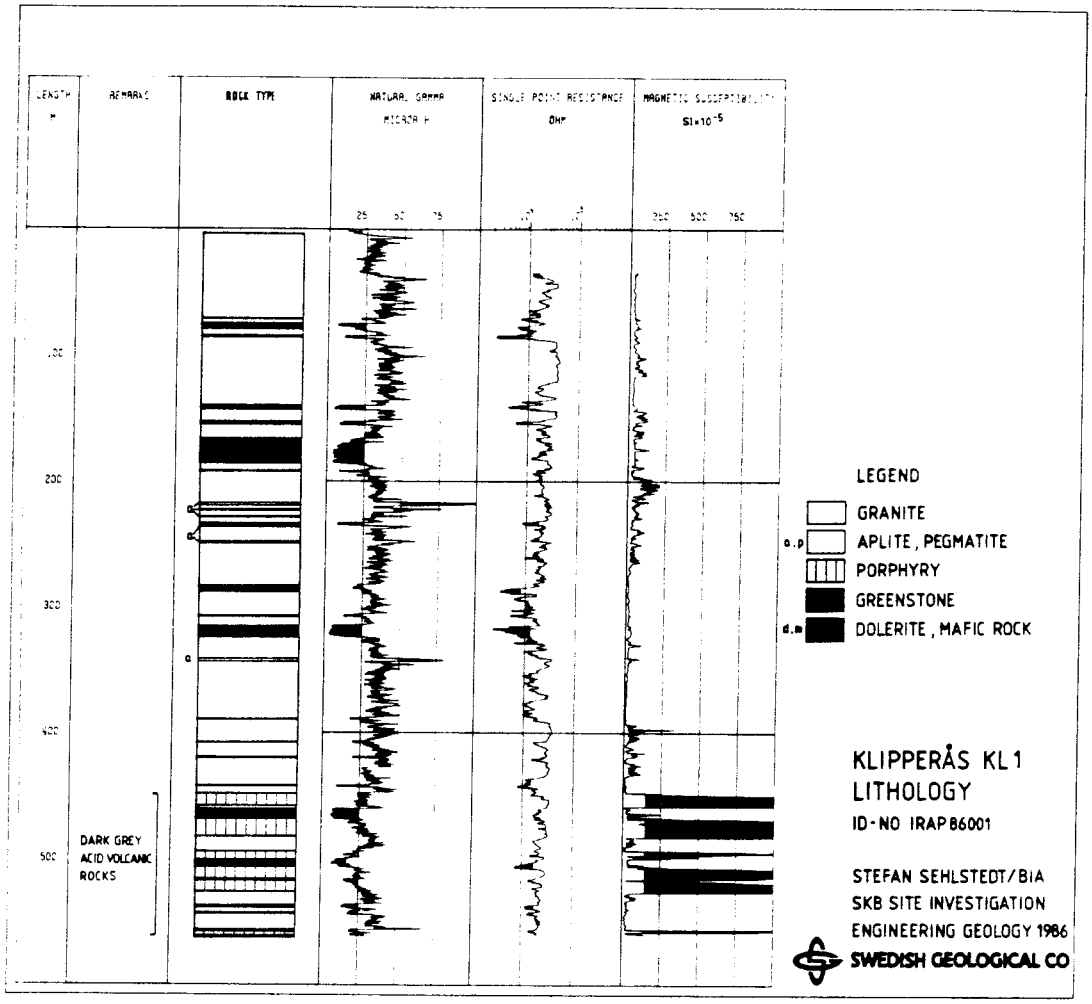

Figure A.1 Geophysical logs sensitive to lithology variations, measured in borehole Kl 1.

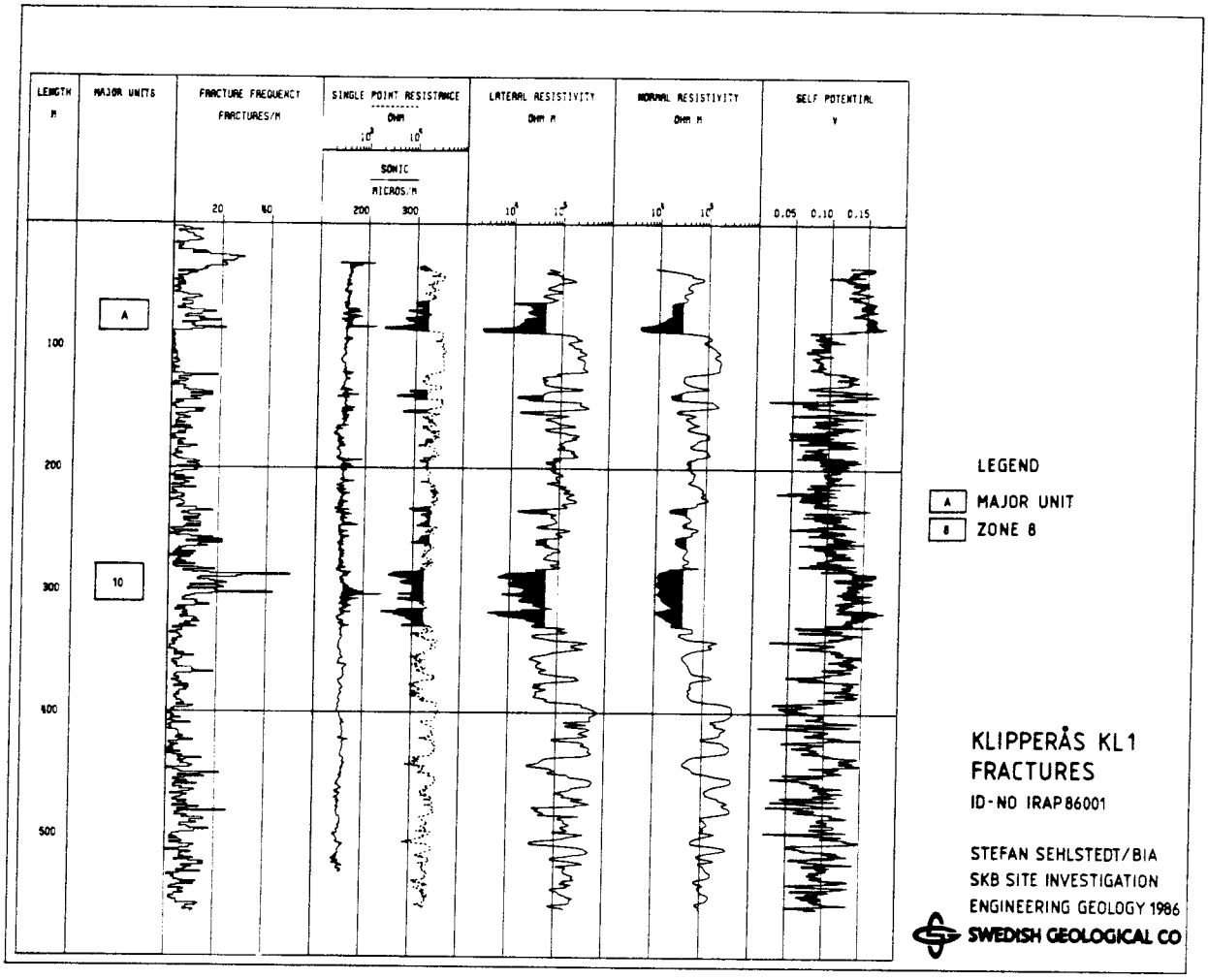

Figure A.2 Geophysical logs sensitive to fracture occurences, measured in borehole Kl 1.

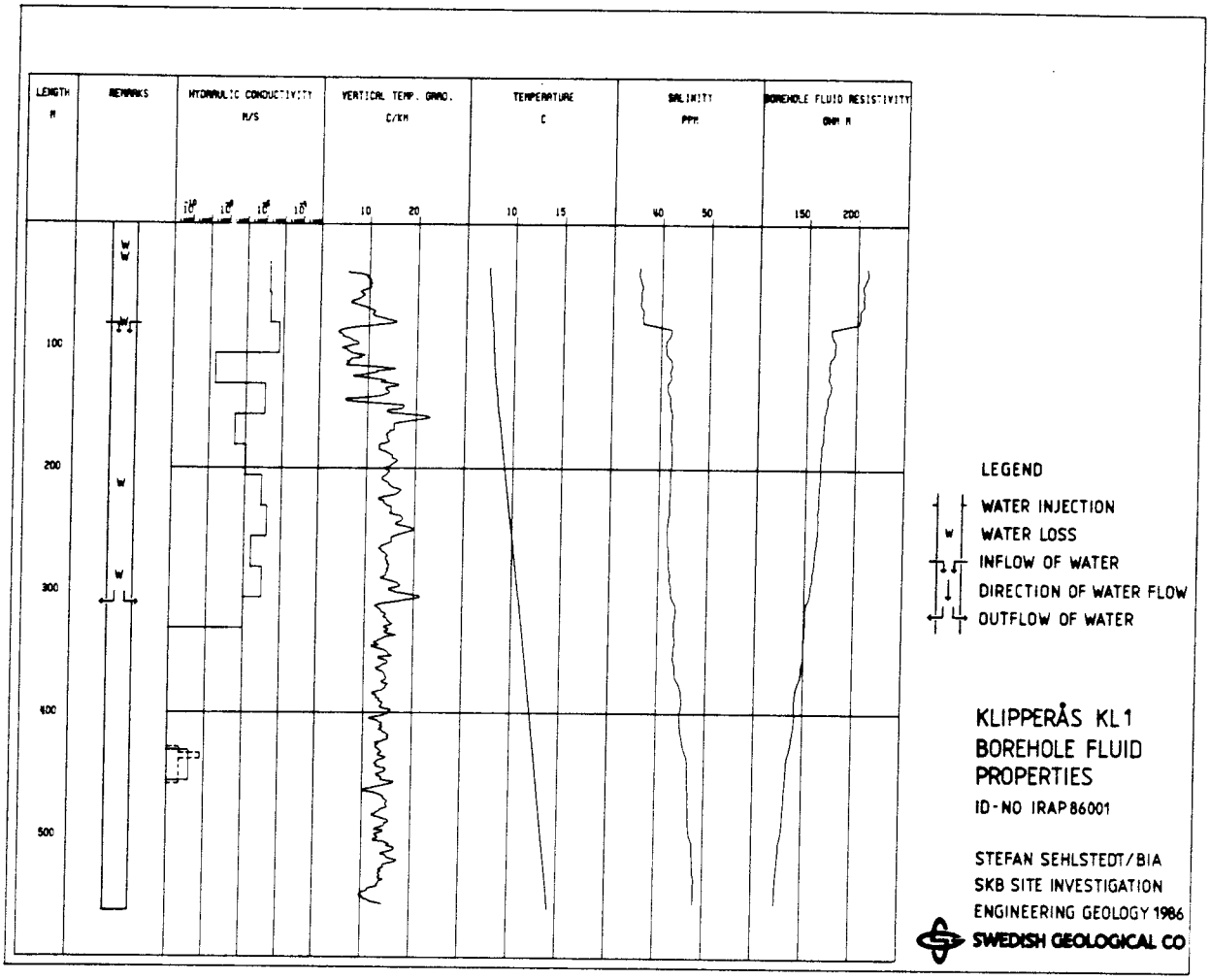

Figure A.3 Geophysical logs sensitive to borehole fluid properties, measured in borehole Kl 1.

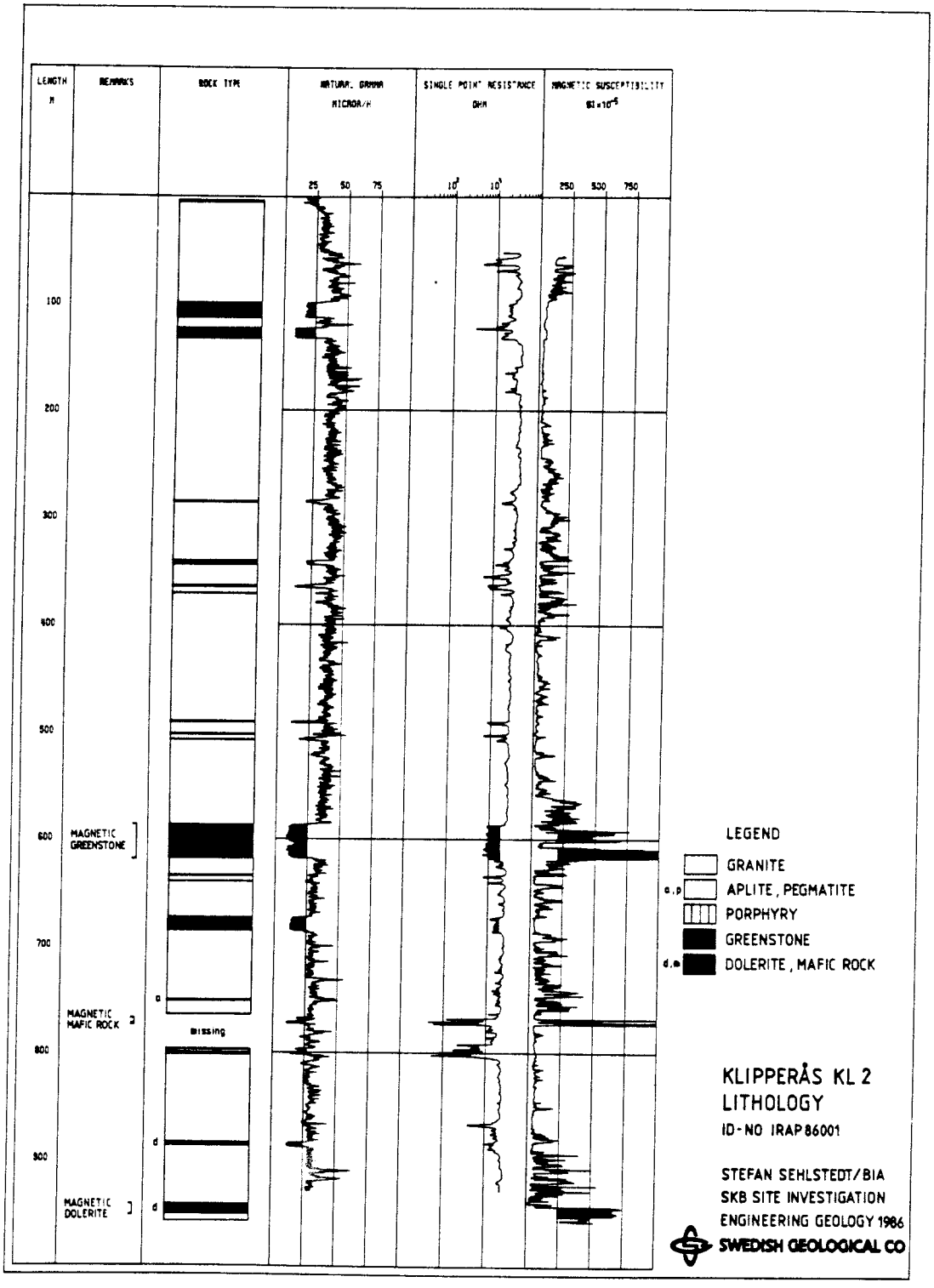

Figure A.4 Geophysical logs sensitive to lithology variations, measured in borehole Kl 2.

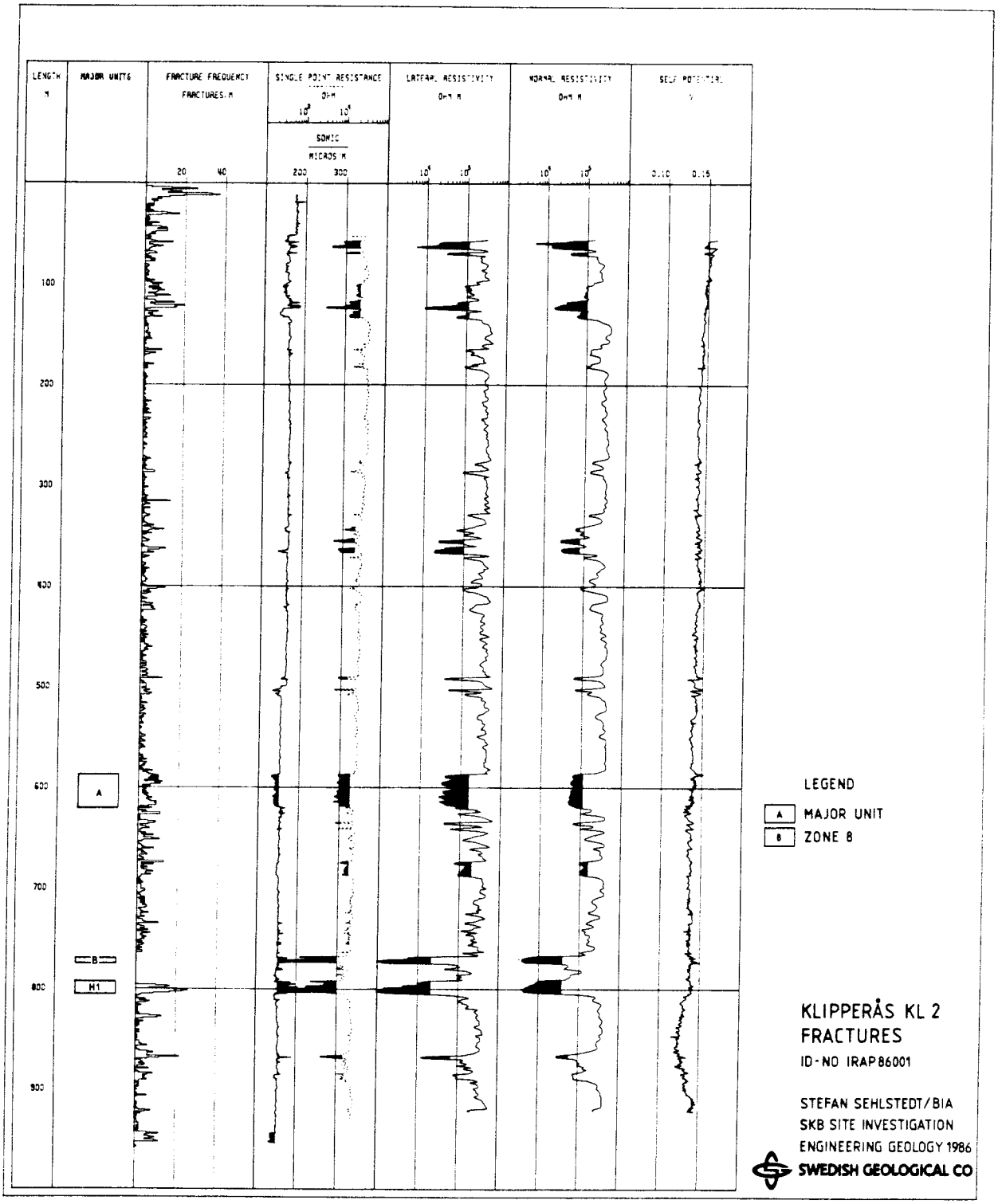

Figure A.5 Geophysical logs sensitive to fracture occurences, measured in borehole Kl 2.

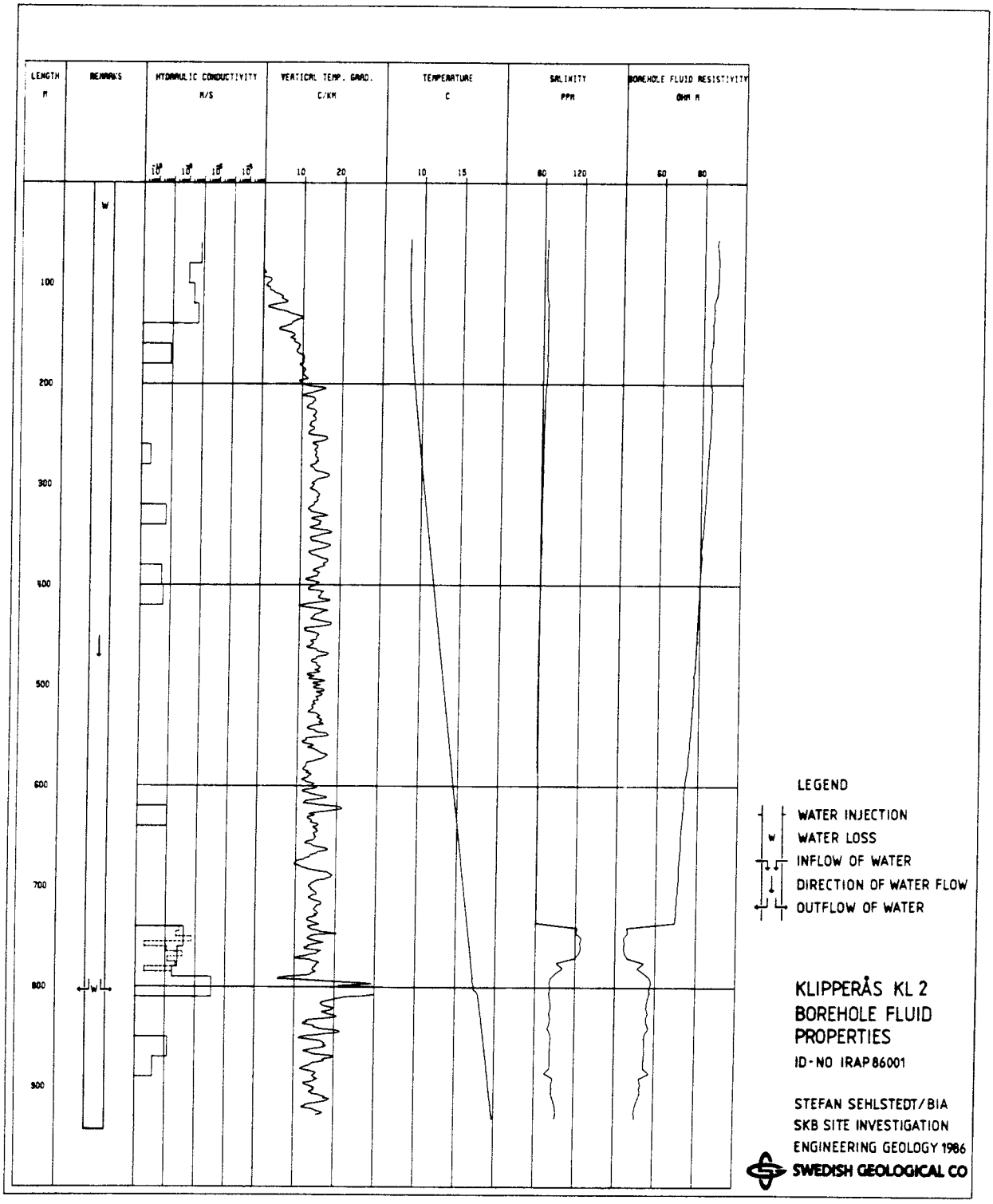

Figure A.6 Geophysical logs sensitive to borehole fluid properties, measured in borehole Kl 2.

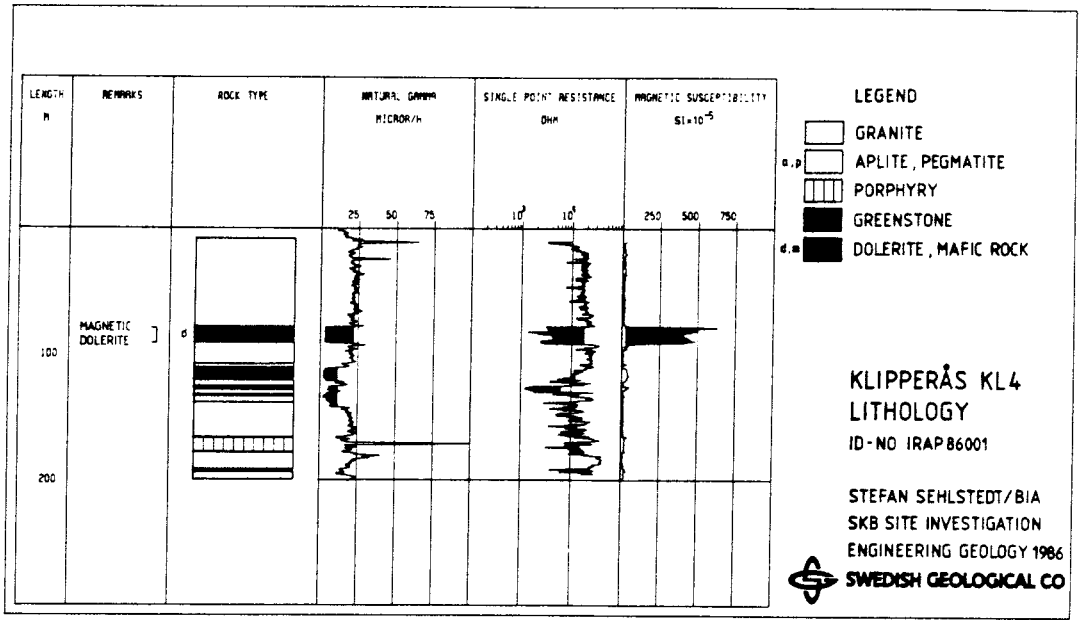

Figure A.7 Geophysical logs sensitive to lithology variations, measured in borehole Kl 4.

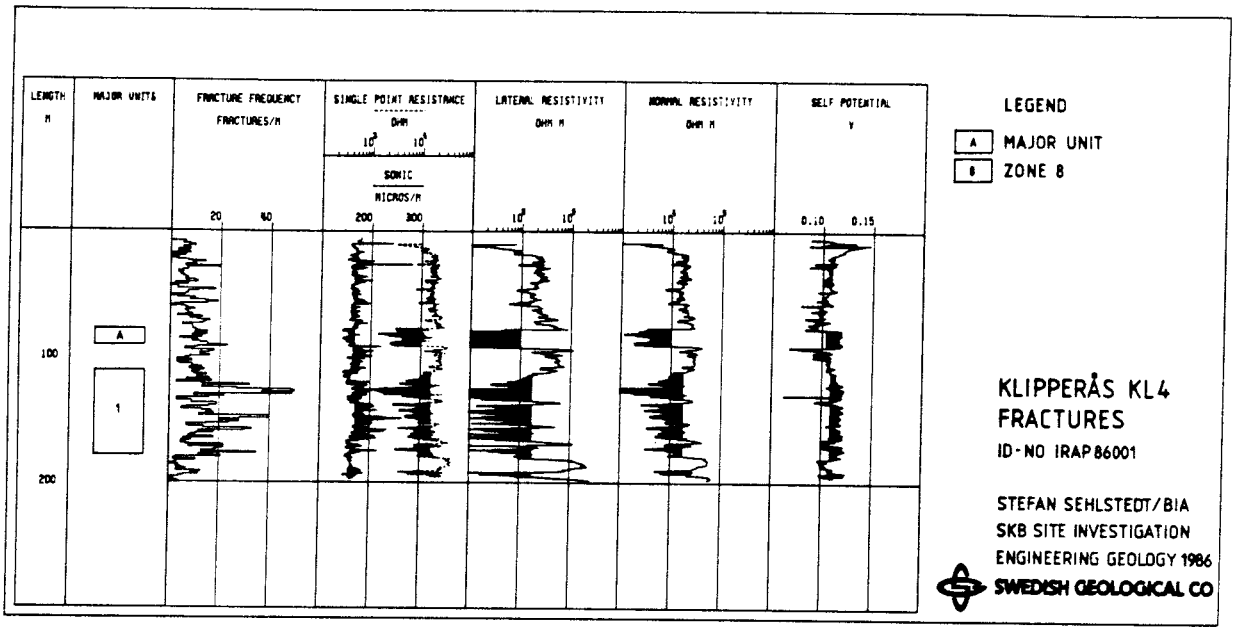

Figure A.8 Geophysical logs sensitive to fracture occurences, measured in borehole Kl 4.

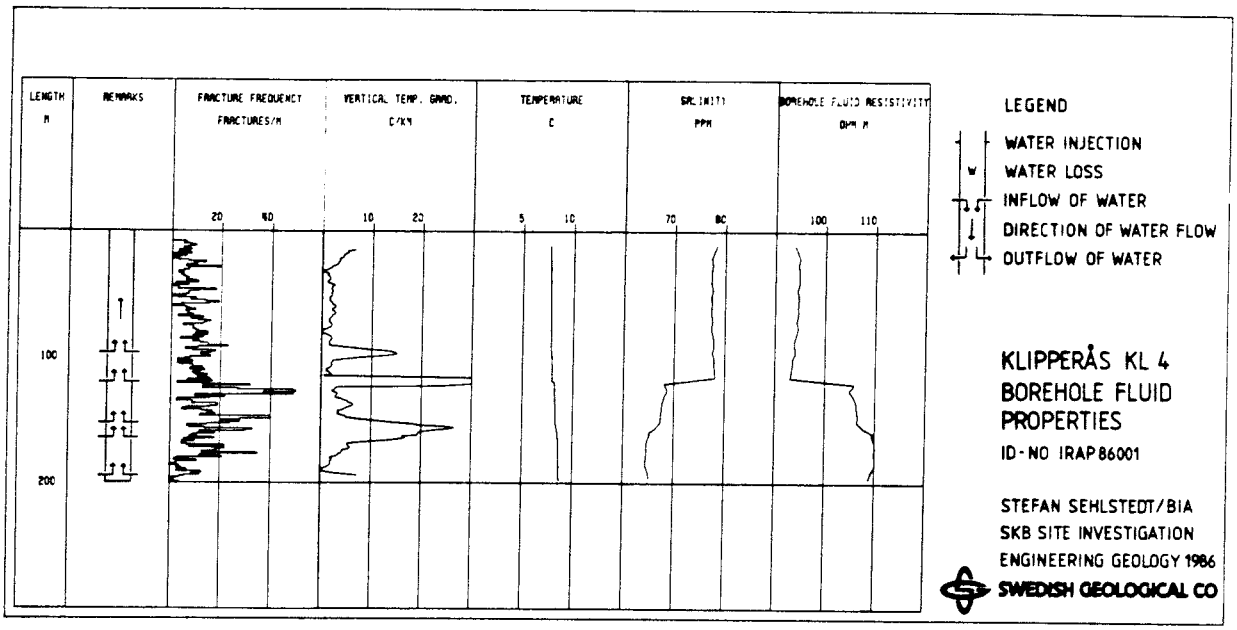

Figure A.9 Geophysical logs sensitive to borehole fluid properties, measured in borehole Kl 4.

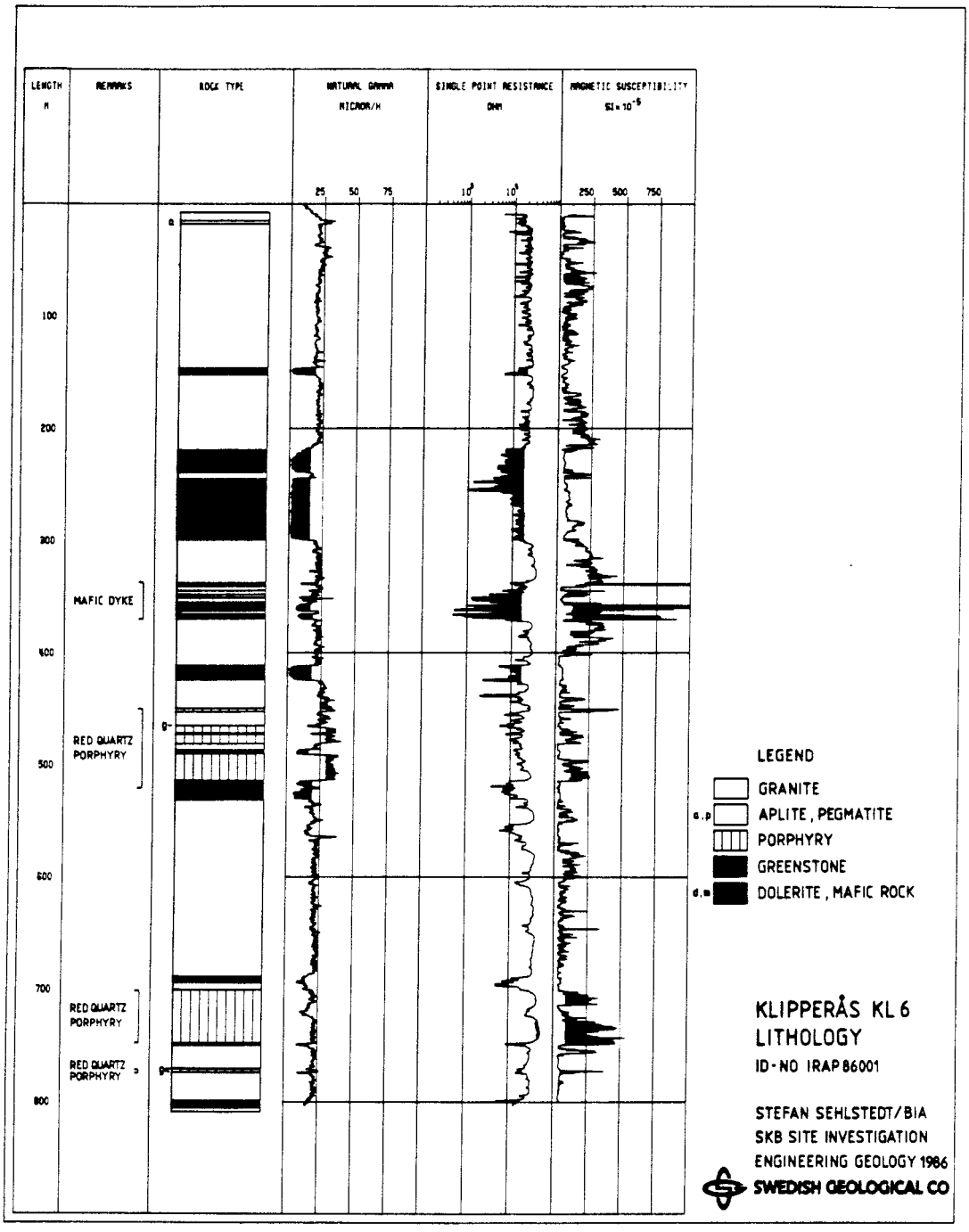

Figure A.10 Geophysical logs sensitive to lithology variations, measured in borehole Kl 6.

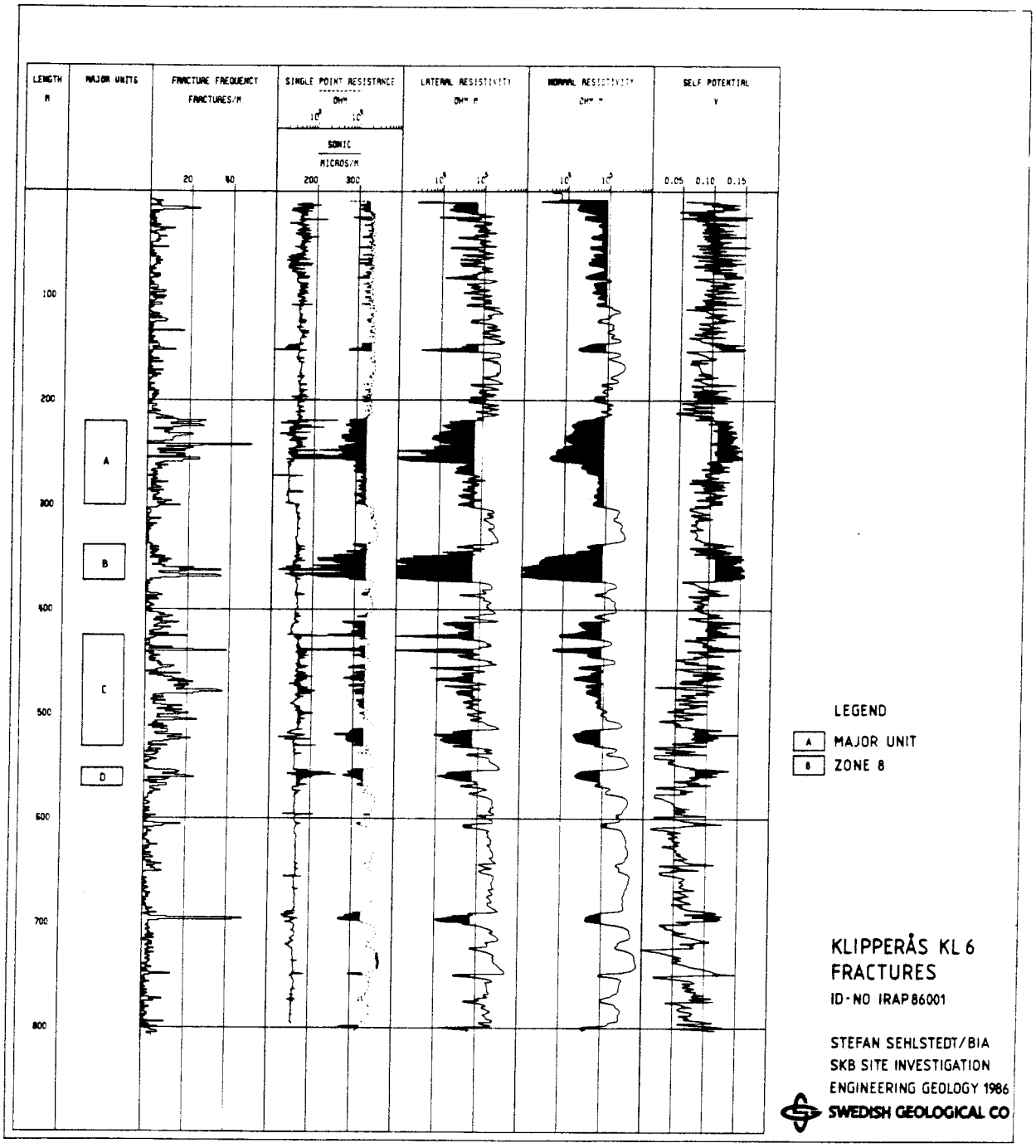

Figure A.11 Geophysical logs sensitive to fracture occurences, measured in borehole Kl 6.

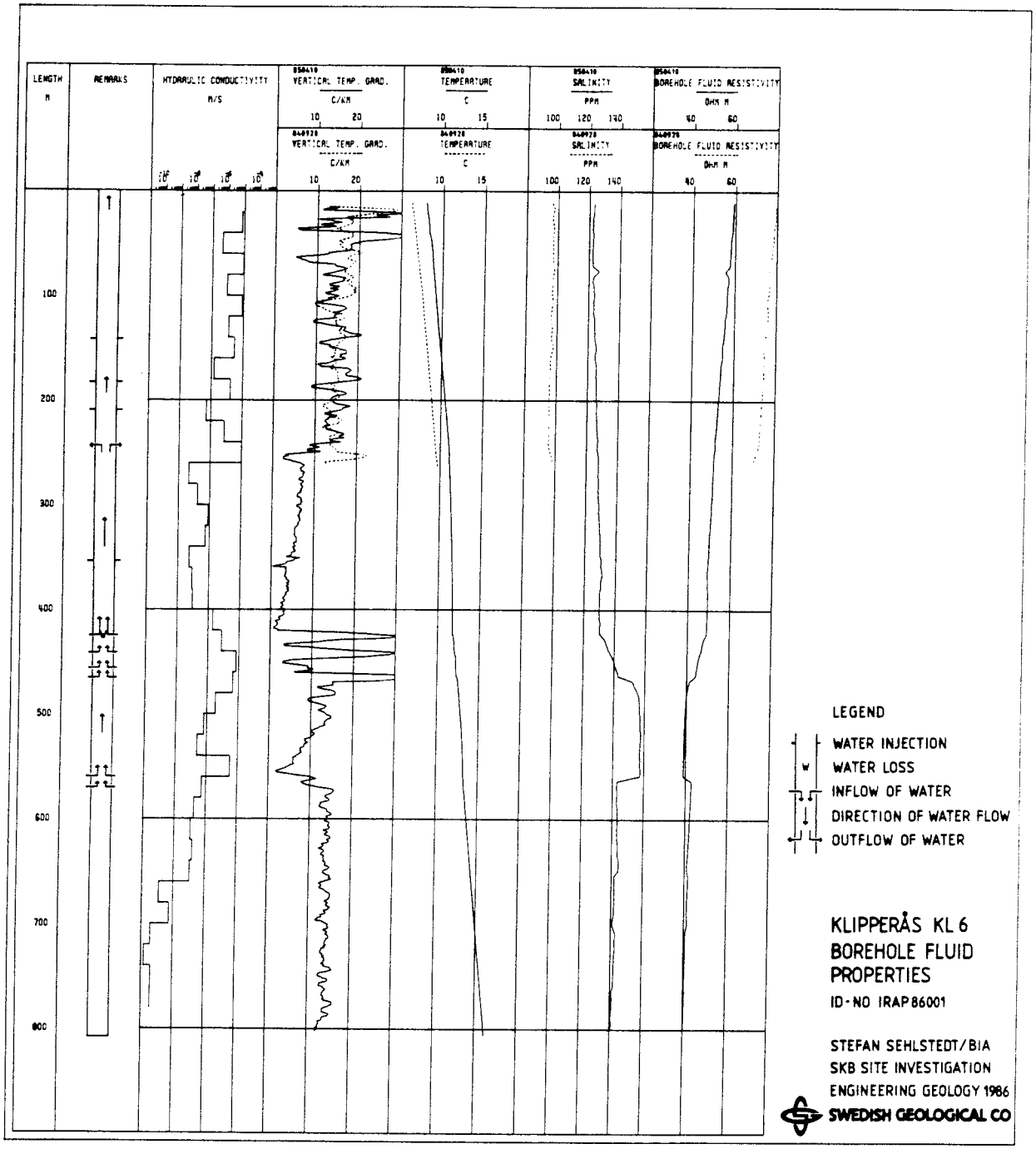

Figure A.12 Geophysical logs sensitive to borehole fluid properties, measured in borehole Kl 6.

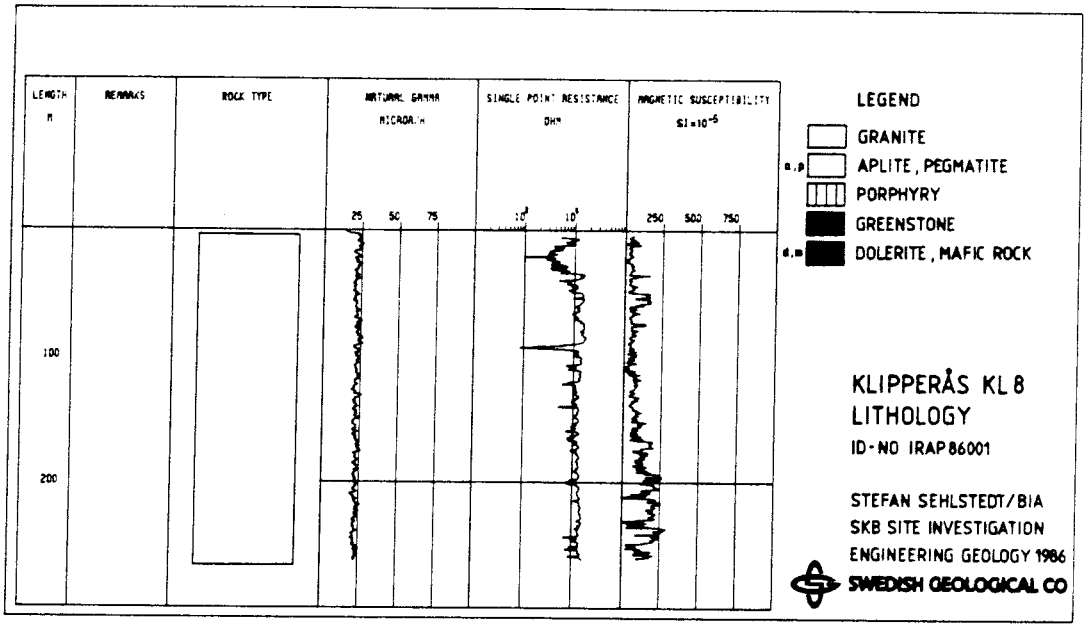

Figure A.13 Geophysical logs sensitive to lithology variations, measured in borehole Kl 8.

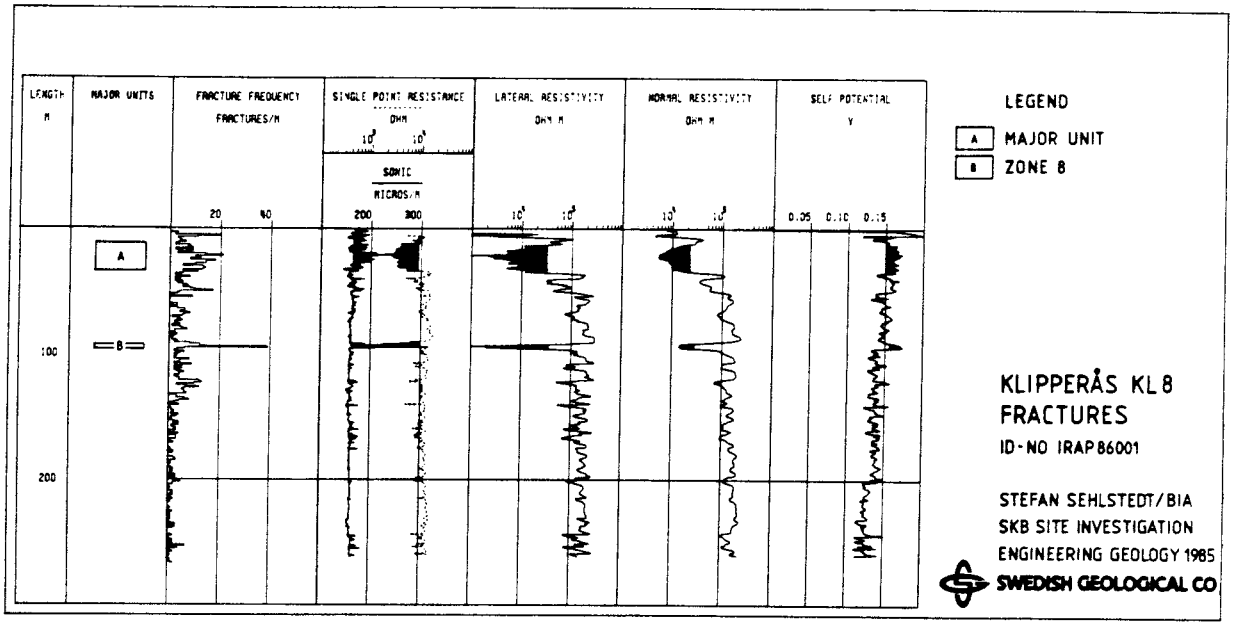

Figure A.14 Geophysical logs sensitive to fracture occurences, measured in borehole Kl 8.

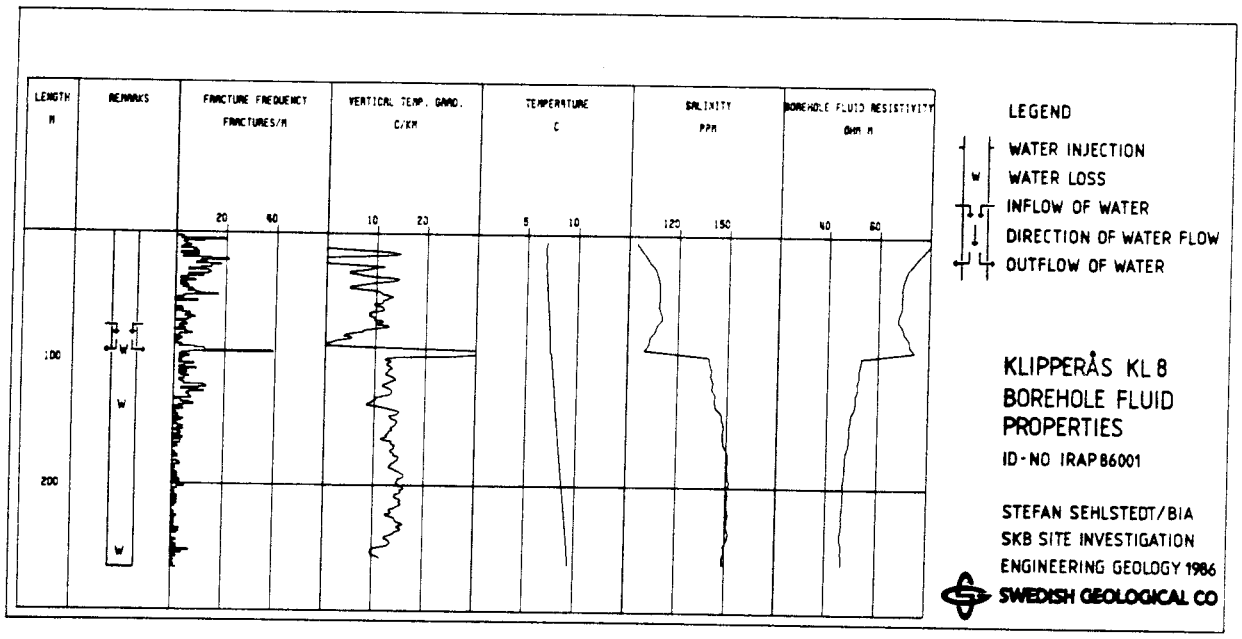

Figure A.15 Geophysical logs sensitive to borehole fluid properties, measured in borehole Kl 8.

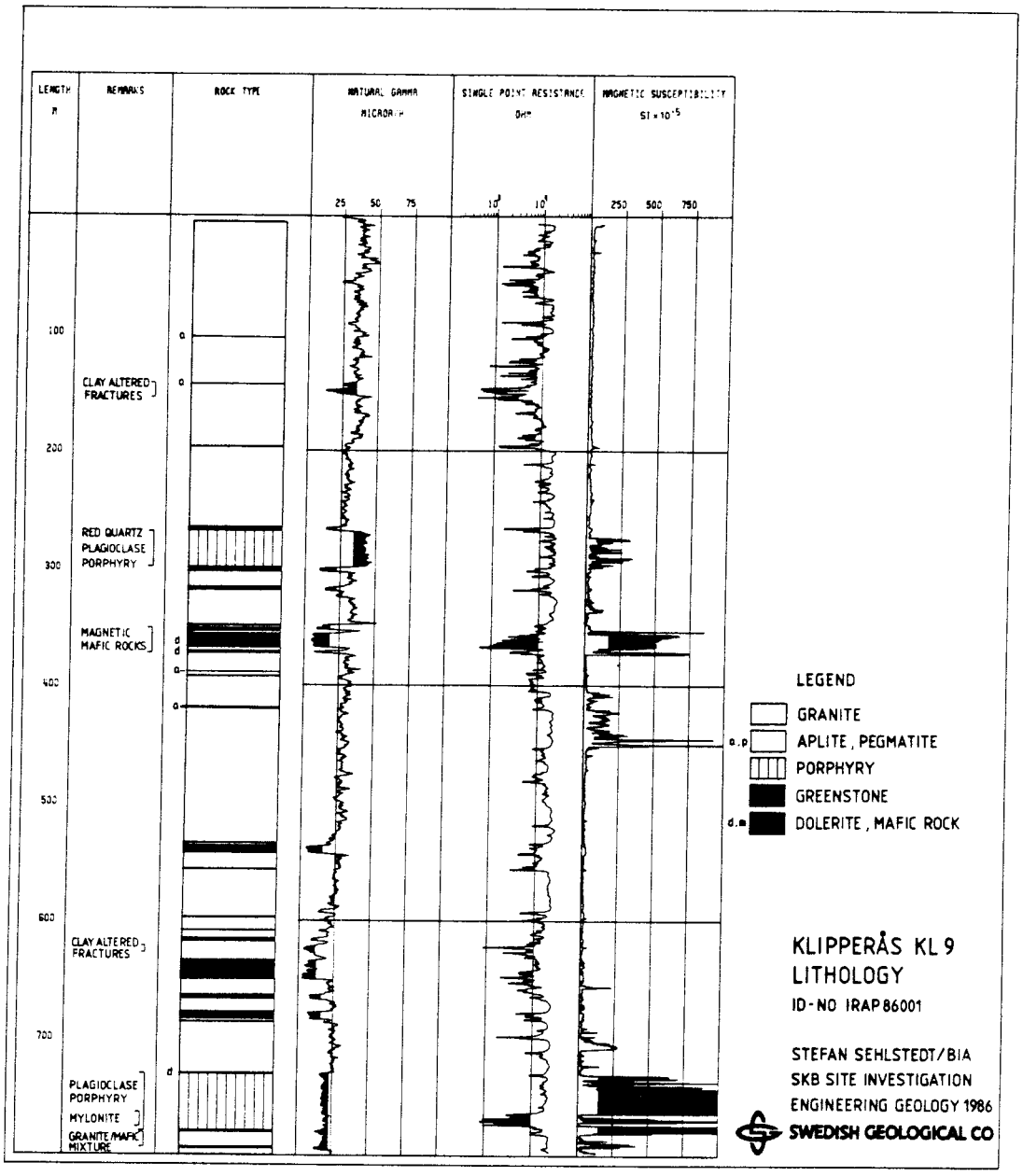

Figure A.16 Geophysical logs sensitive to lithology variations, measured in borehole Kl 9.

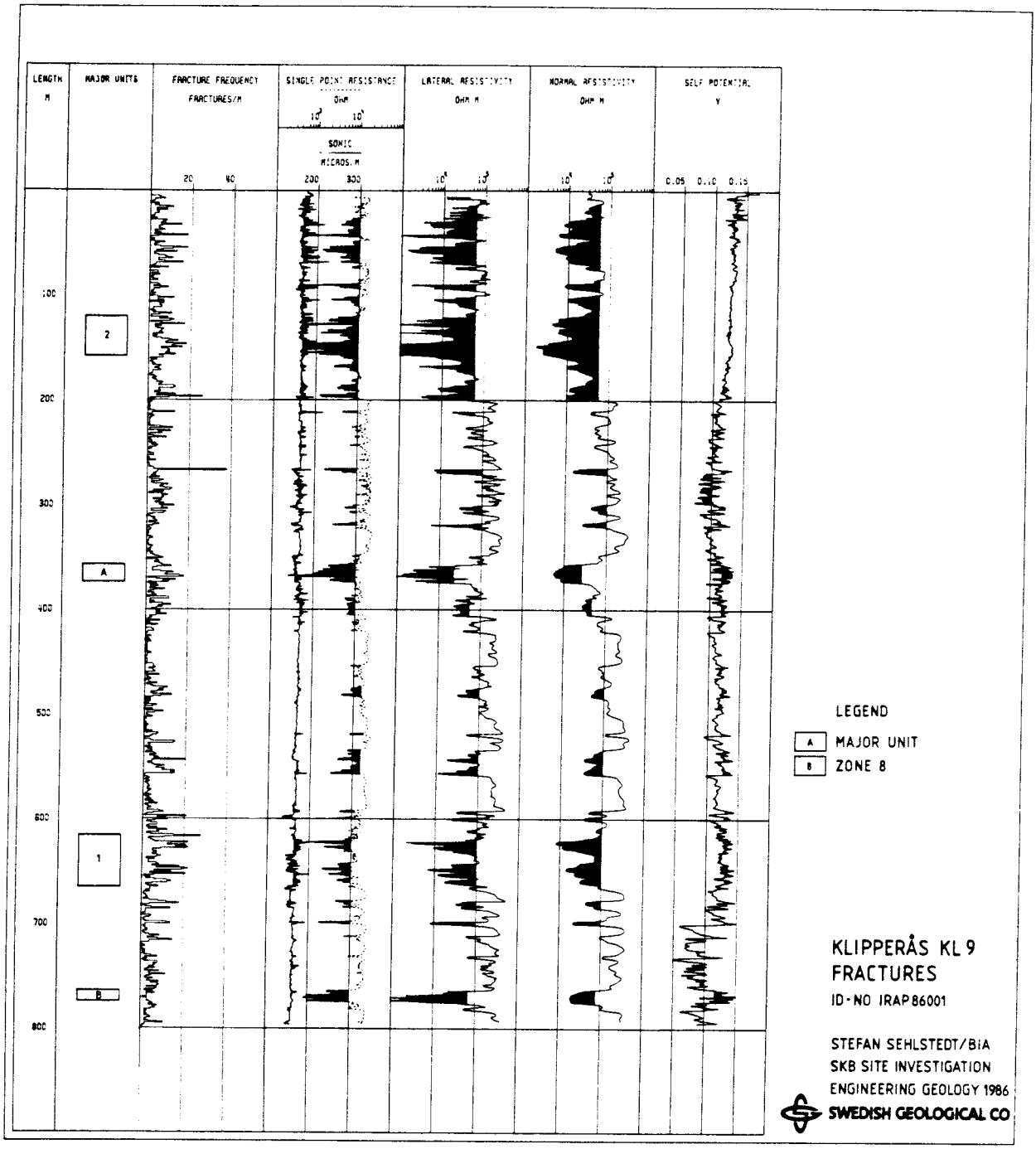

Figure A.17 Geophysical logs sensitive to fracture occurences, measured in borehole Kl 9.

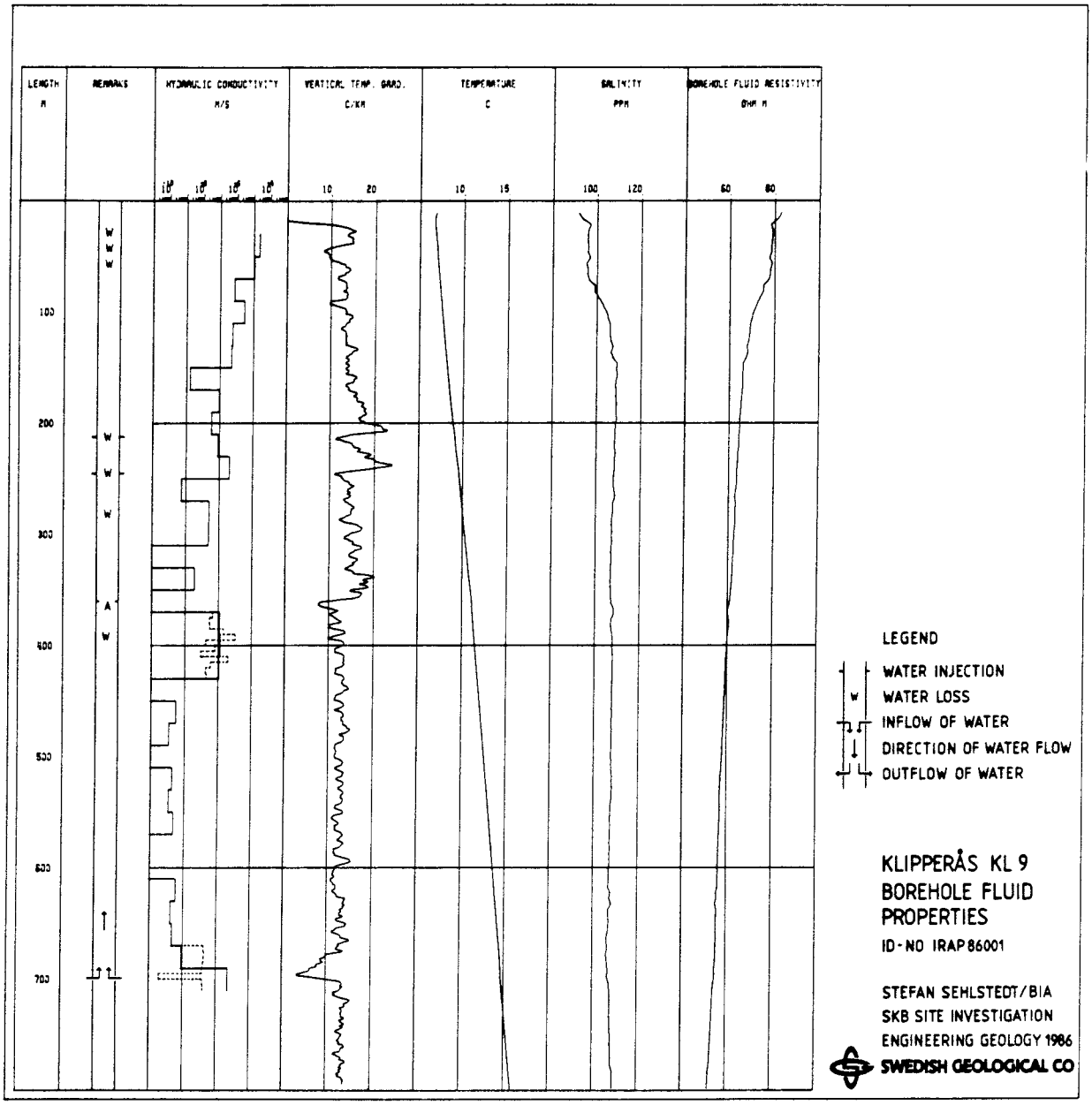

Figure A.18 Geophysical logs sensitive to borehole fluid properties, measured in borehole Kl 9.

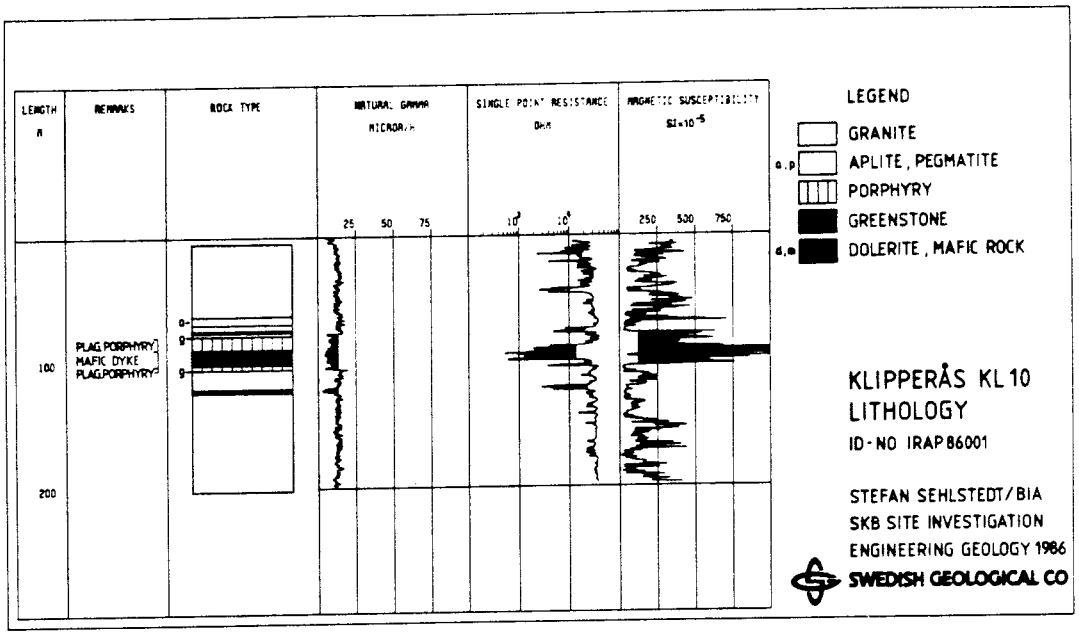

Figure A.19 Geophysical logs sensitive to lithology variations, measured in borehole Kl 10.

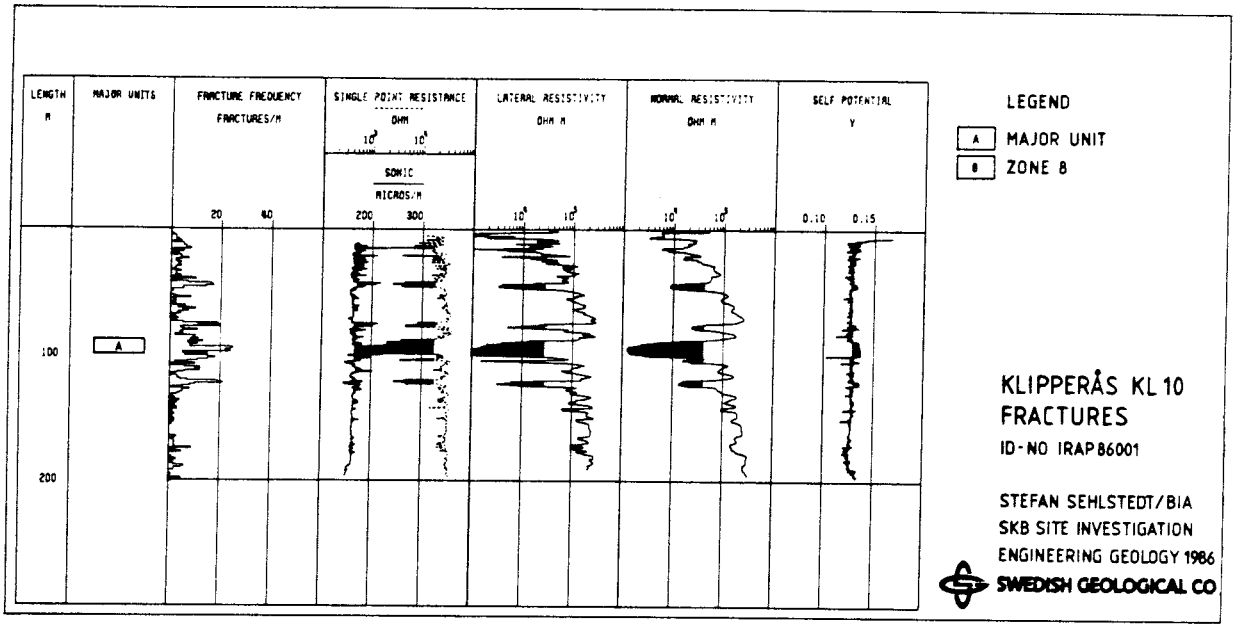

Figure A.20 Geophysical logs sensitive to fracture occurences, measured in borehole Kl 10.

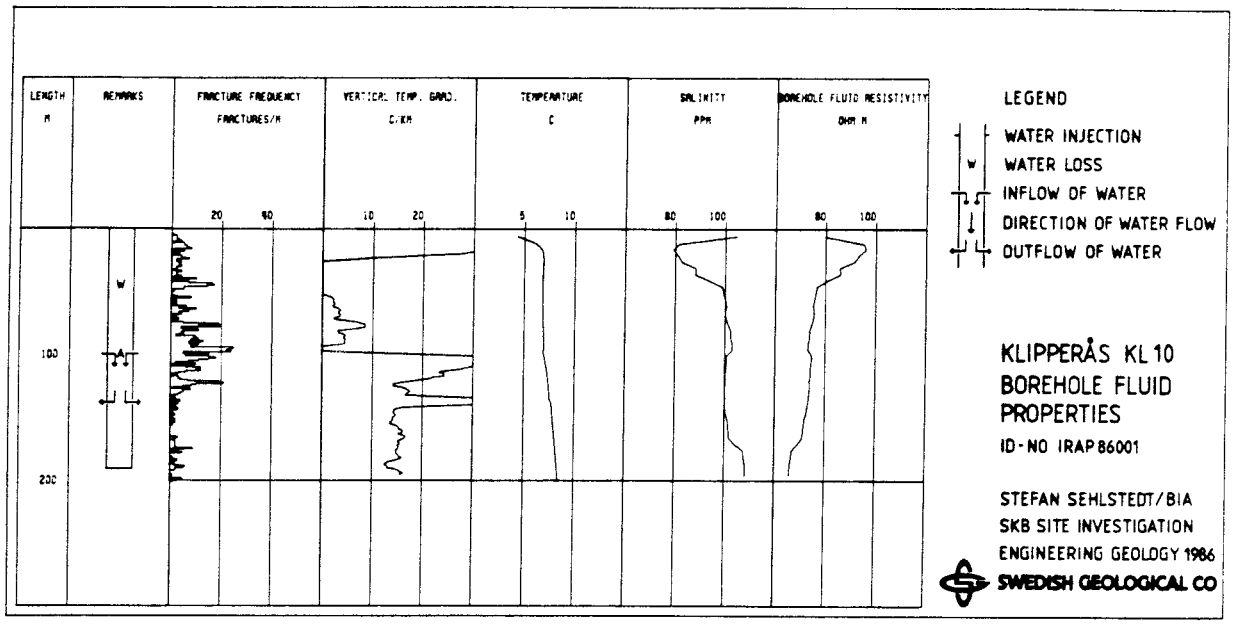

Figure A.21 Geophysical logs sensitive to borehole fluid properties, measured in borehole Kl 10.

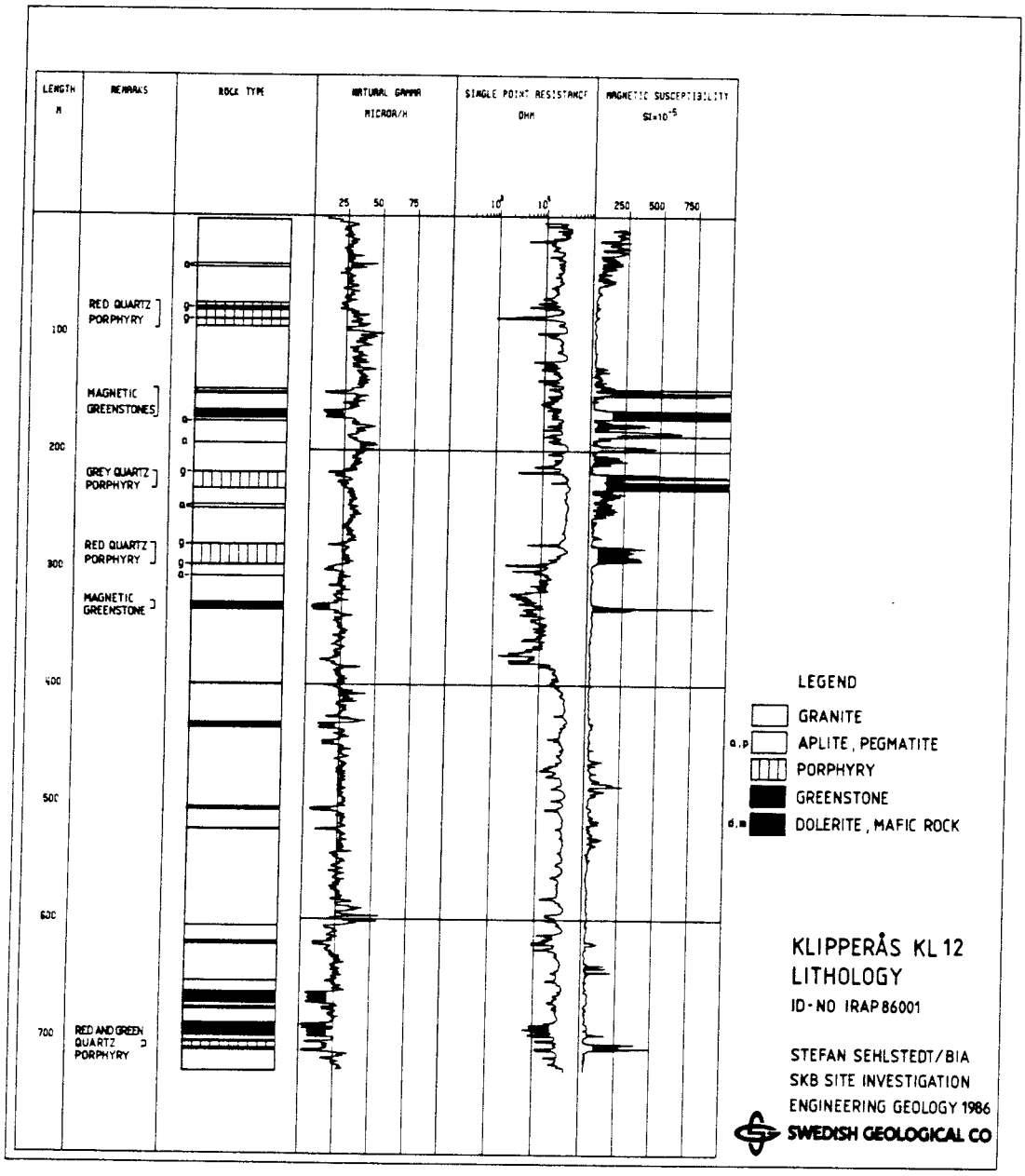

Figure A.22 Geophysical logs sensitive to lithology variations, measured in borehole Kl 12.

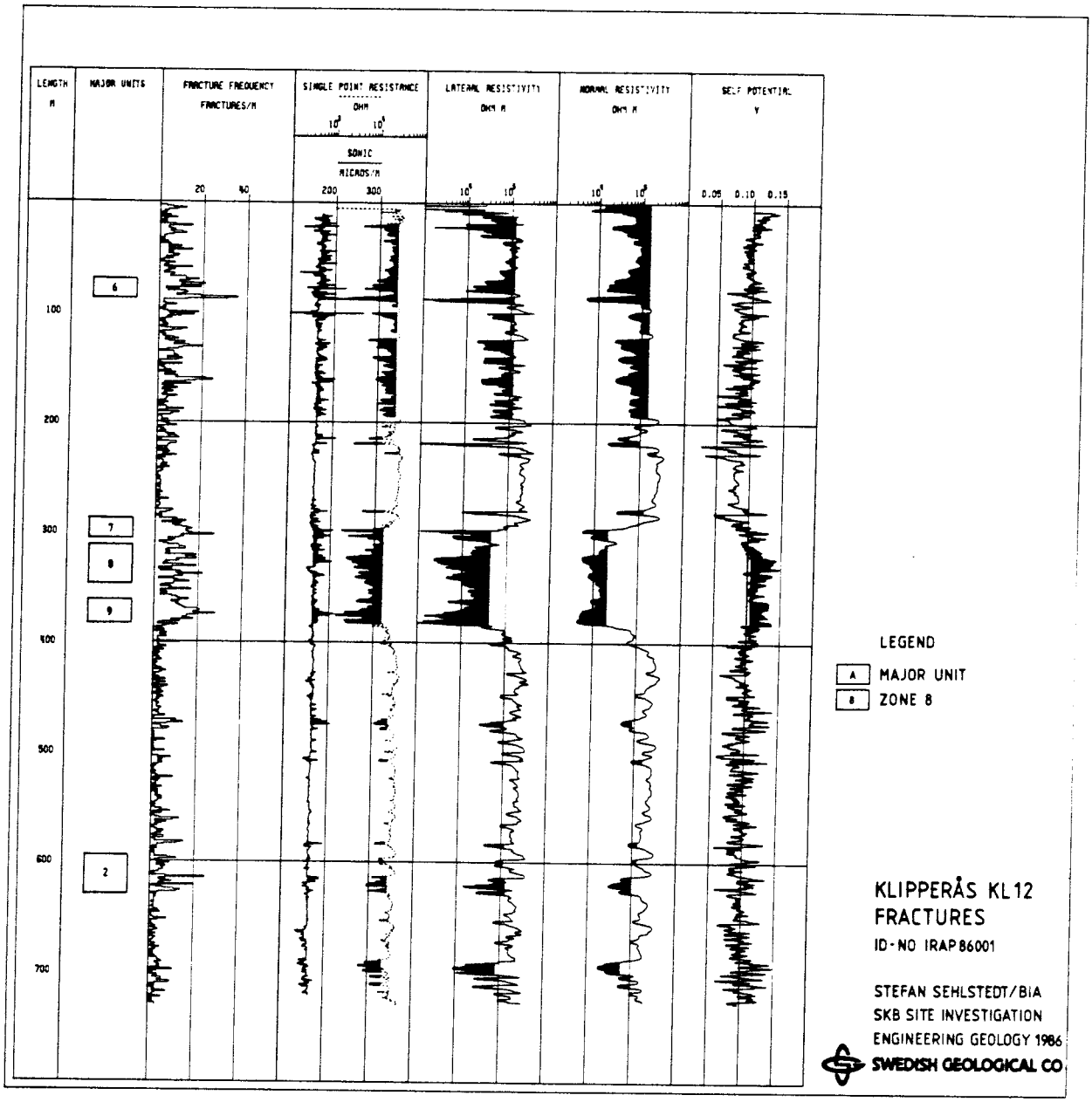

Figure A.23 Geophysical logs sensitive to fracture occurences, measured in borehole Kl 12.

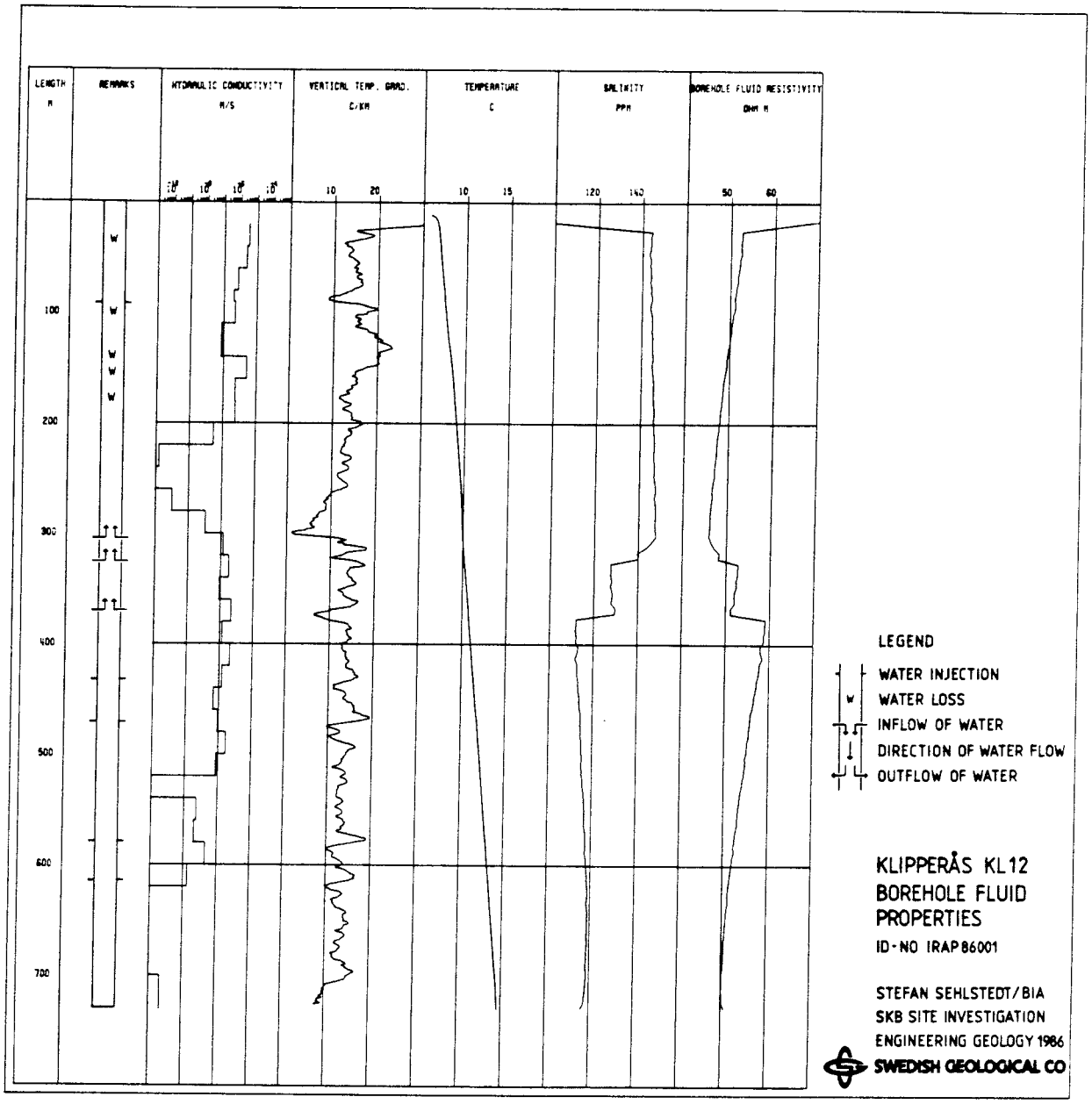

Figure A.24 Geophysical logs sensitive to borehole fluid properties, measured in borehole Kl 12.

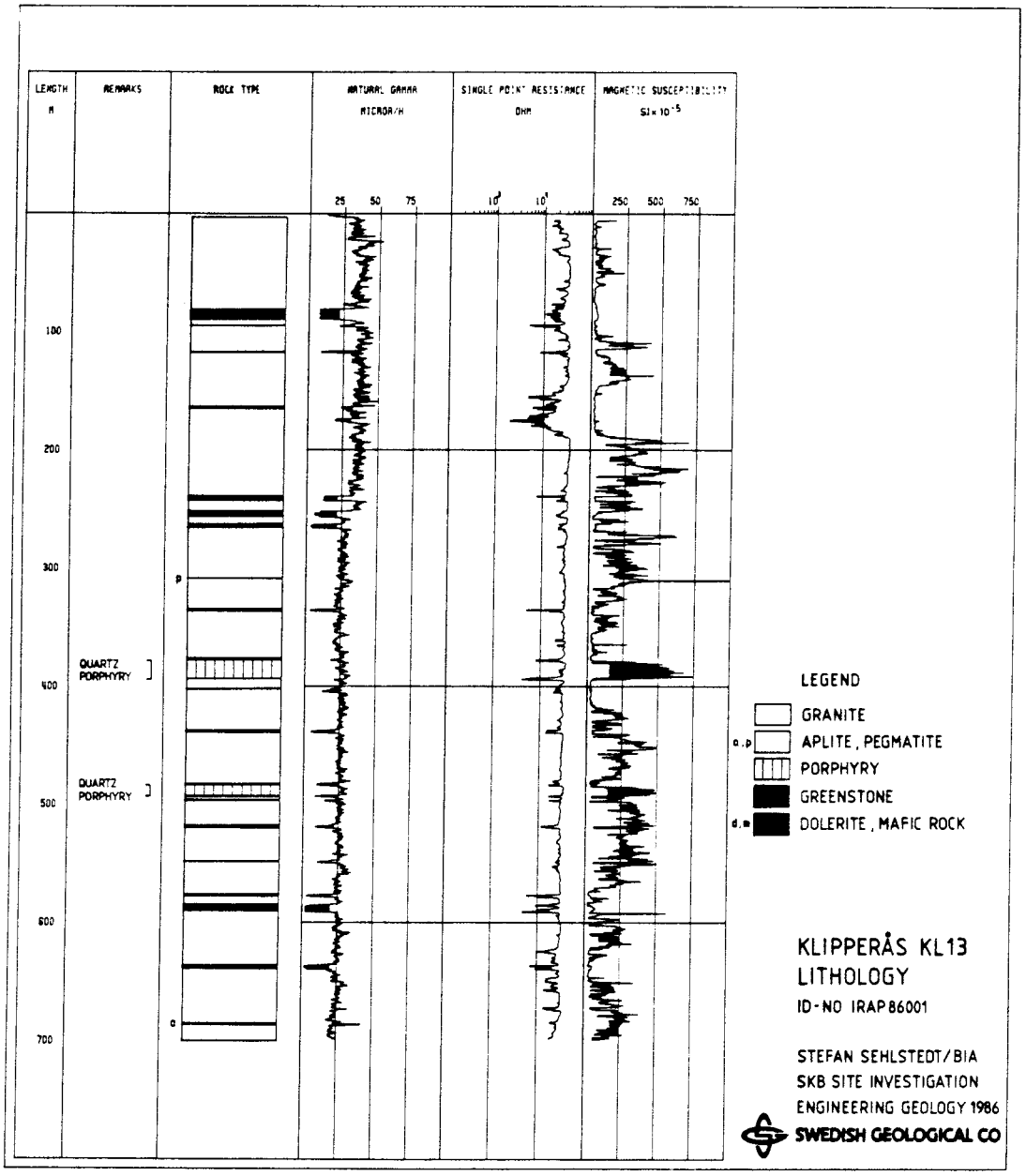

Figure A.25 Geophysical logs sensitive to lithology variations, measured in borehole Kl 13.

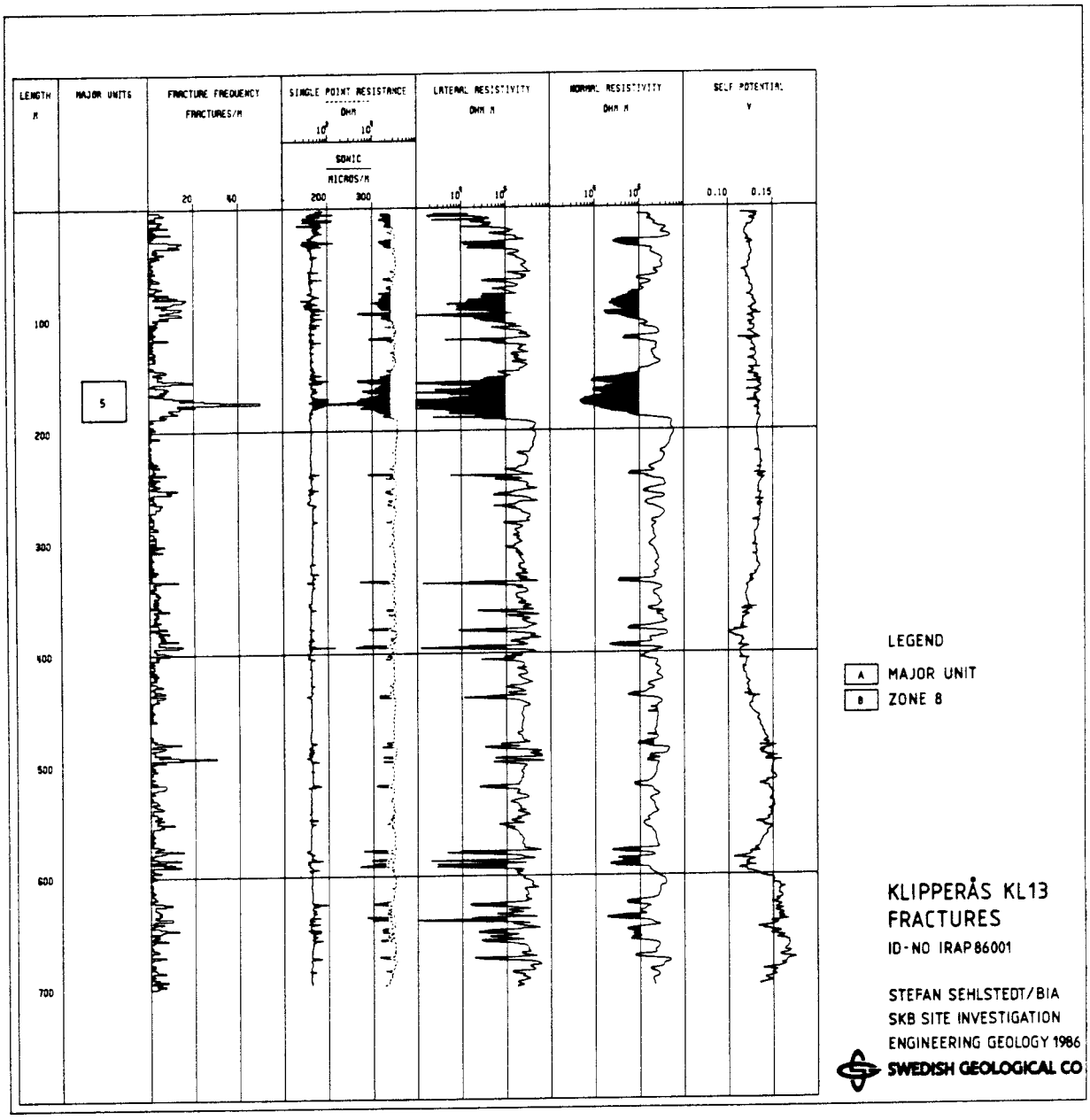

Figure A.26 Geophysical logs sensitive to fracture occurences, measured in borehole Kl 13.

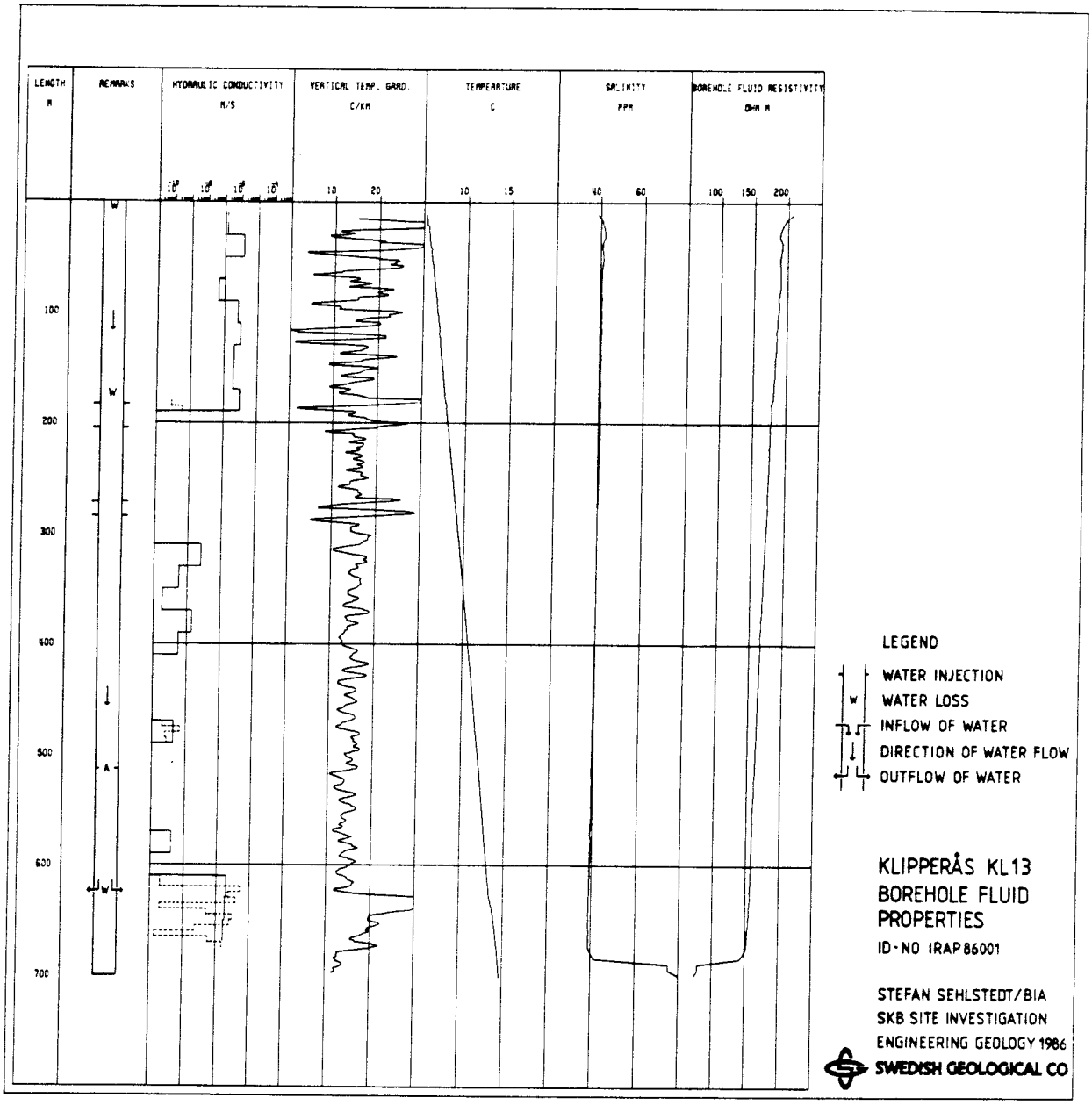

Figure A.27 Geophysical logs sensitive to borehole fluid properties, measured in borehole Kl 13.

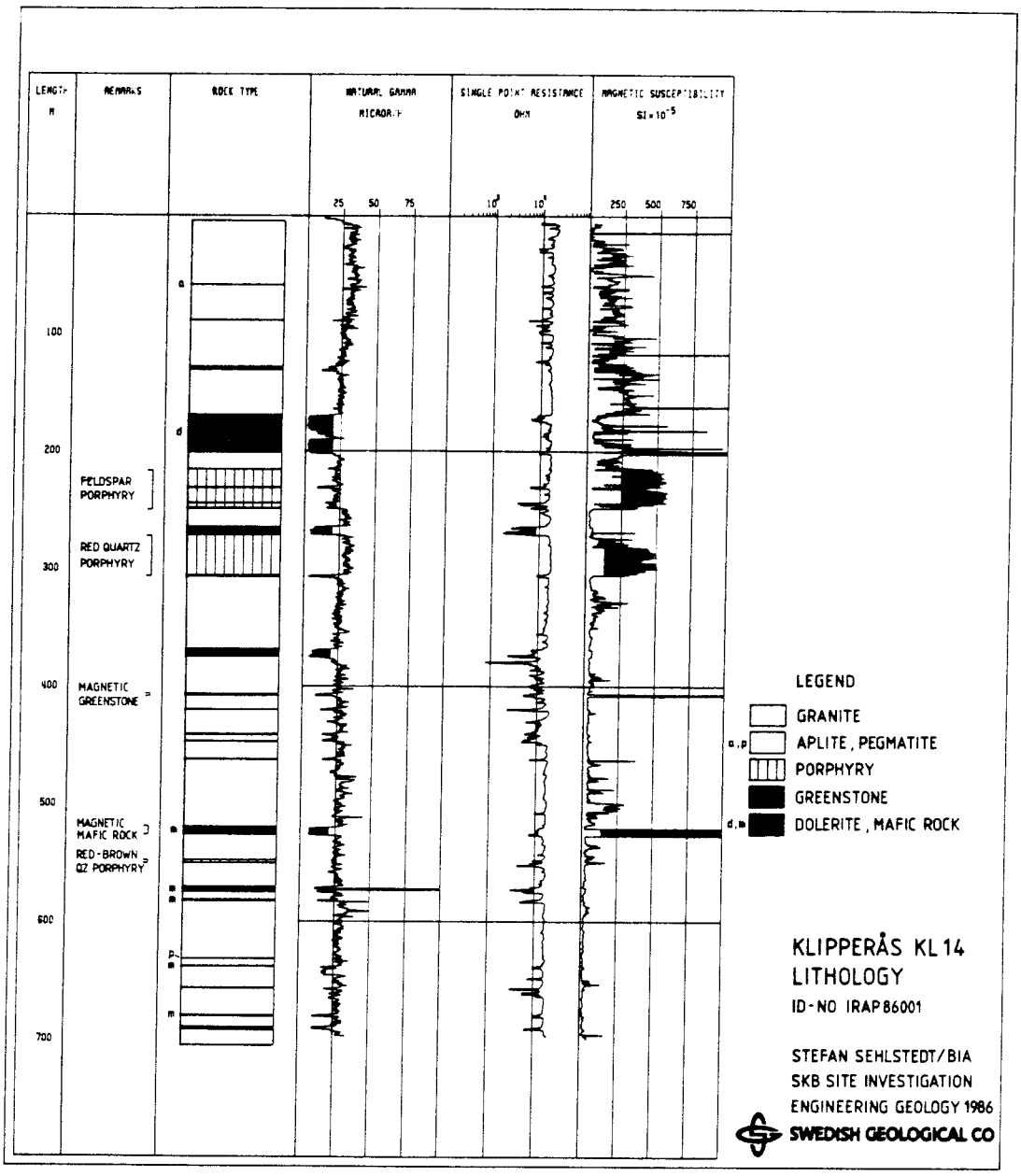

Figure A.28 Geophysical logs sensitive to lithology variations, measured in borehole Kl 14.

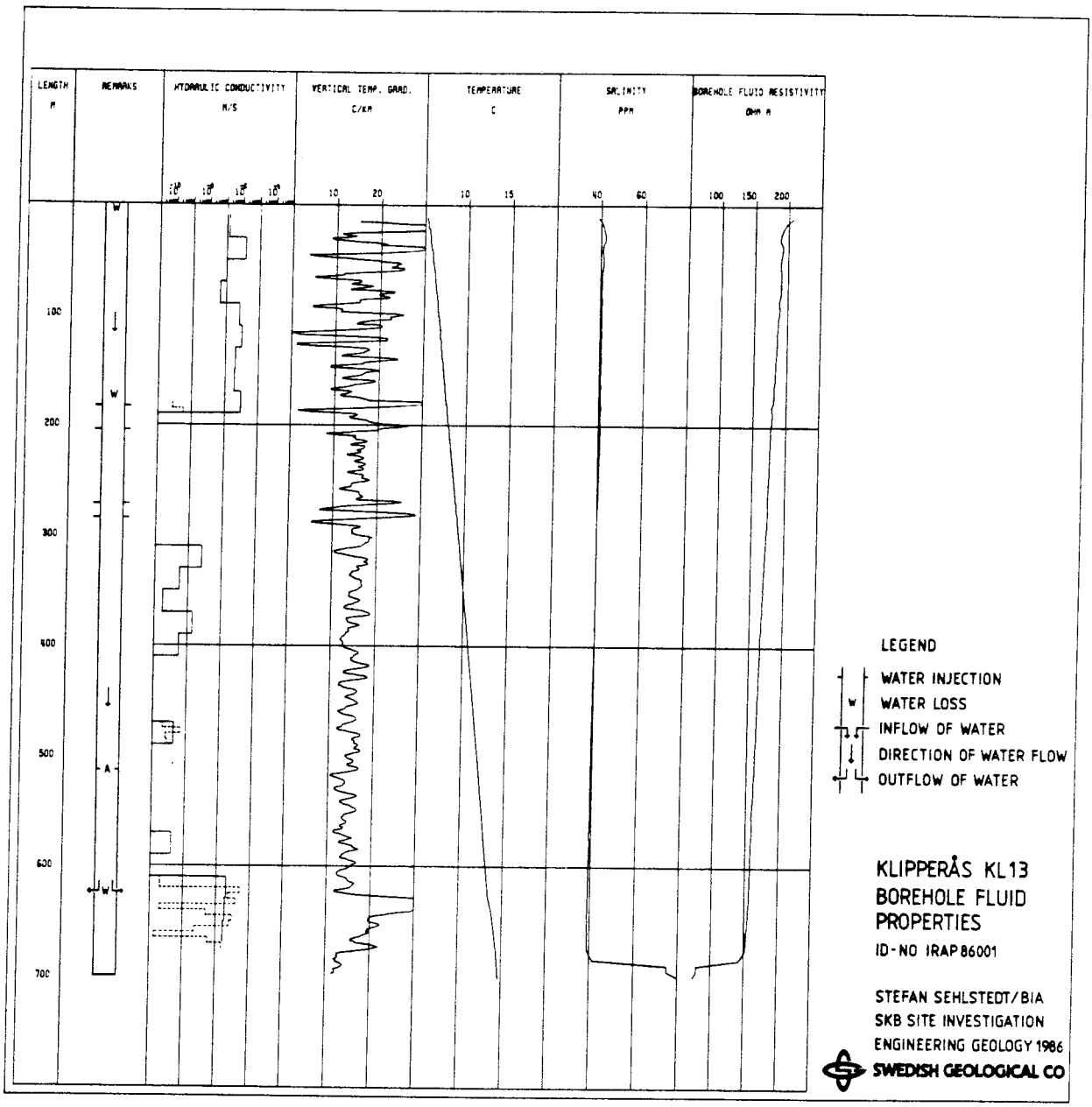

Figure A.27 Geophysical logs sensitive to borehole fluid properties, measured in borehole Kl 13.

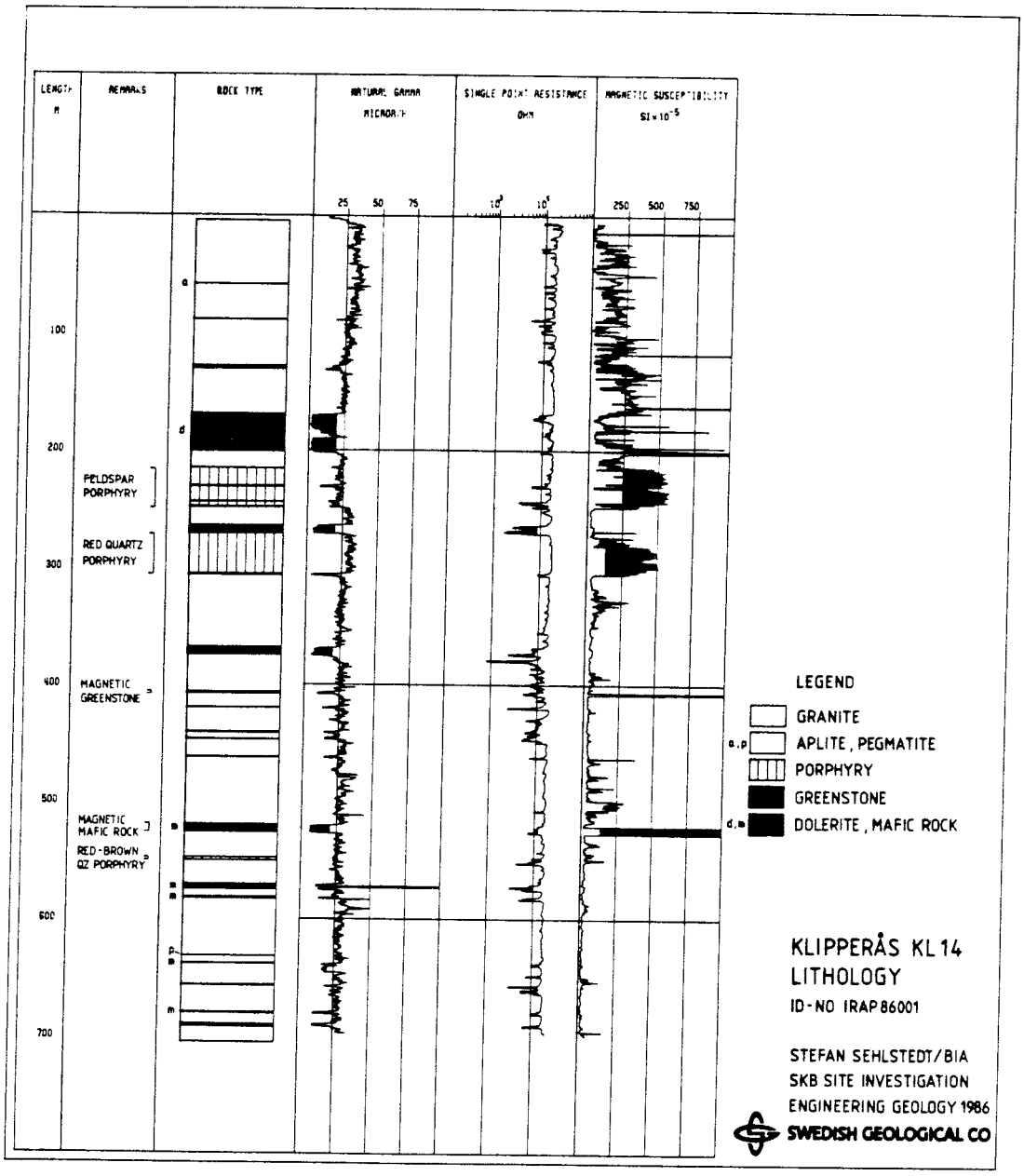

Figure A.28 Geophysical logs sensitive to lithology variations, measured in borehole Kl 14.

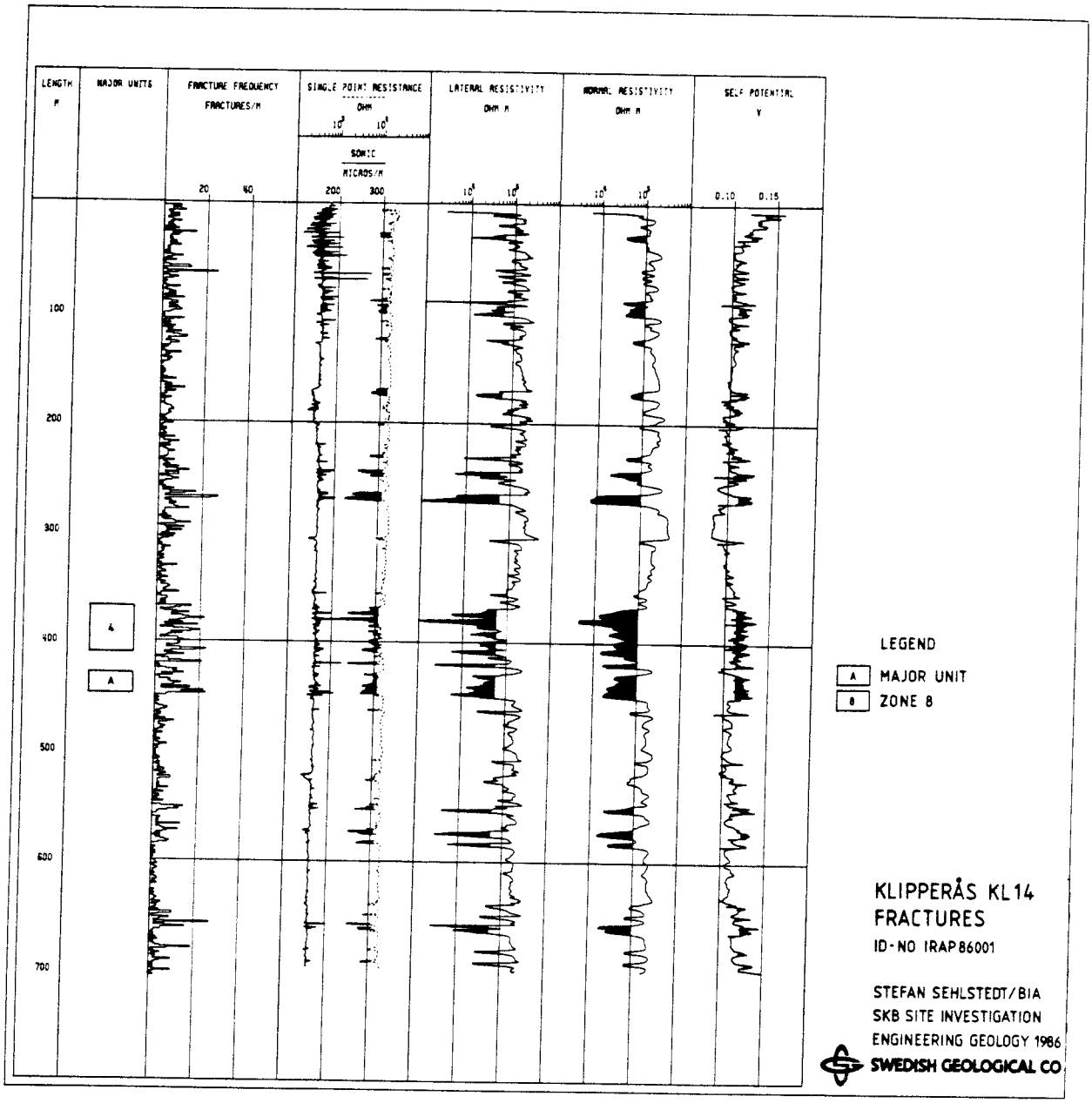

Figure A.29 Geophysical logs sensitive to fracture occurences, measured in borehole Kl 14.

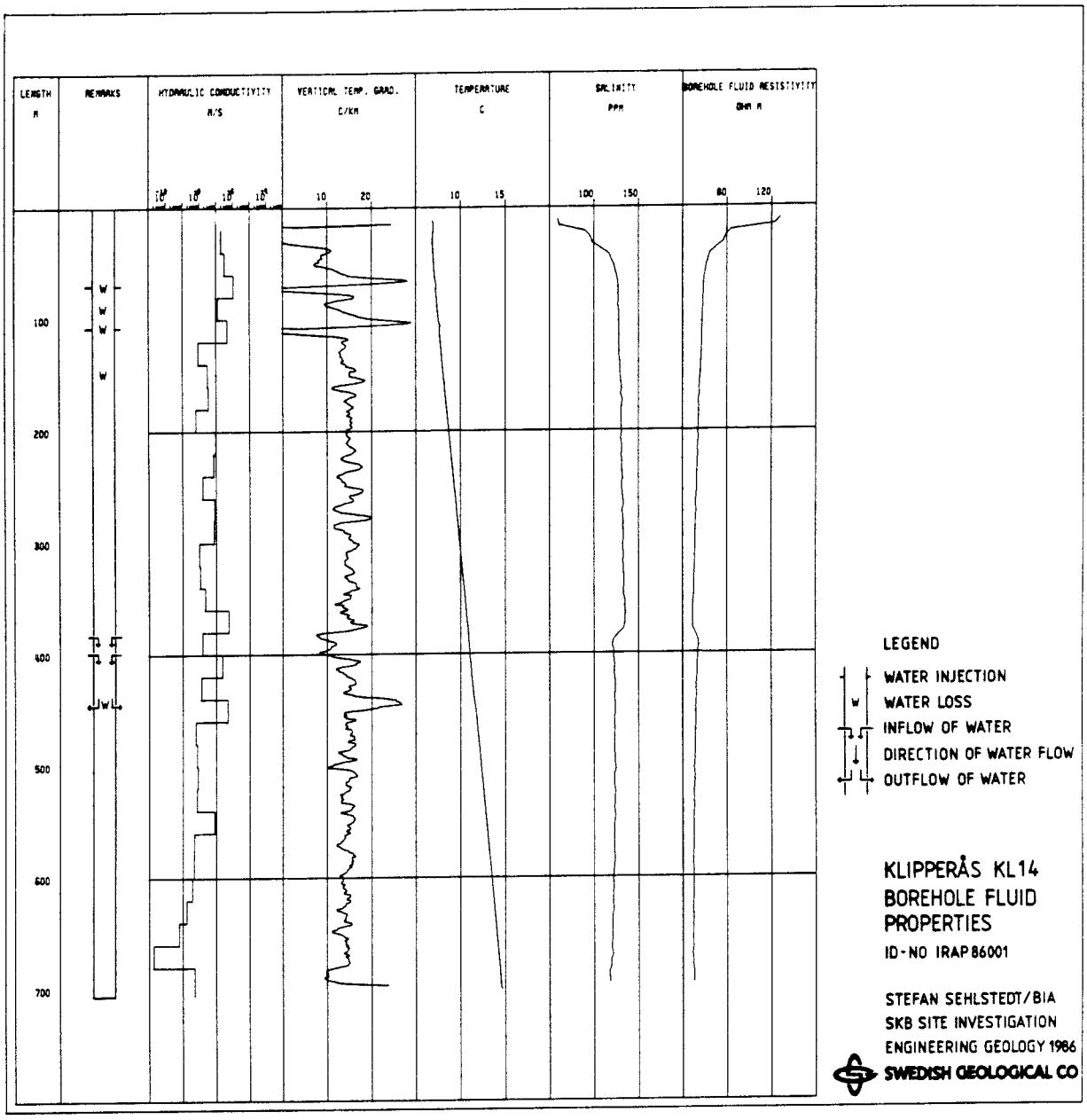

Figure A.30 Geophysical logs sensitive to borehole fluid properties, measured in borehole Kl 14.

APPENDIX B

Radar maps from the investigated boreholes.

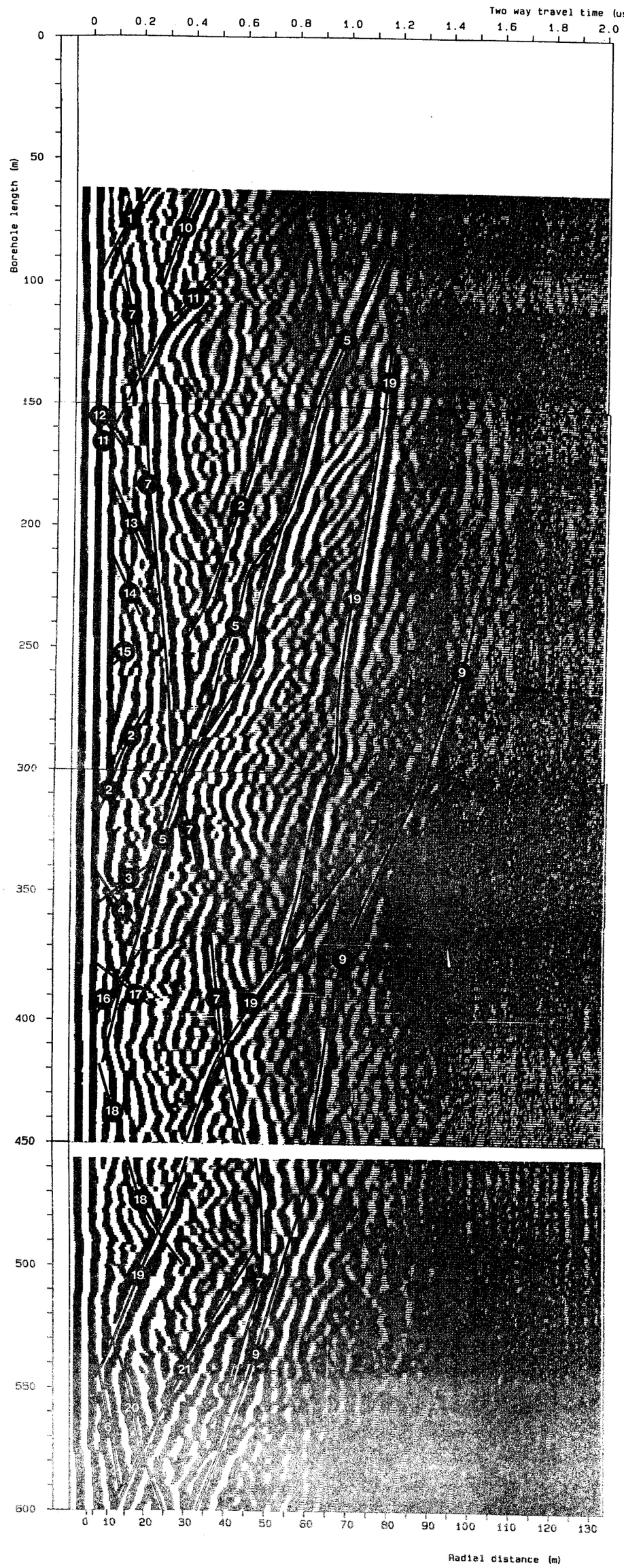

Figure B.3 Radar map for borehole Kl 2, 22 MHz (Part I).

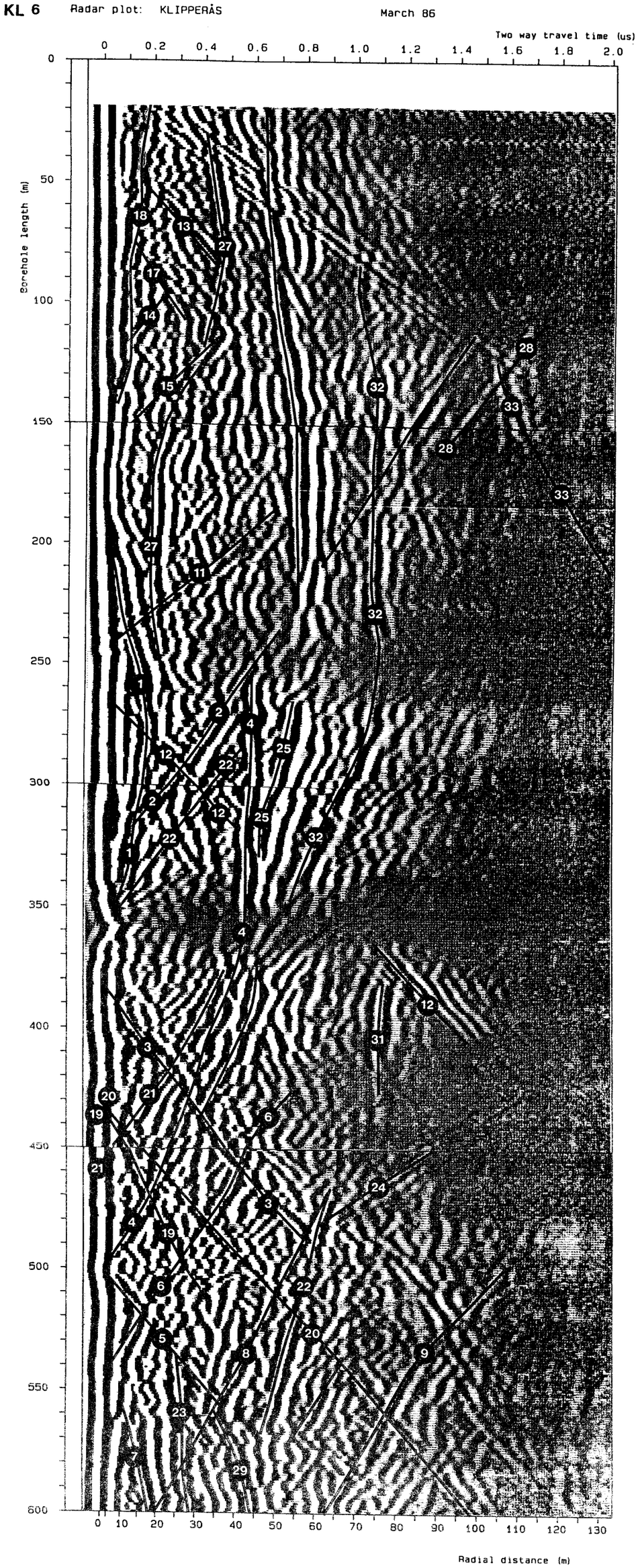

Figure B.9 Radar map for borehole Kl 6, 22 MHz (Part I).

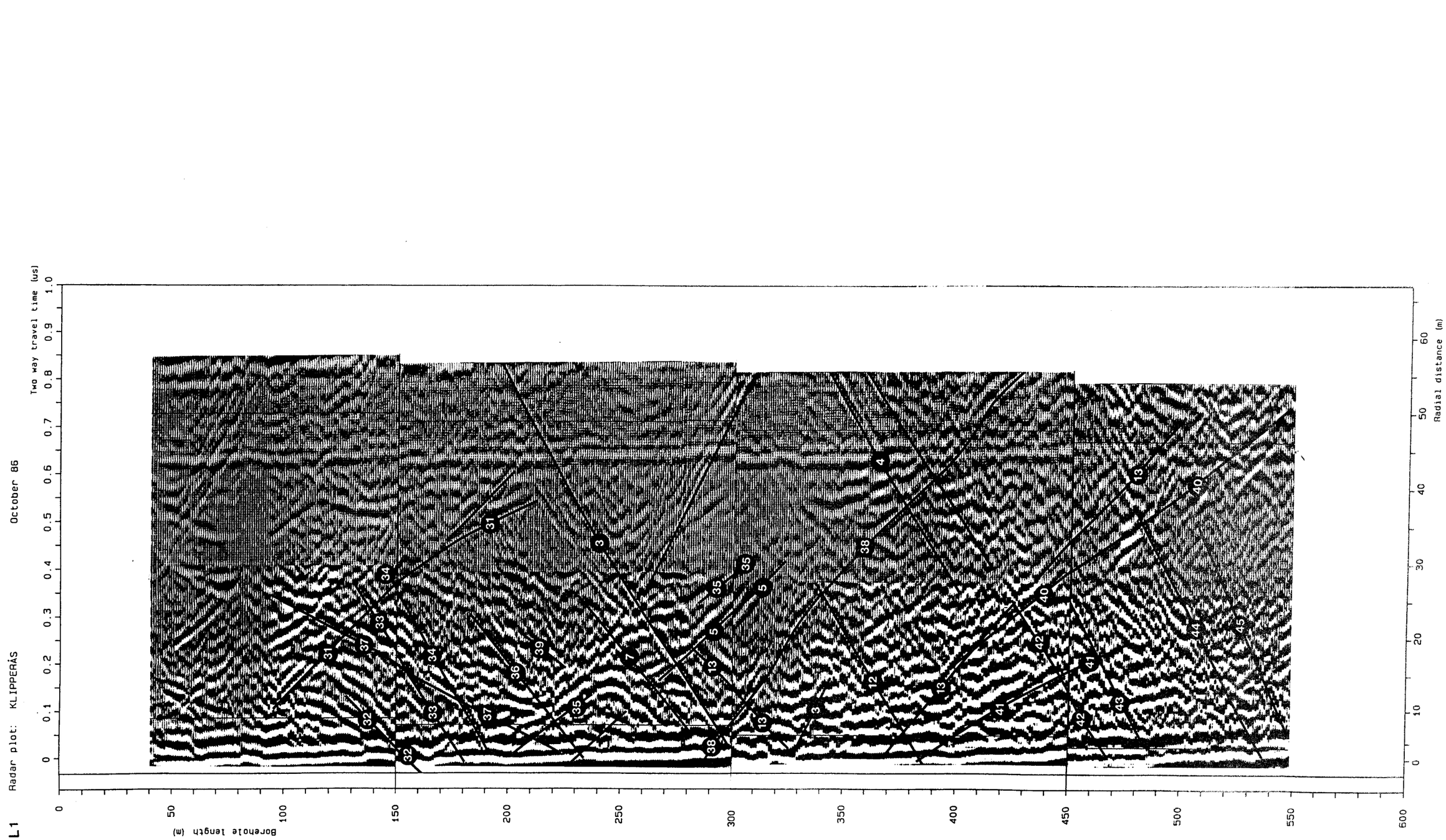

Figure B.2 Radar map for borehole Kl 1, 60 MHz.

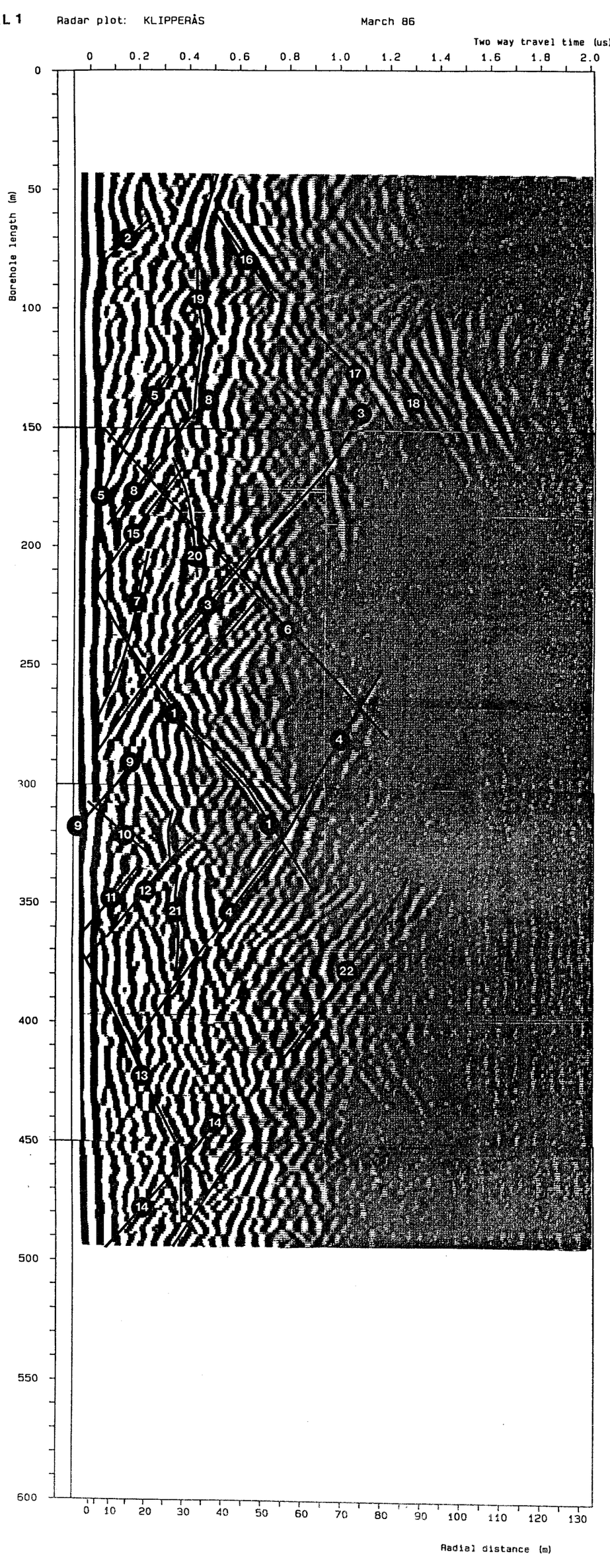

Figure B.1 Radar map for borehole Kl 1, 22 MHz.

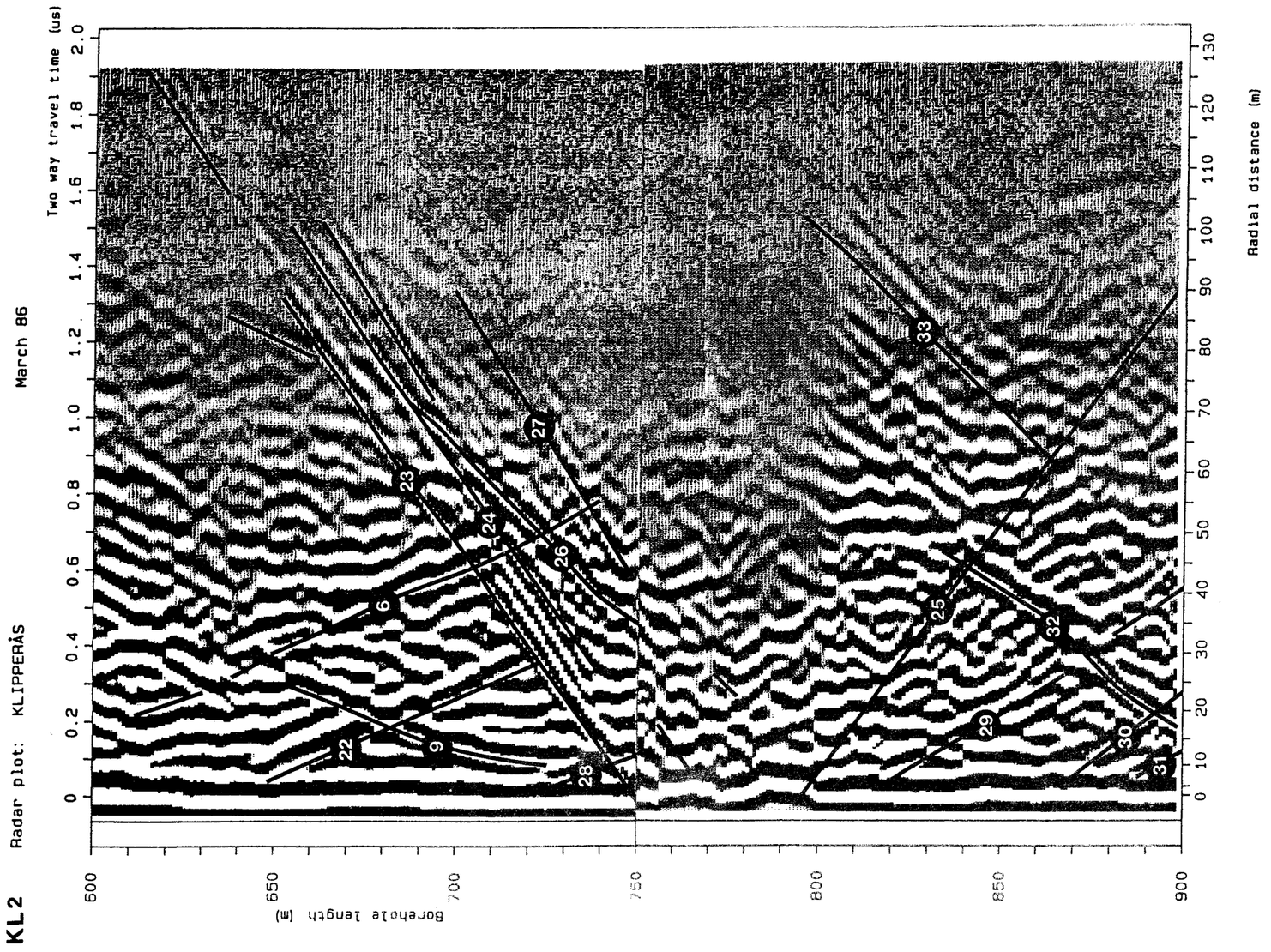

Figure B.5 Radar map for borehole Kl 2, 22 MHz (Part III).

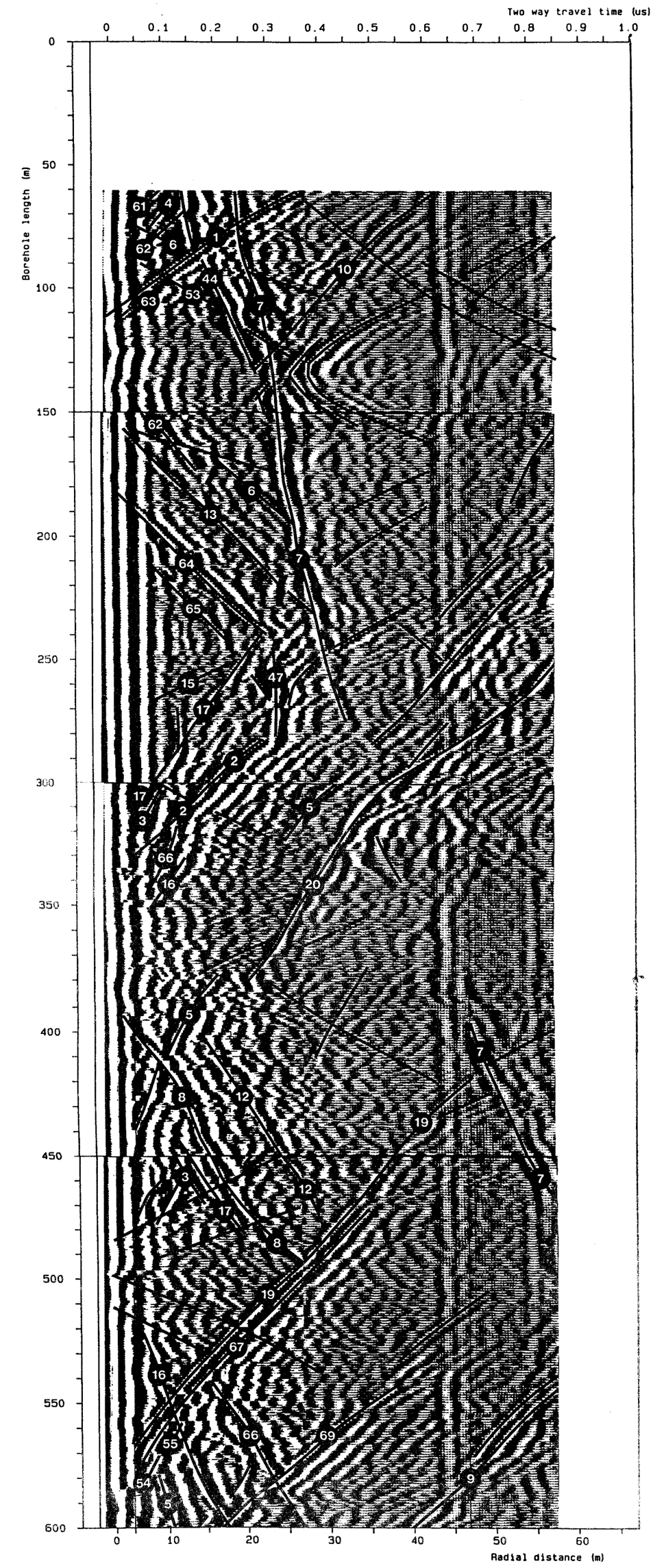

Figure B.6 Radar map for borehole Kl 2, 60 MHz (Part I).

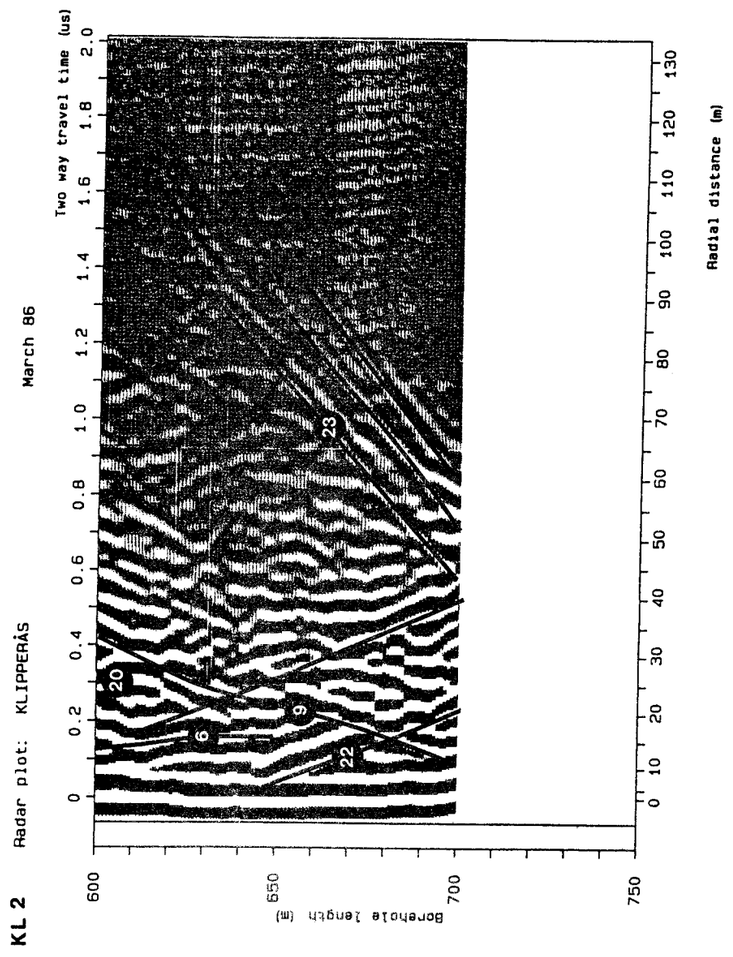

Figure B.4 Radar map for borehole Kl 2, 22 MHz (Part II).

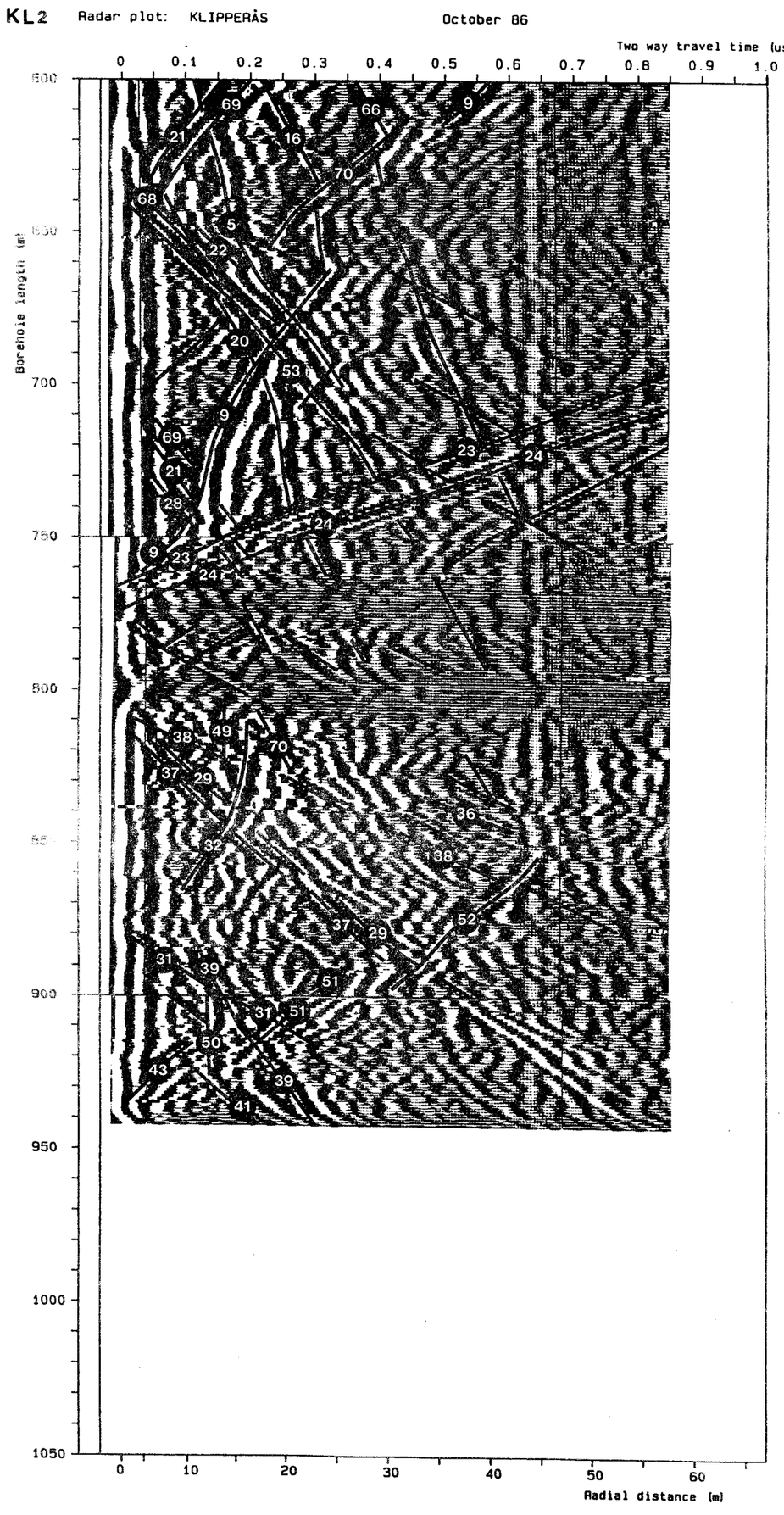

Figure B.7 Radar map for borehole KL 2, 60 MHz (Part II).

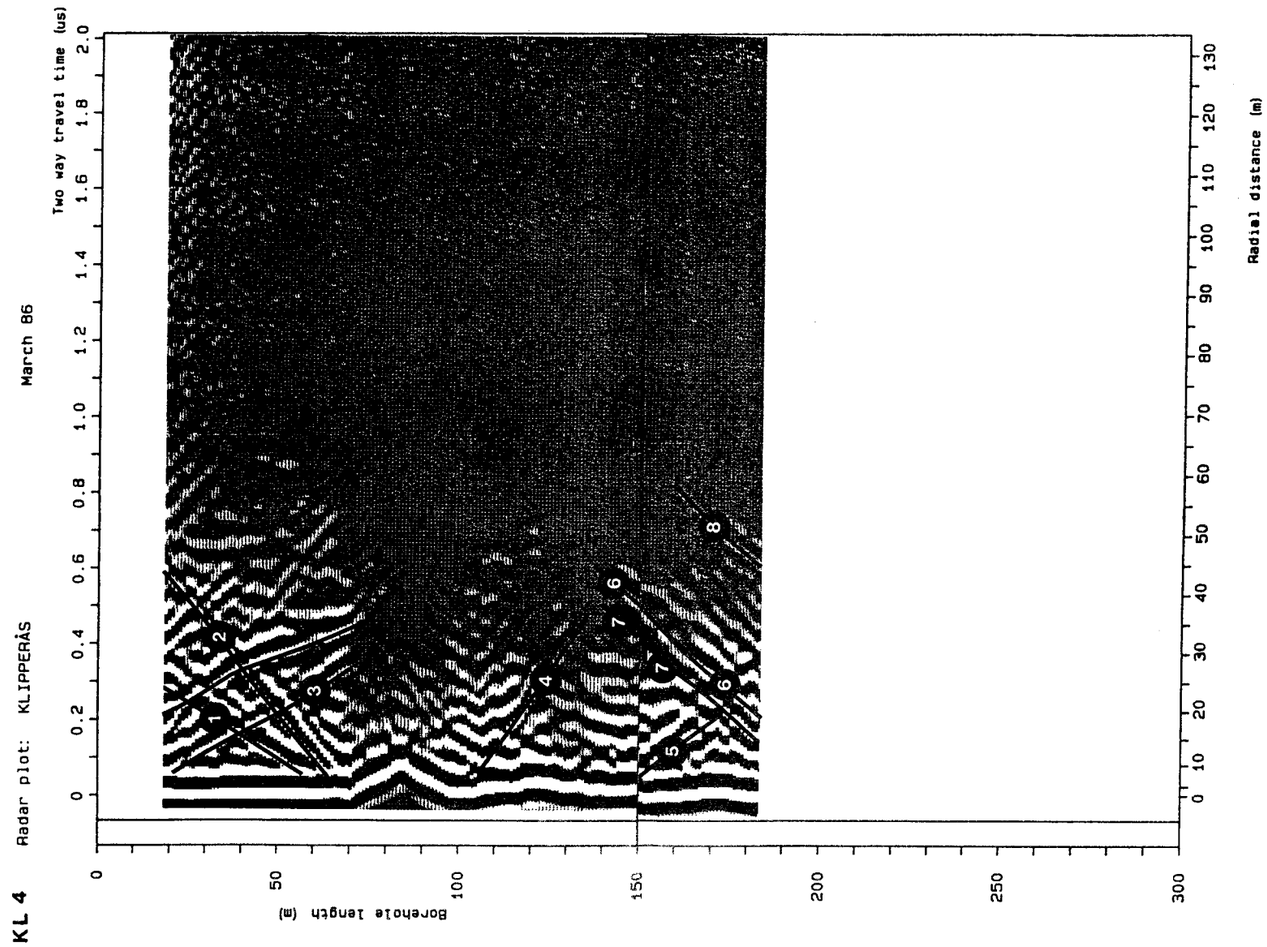

Figure B.8 Radar map for borehole KI 4, 22 MHz.

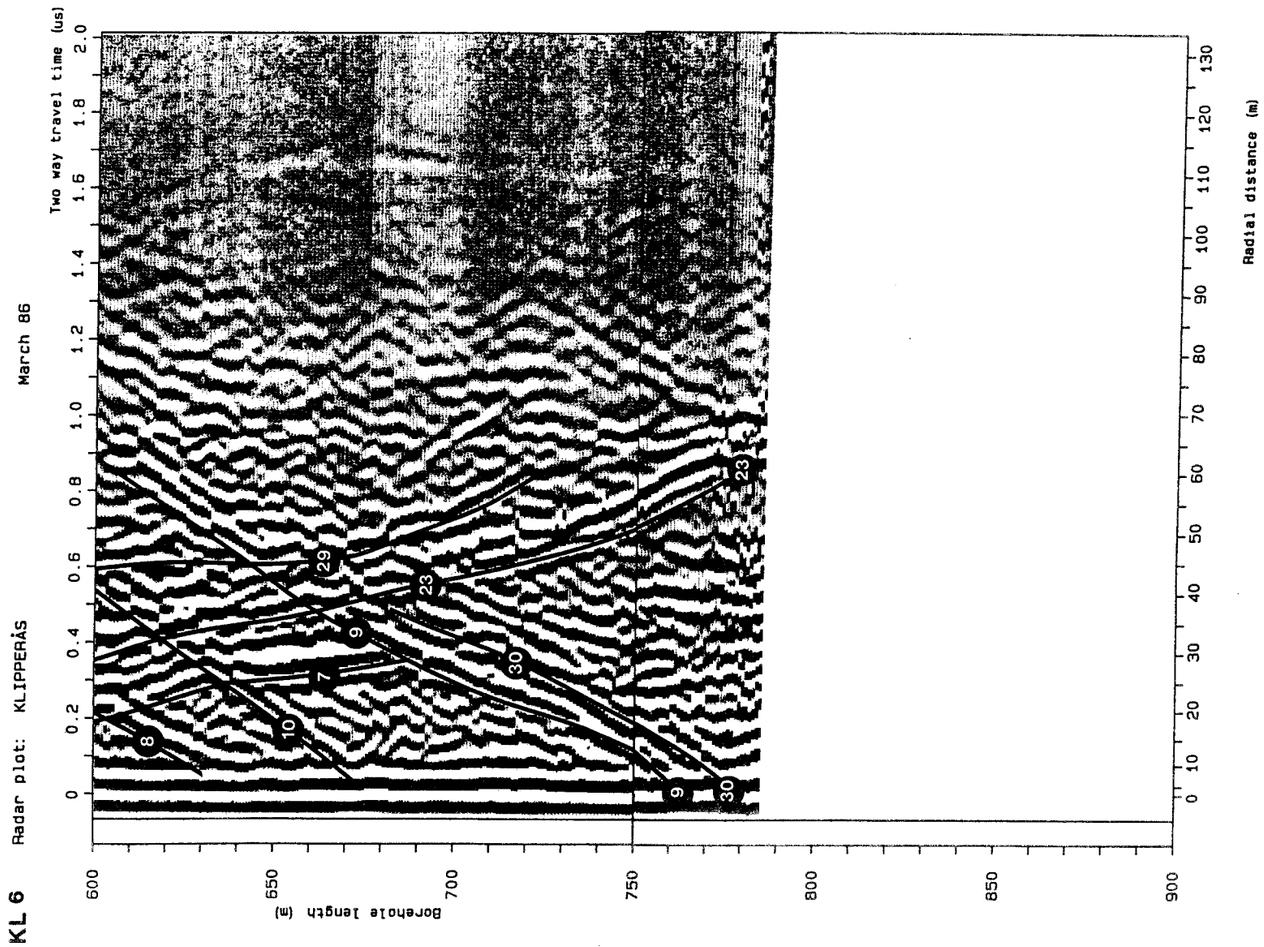

Figure B.10 Radar map for borehole Kl 6, 22 MHz (Part II).

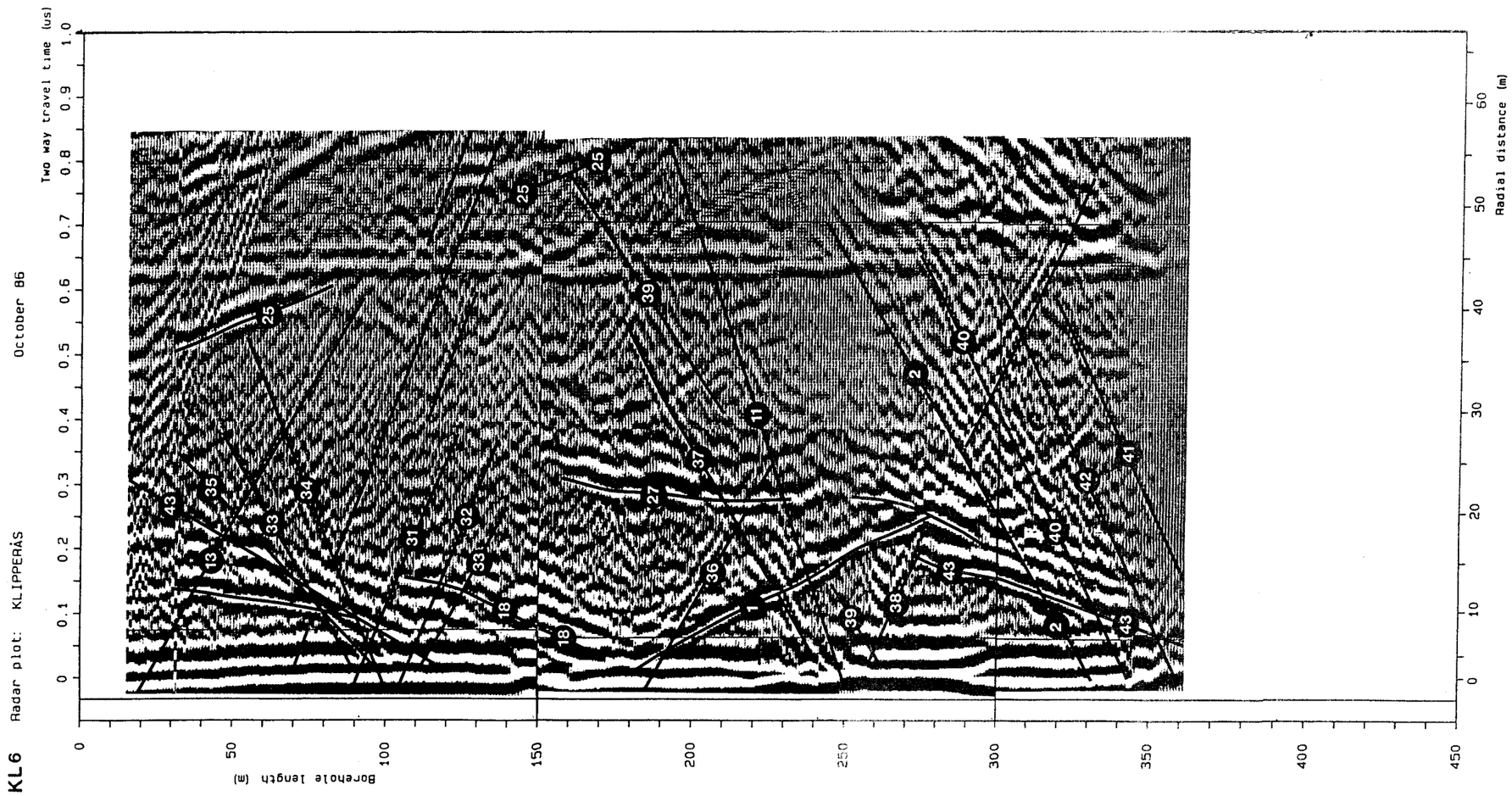

Figure B.11 Radar map for borehole Kl 6, 60 MHz.

KL 8 Radar plot: KLIPPERÅS March 86

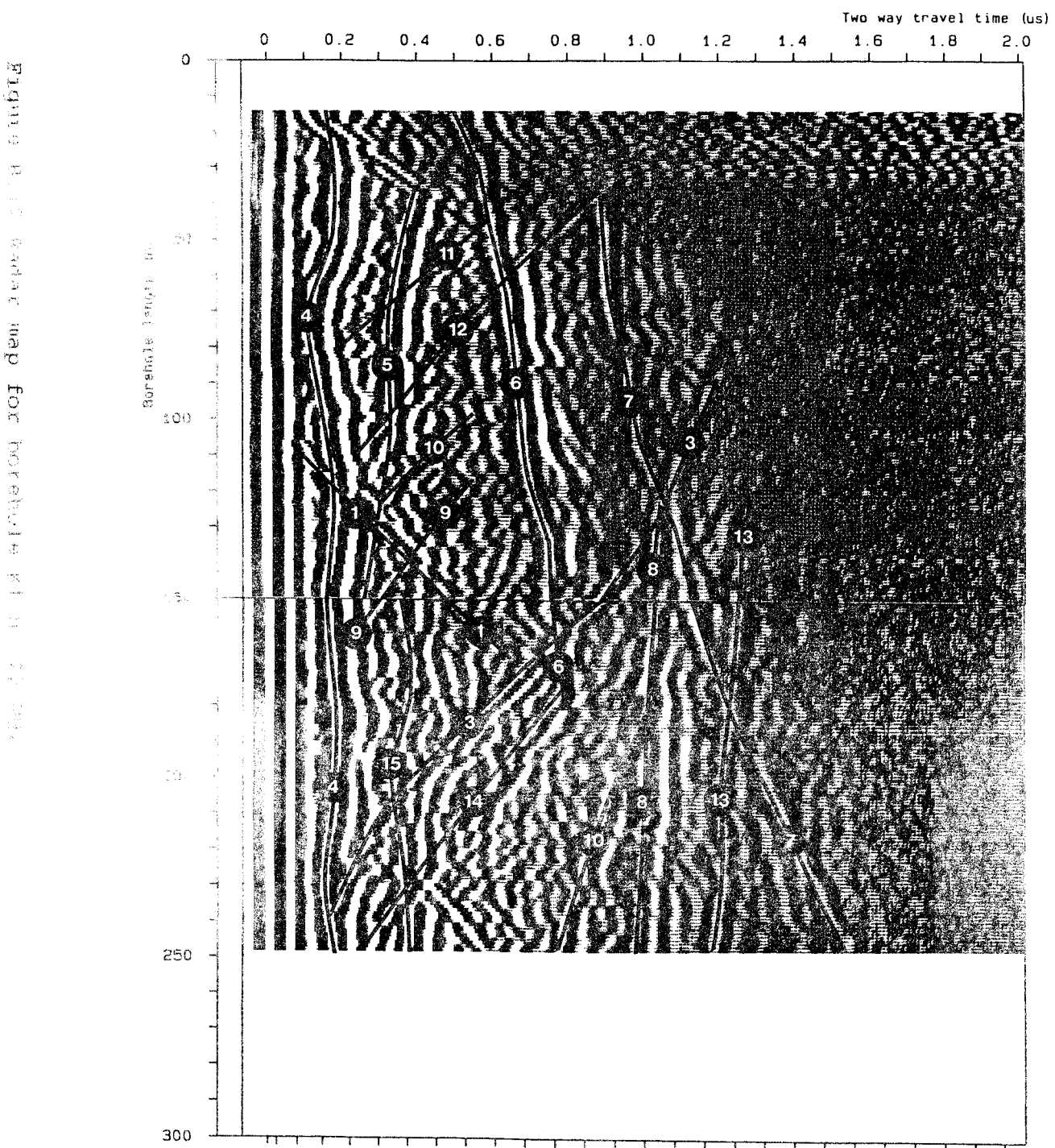

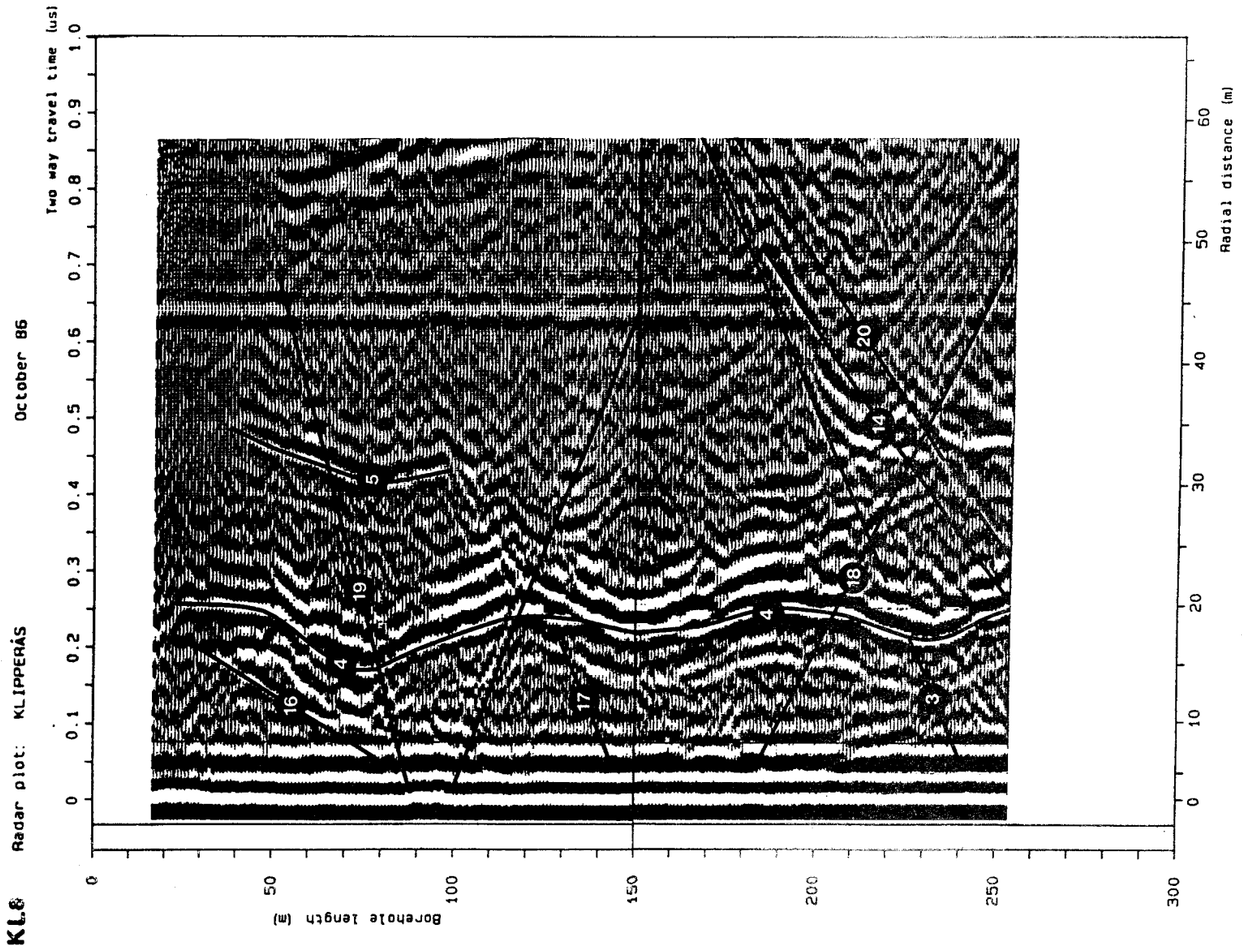

Figure B.13 Radar map for borehole Kl 8, 60 MHz.

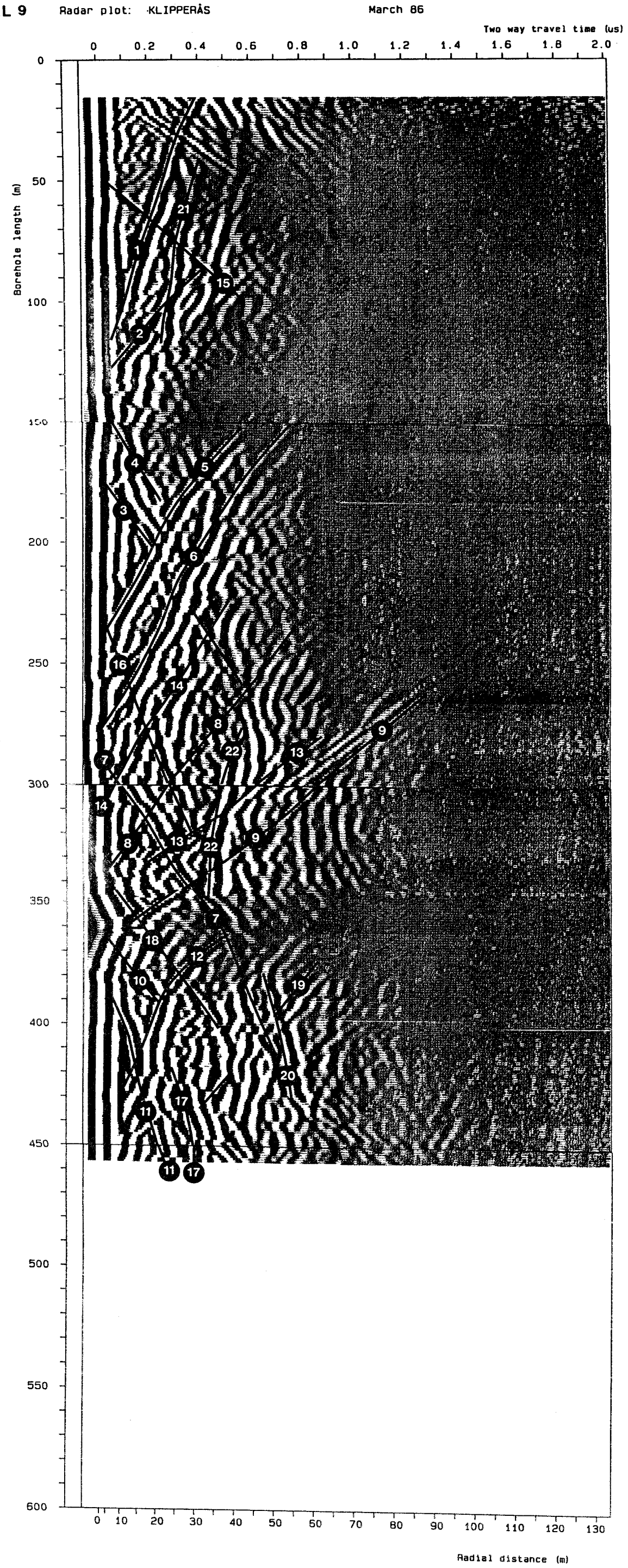

Figure B.14 Radar map for borehole Ki 9, 22 MHz (part 1).

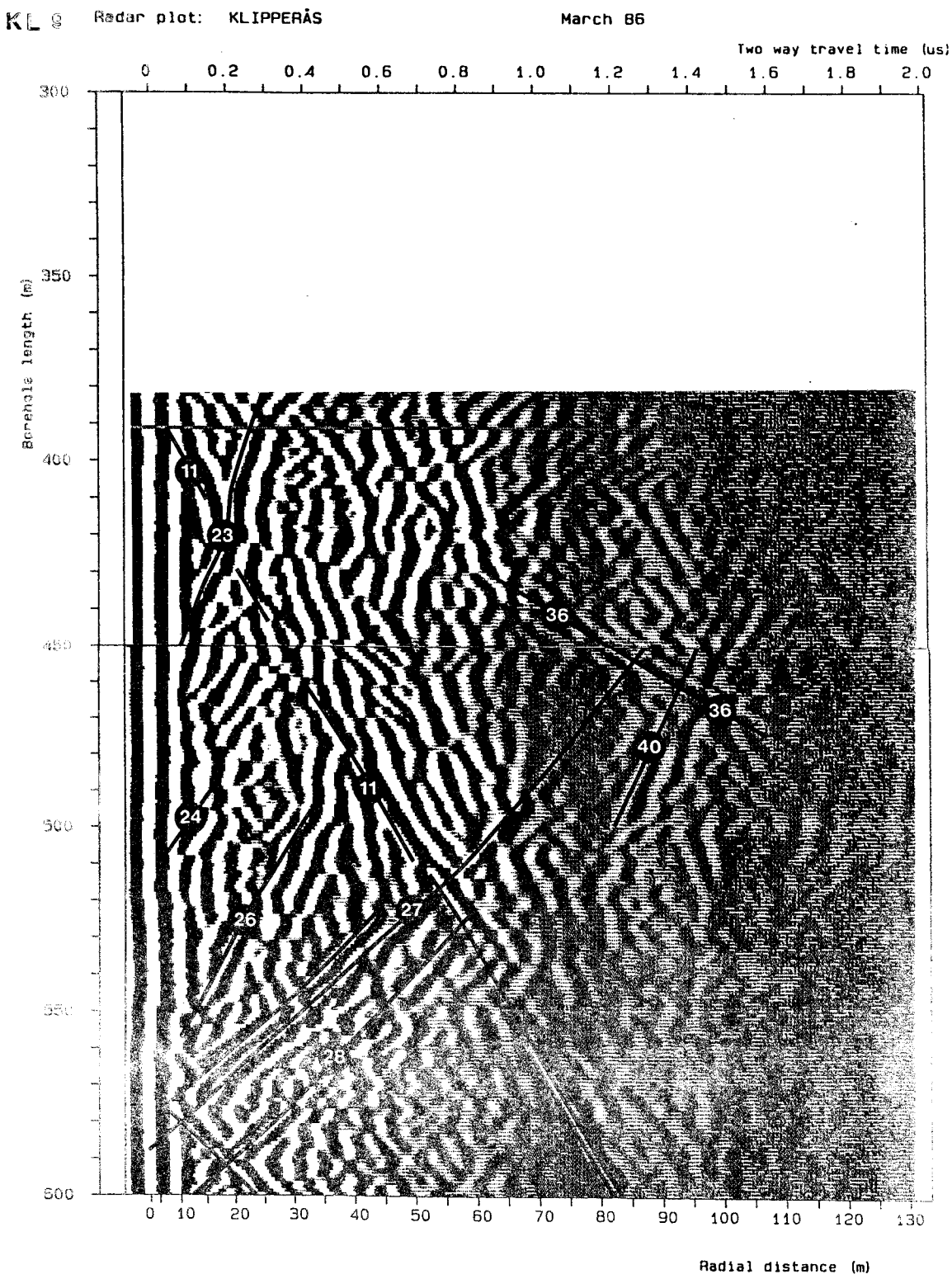

Figure B.15 Radar map for boreHole KL 9, 22 MHz (part II).

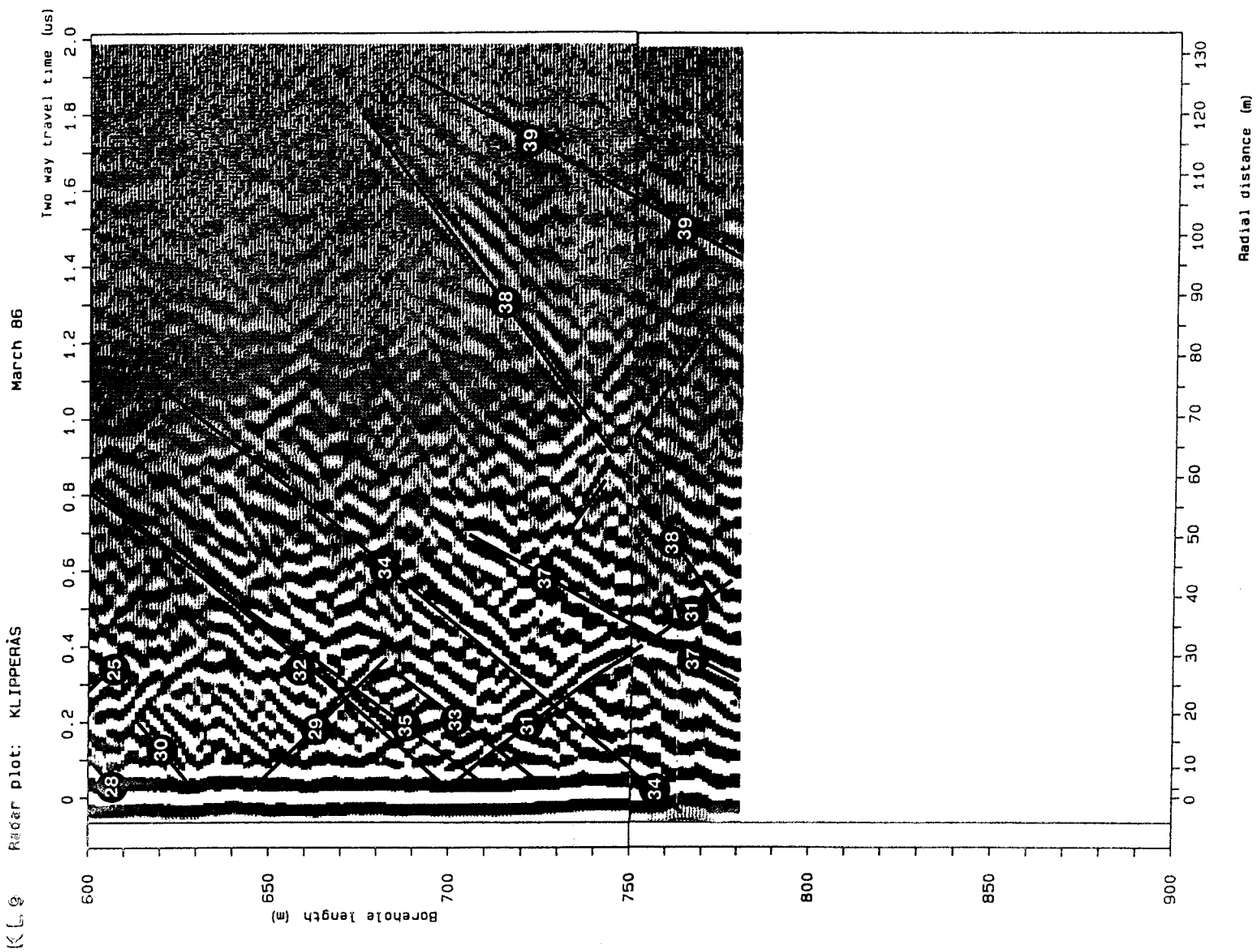

Figure B.16 Radar map for borehole Kl 9, 22 MHz (Part III).

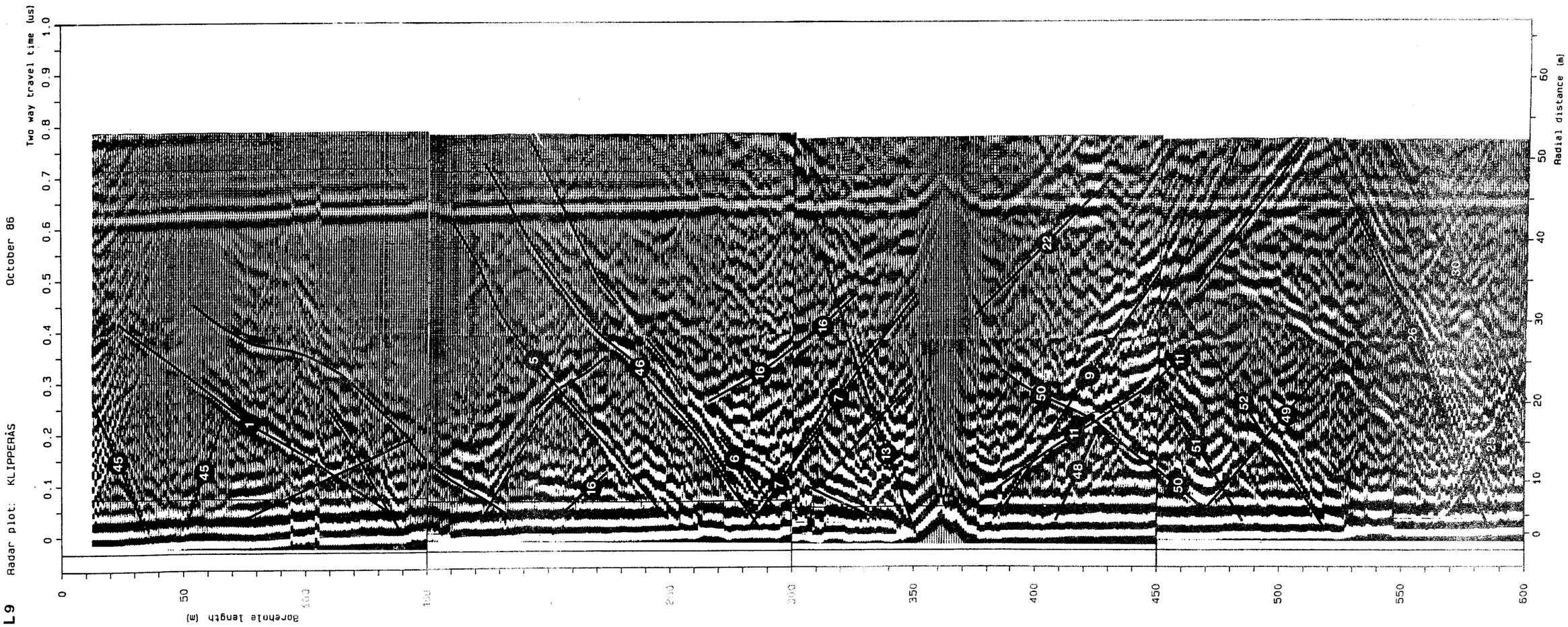

Figure B.17 Radar map for borehole KL9, 60 MHz (Part I).

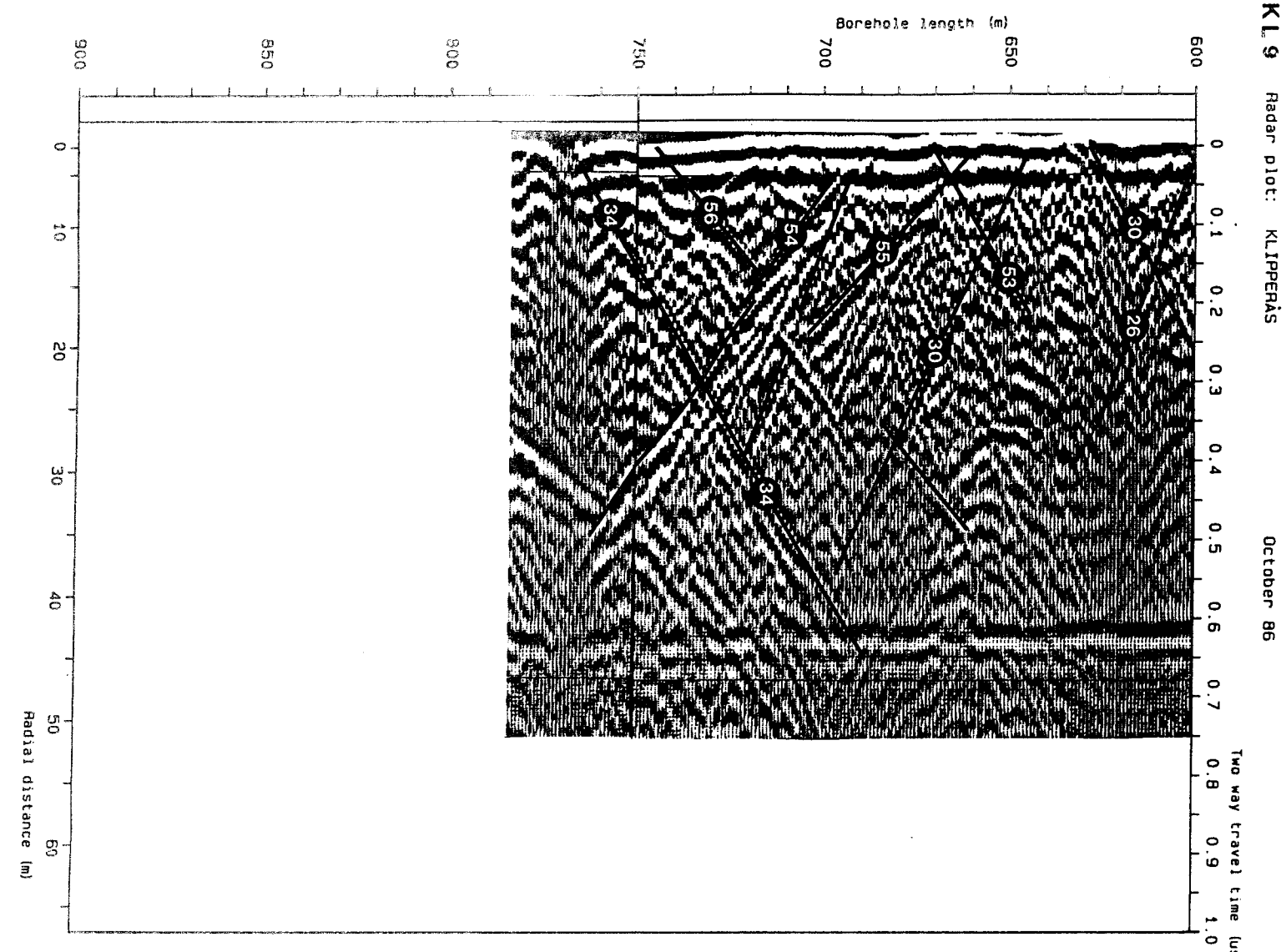

Figure B.18 Radar map for borehole KI 9, 60 MHz (part II).

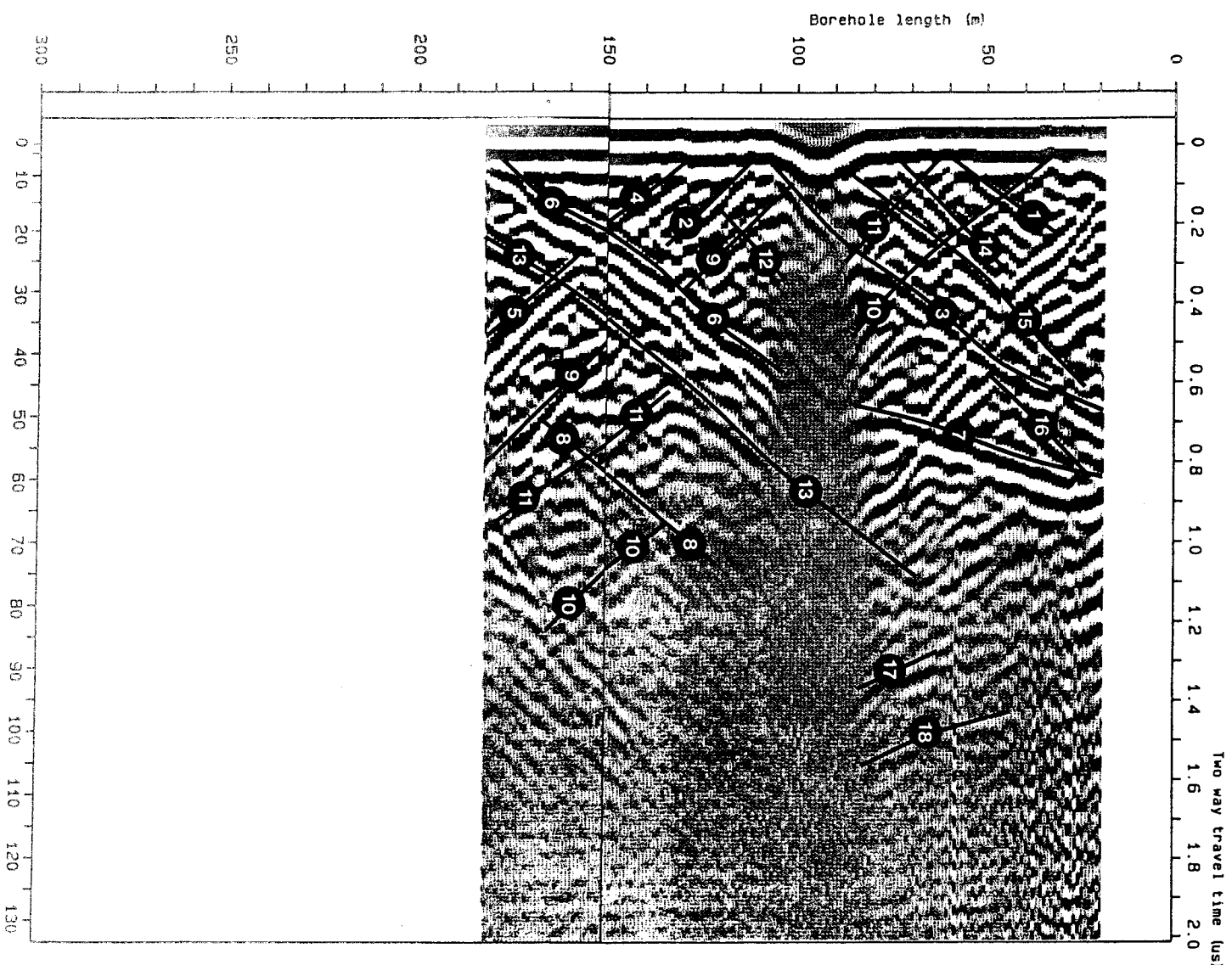

Figure B.19 Radar map for borehole KI 10, 22 MHz.

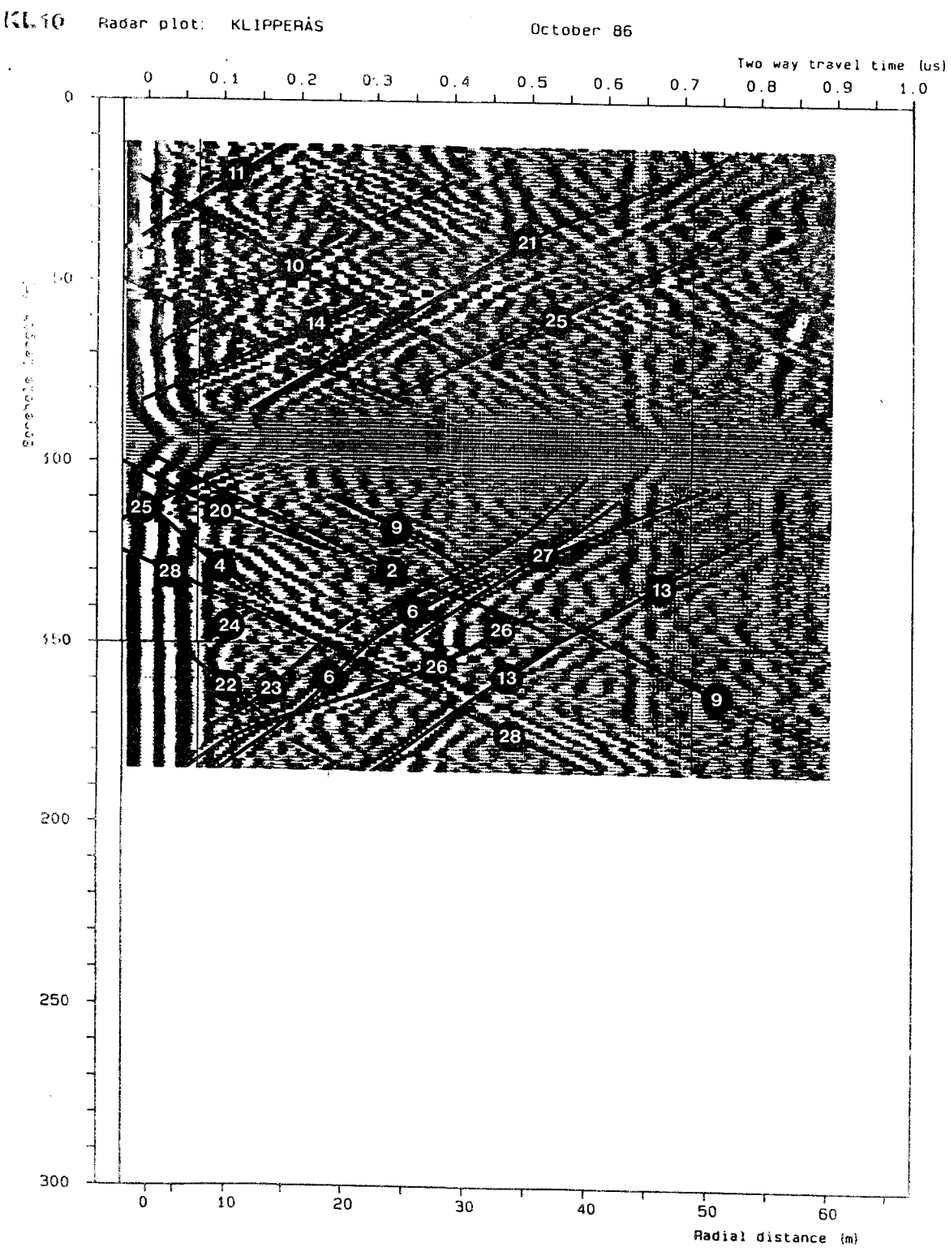

Figure 5.20 Radar map for borehole KL 10, 60 MHz.

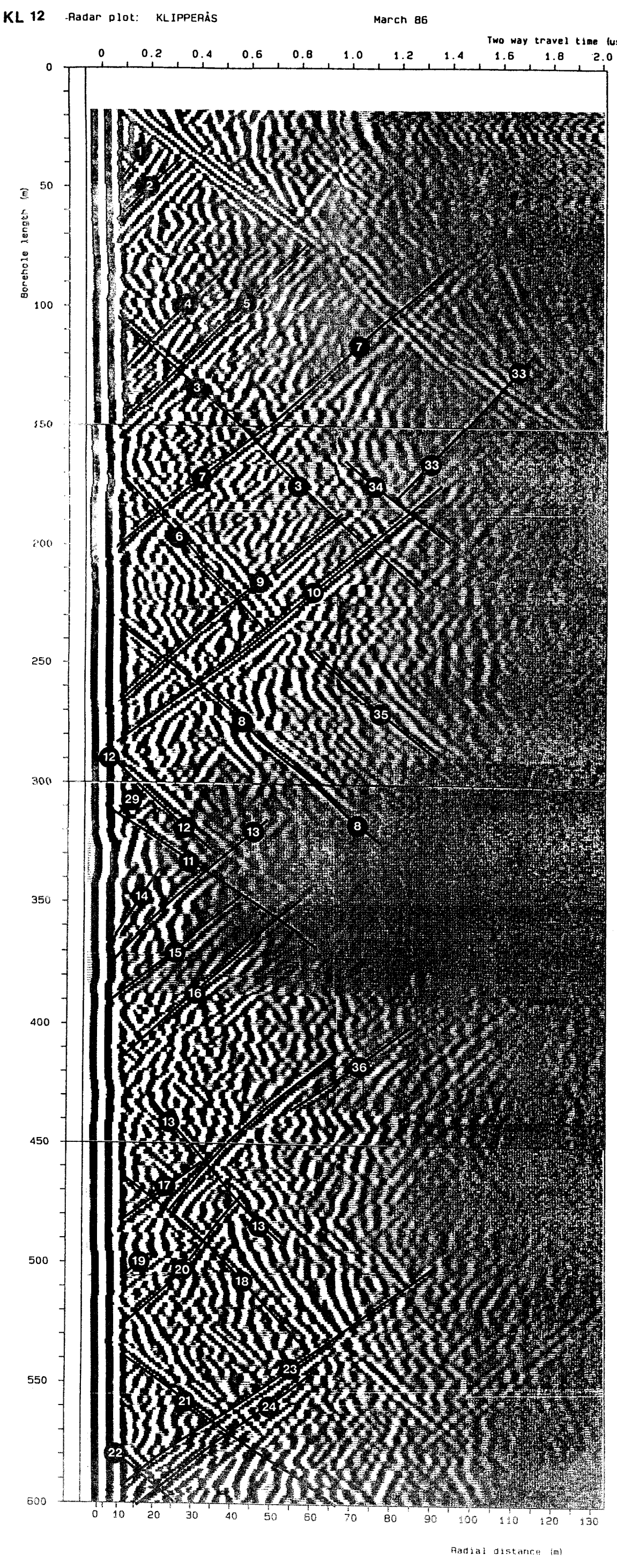

Figure B.21 Radar map for borehole KL 12, 22 MHz (Part 1).

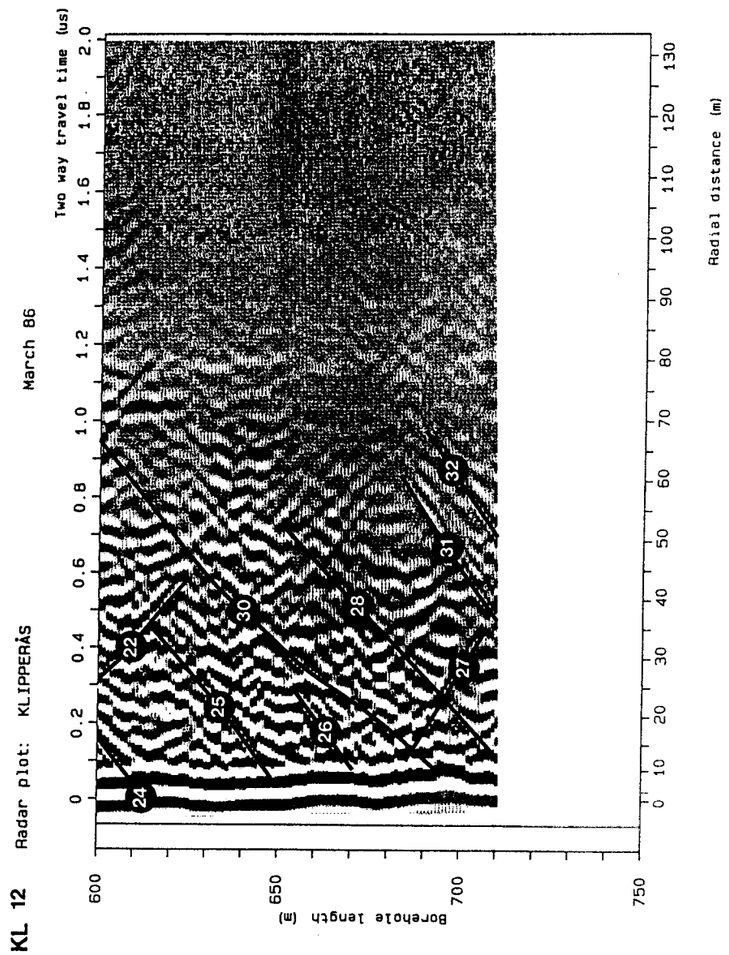

Figure B.22 Radar map for borehole Kl 12, 22 MHz (Part II).

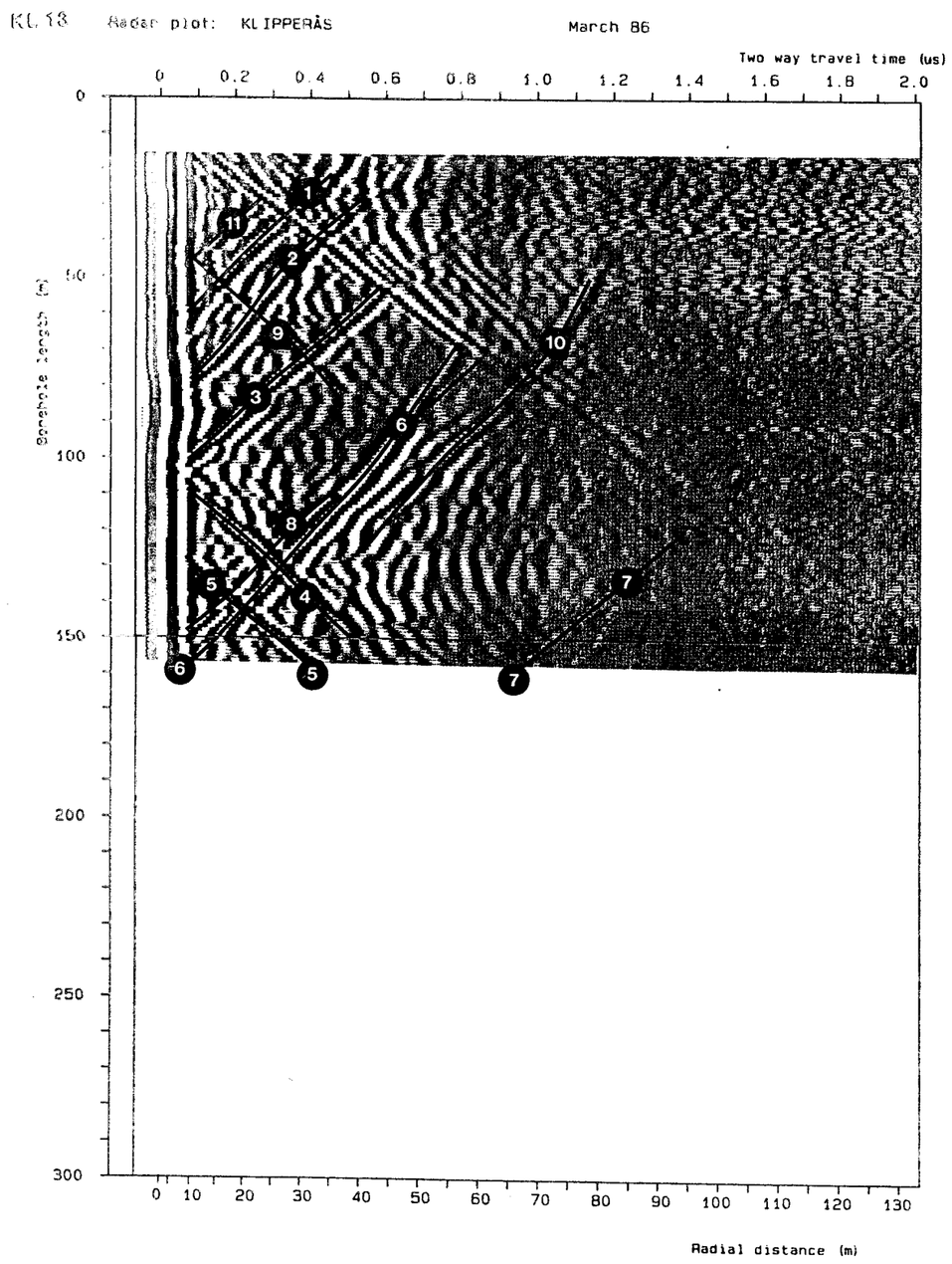

Figure B.23 Radar map for borehole KL 13, 22 MHz.

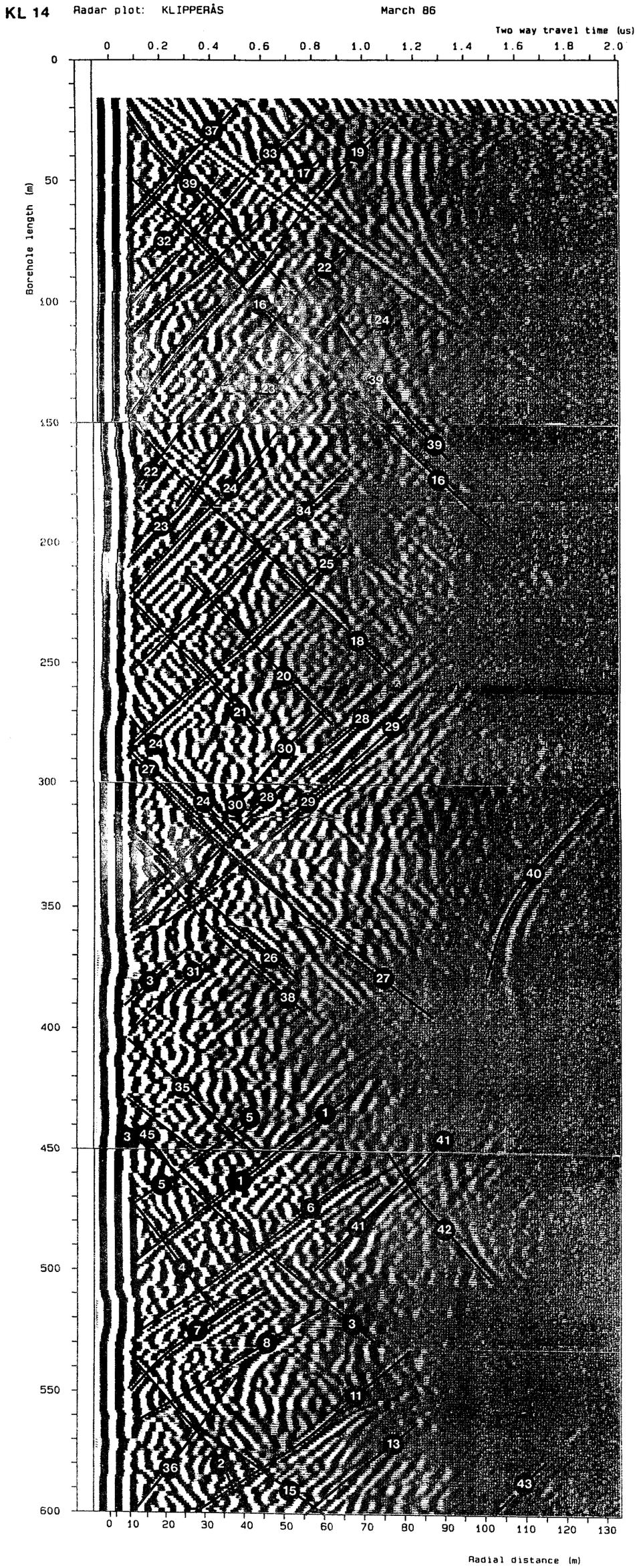

Figure B.24 Radar map for borehole Kl 14, 22 MHz (Part I).

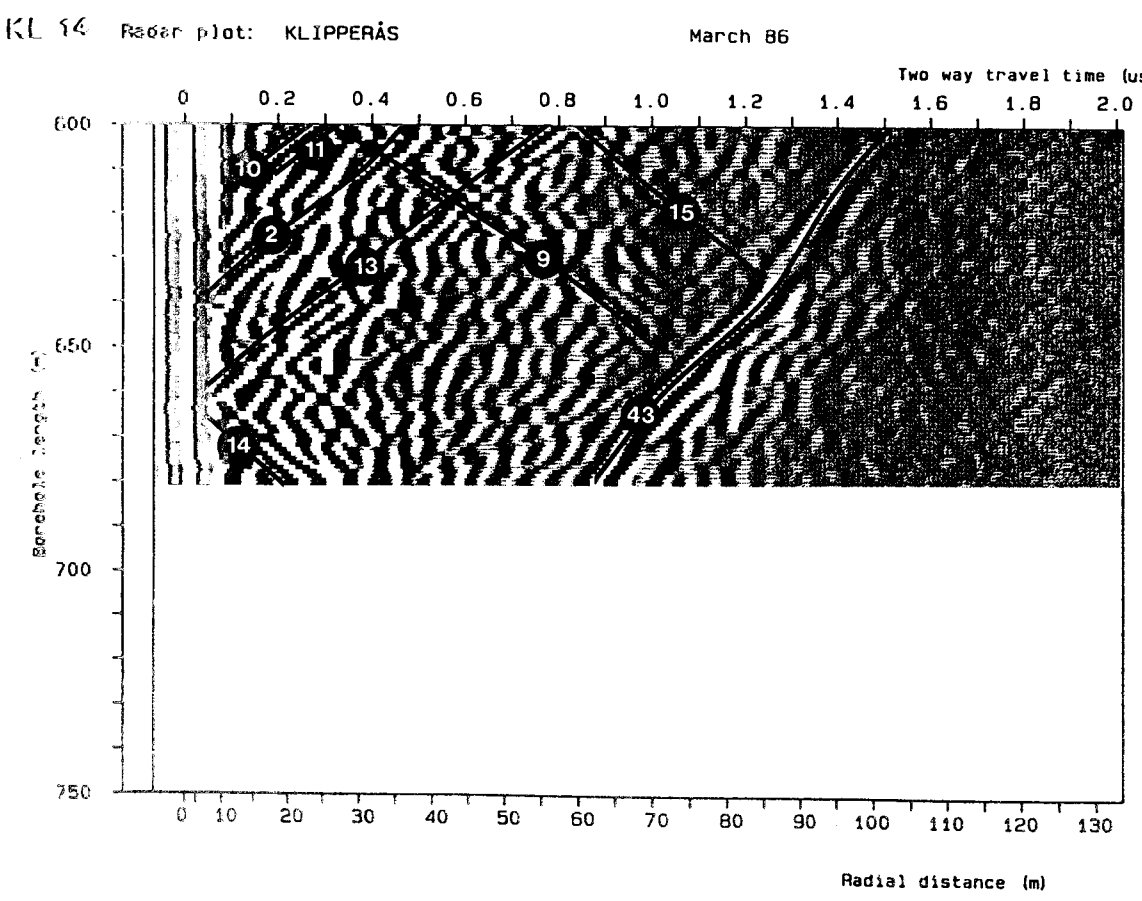

Figure 3.25 Radar map for borehole KL 14, 22 MHz (Part III).

APPENDIX C

VRP maps from the investigated boreholes.

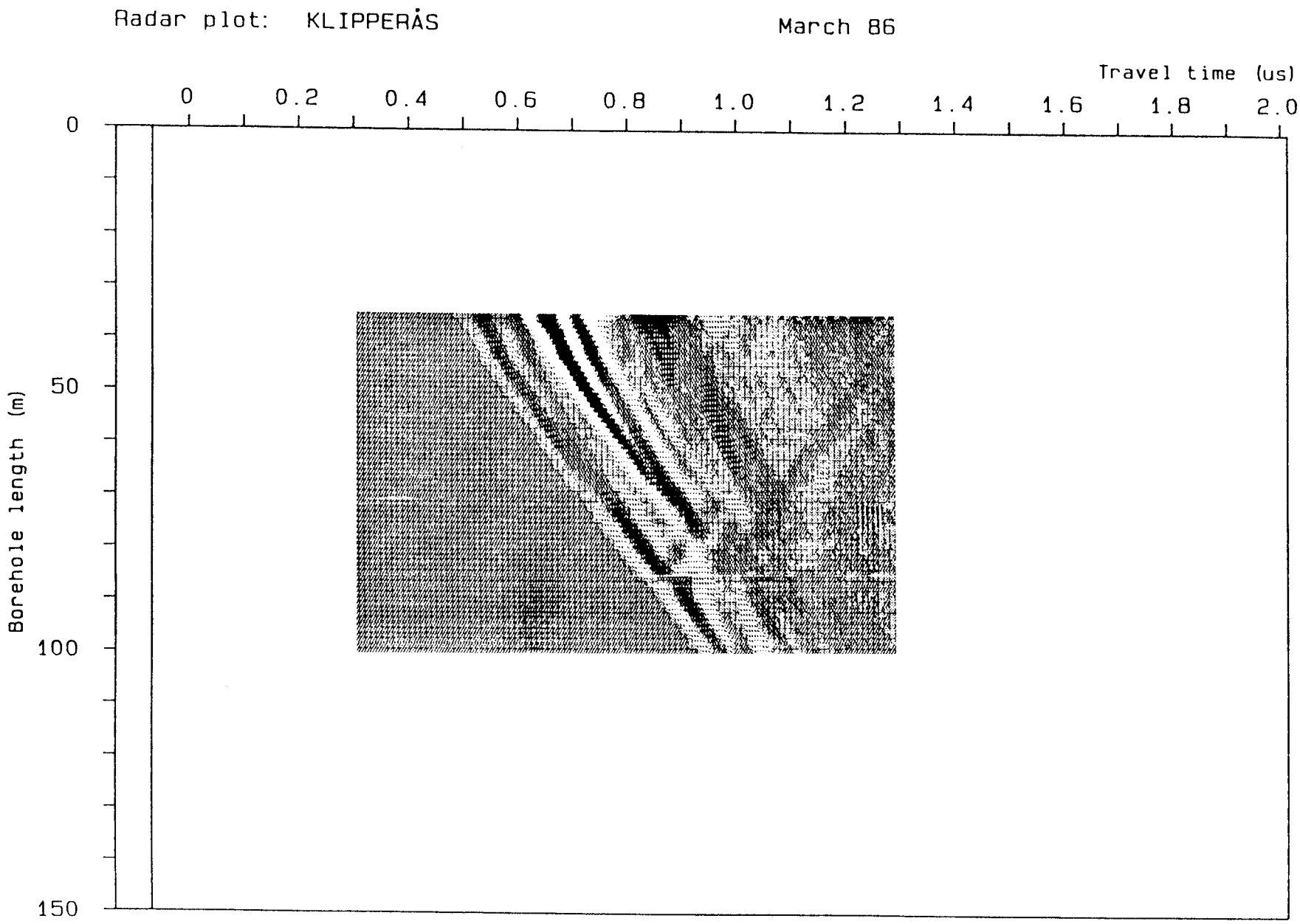

Figure C.1 VRP map from borehole K1 1.
Direction N42E.

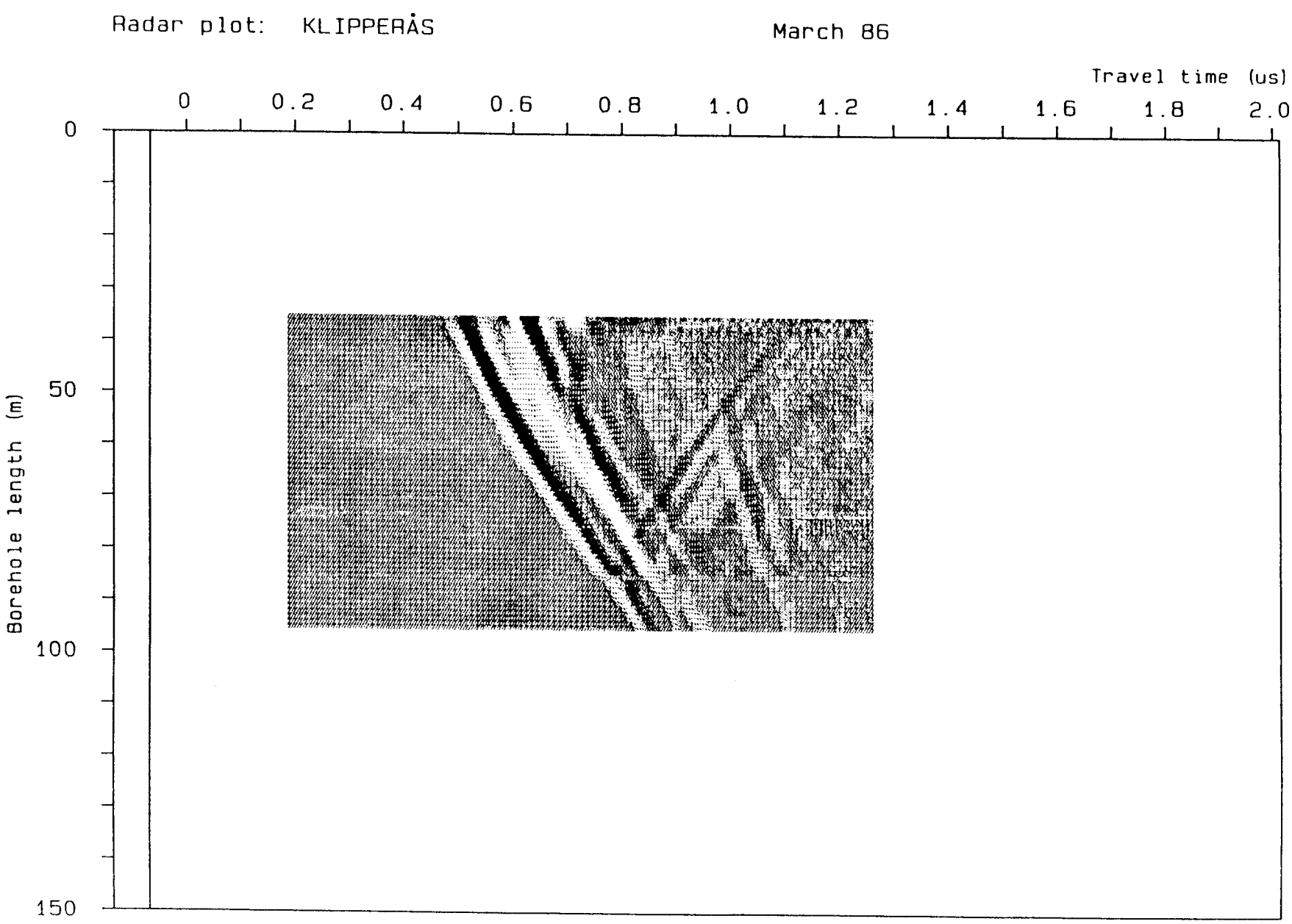

Figure C.2 VRP map from borehole Kl 1.
Direction S48E.

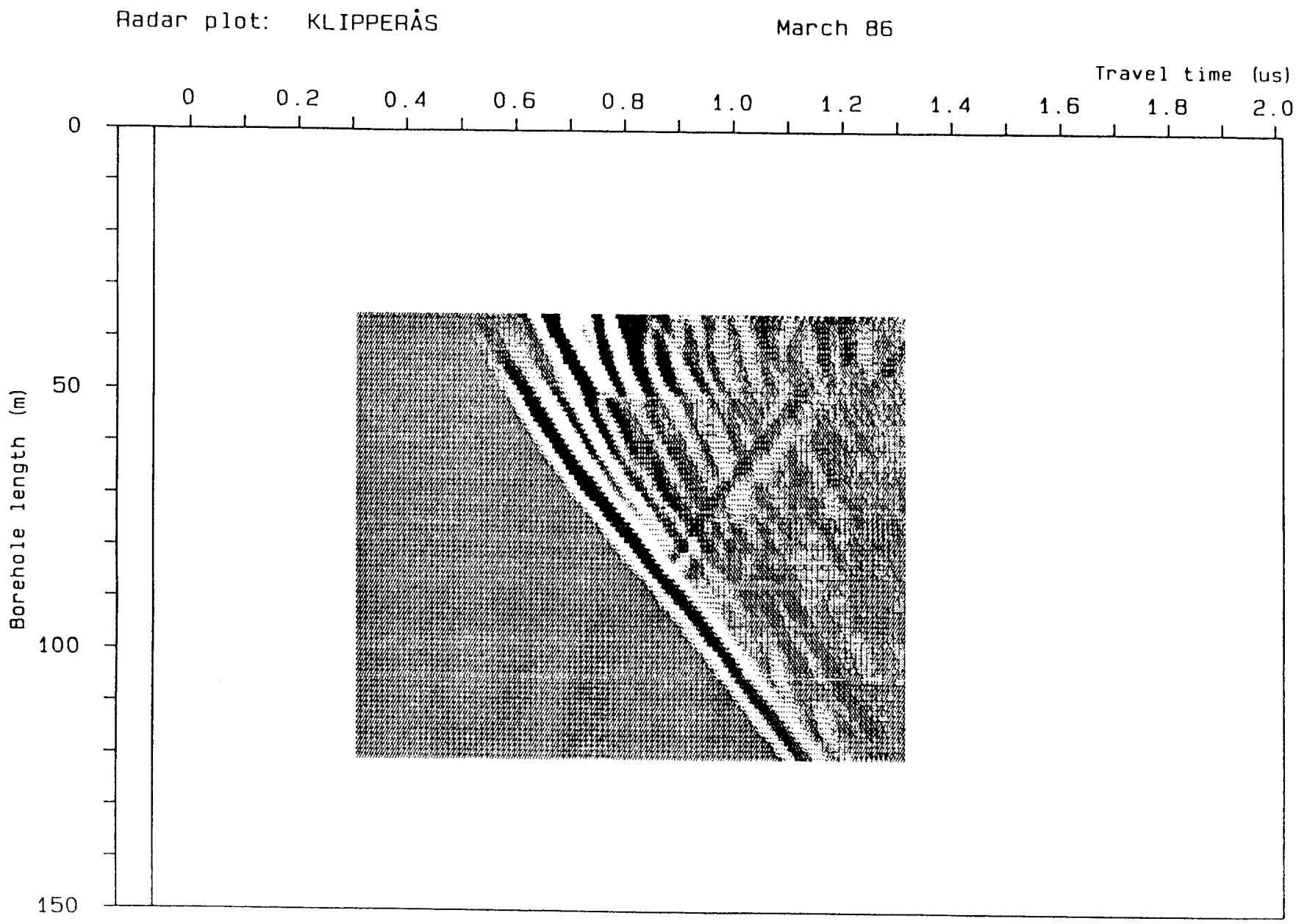

Figure C.3 VRP map from borehole Kl 1.
Direction S42W.

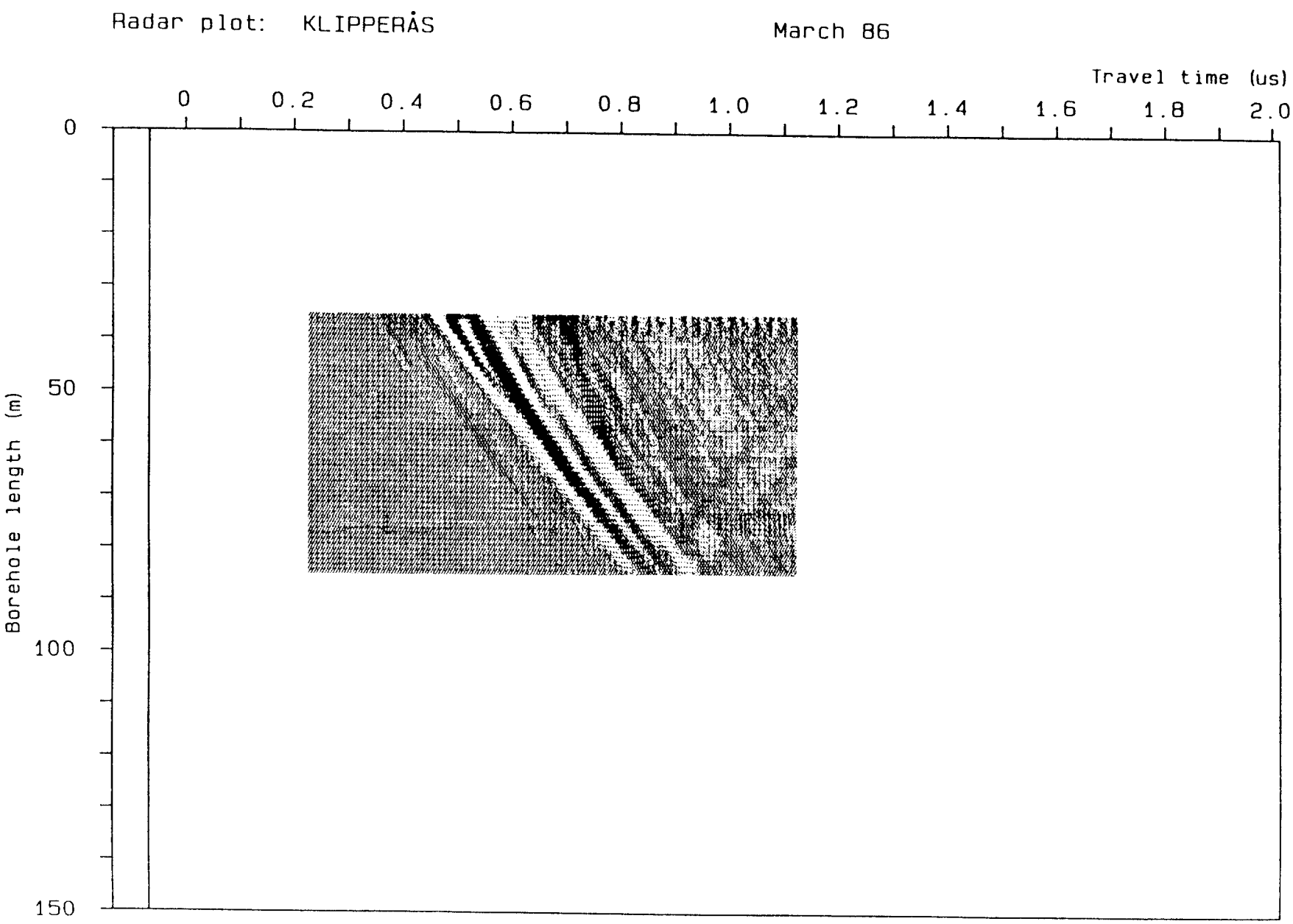

Figure C.4 VRP map from borehole Kl 1.
Direction N48W.

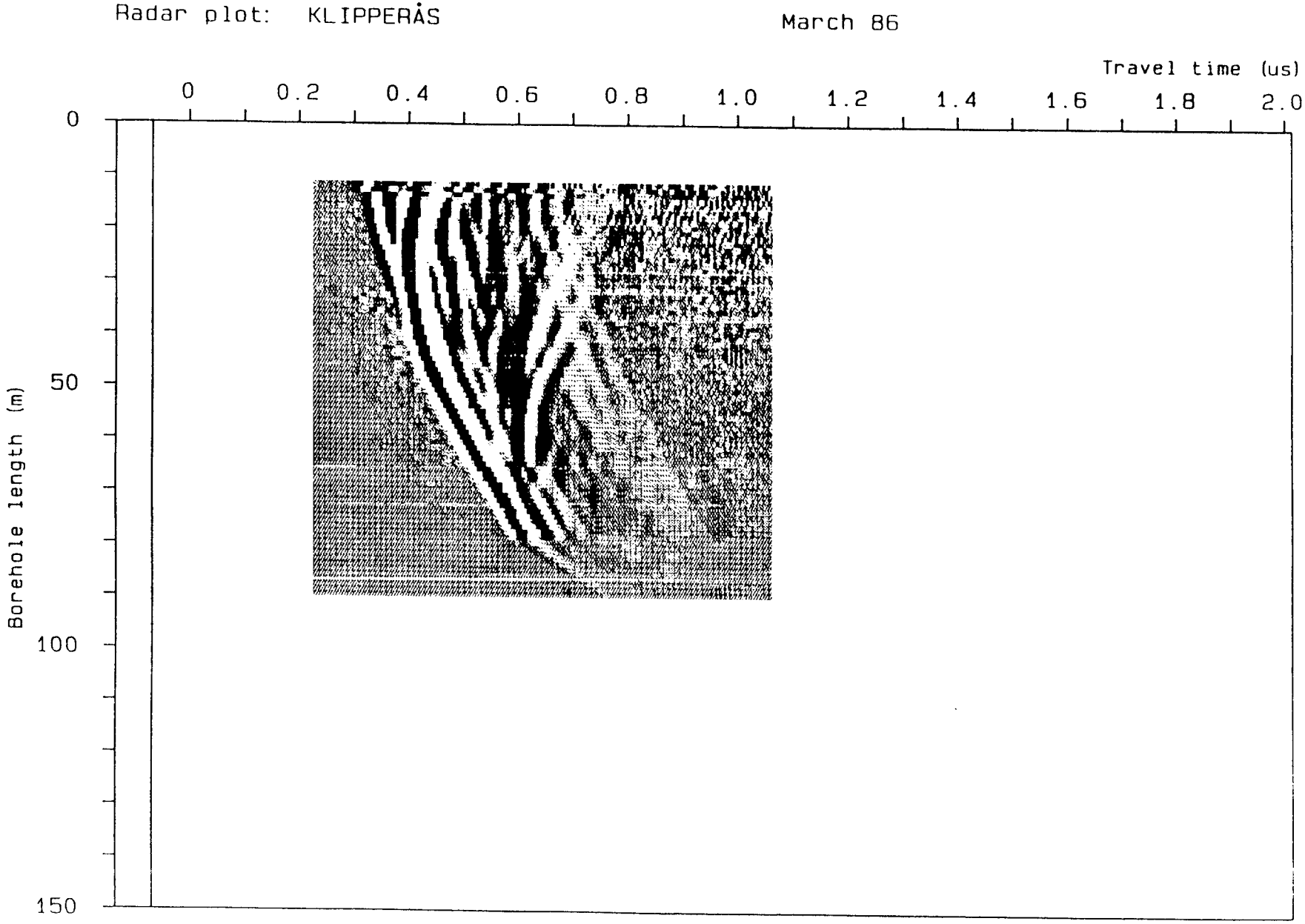

Figure C.5 VRP map from borehole Kl 4.

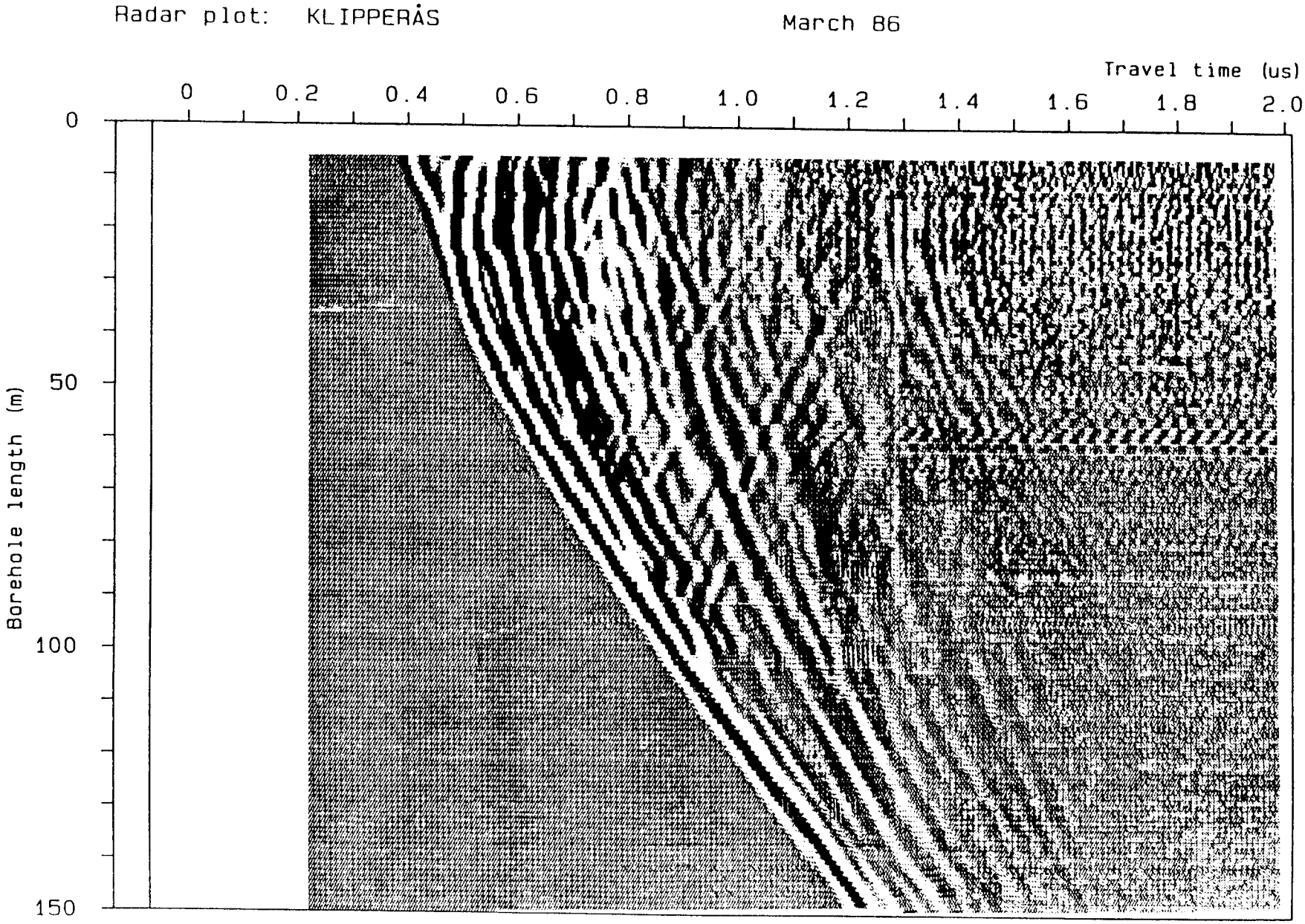

Figure C.6 VRP map from borehole Kl 6.

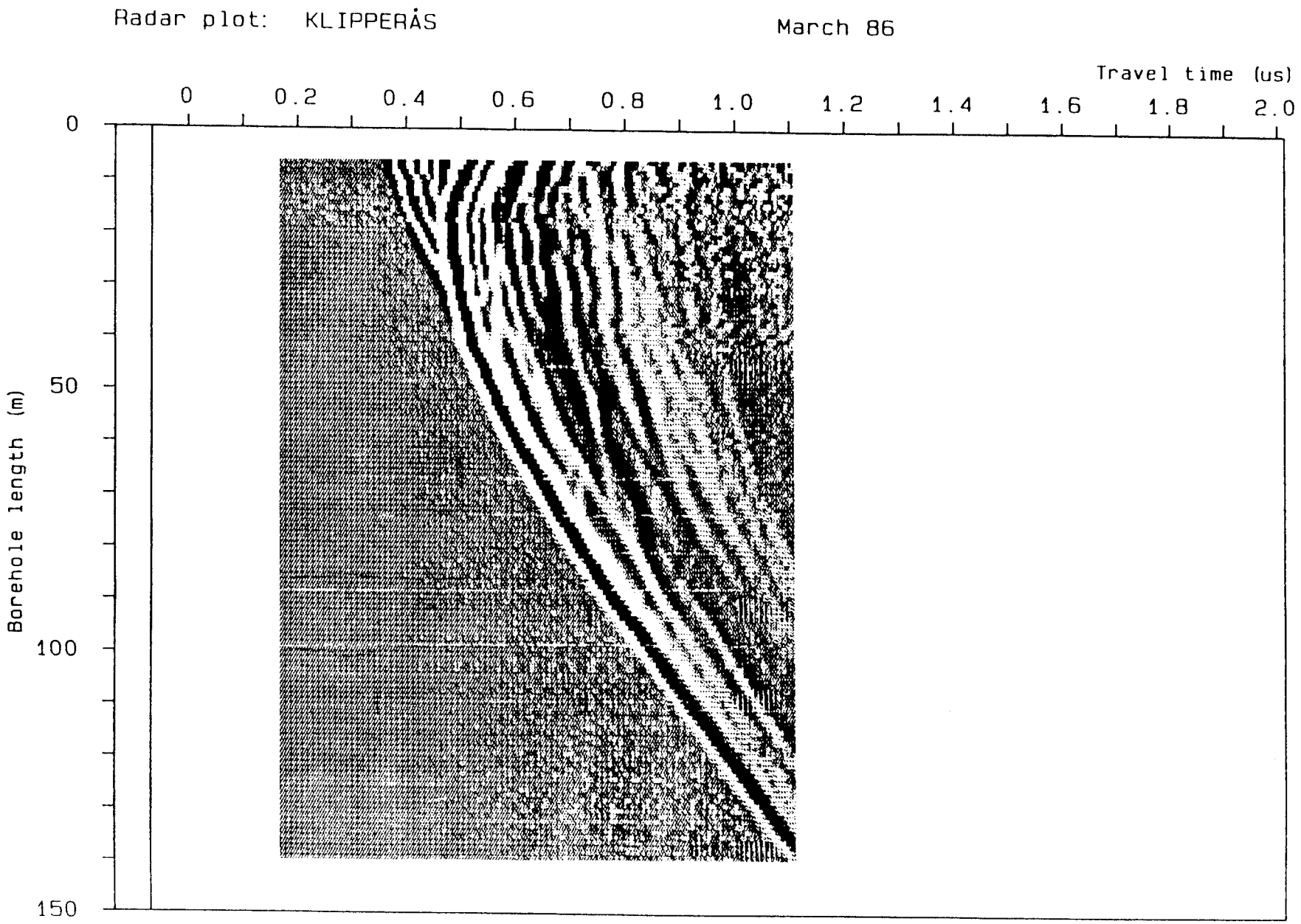

Figure C.7 VRP map from borehole Kl 8.

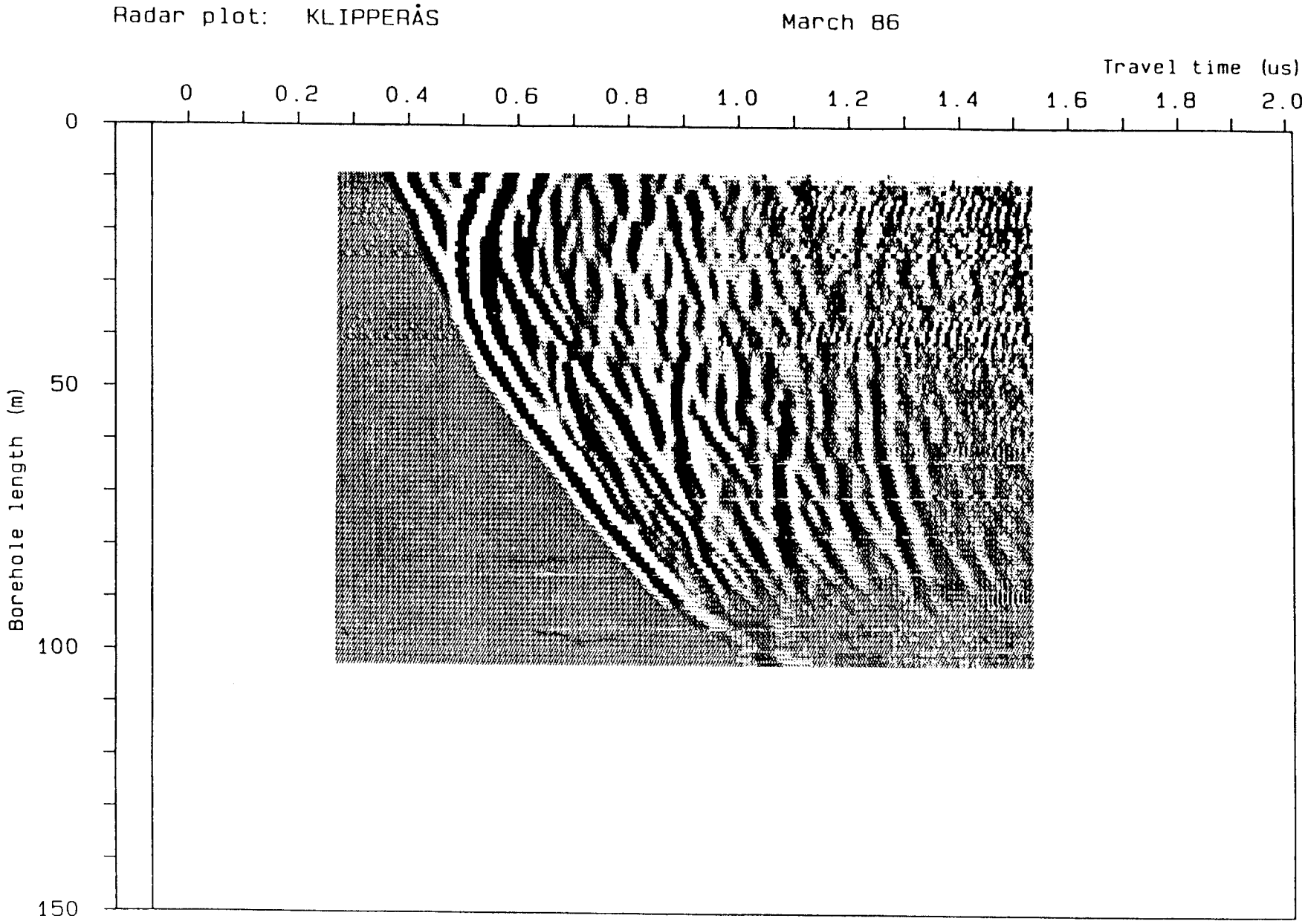

Figure C.8 VRP map from borehole Kl 9.

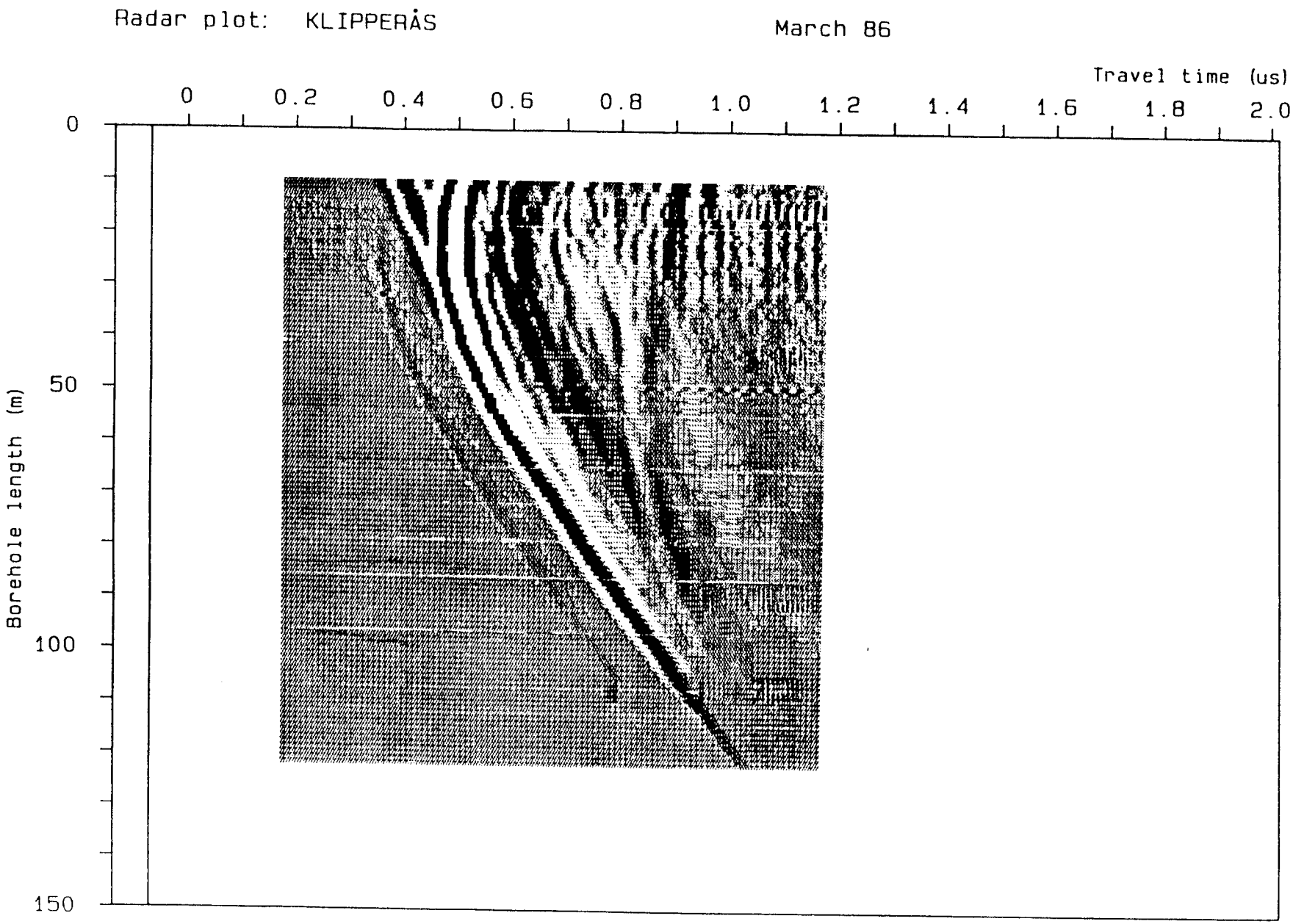

Figure C.9 VRP map from borehole Kl 10.

List of SKB reports

Annual Reports

1977–78
TR 121
KBS Technical Reports 1 – 120.
Summaries. Stockholm, May 1979.

1979
TR 79–28
The KBS Annual Report 1979.
KBS Technical Reports 79-01 – 79-27.
Summaries. Stockholm, March 1980.

1980
TR 80–26
The KBS Annual Report 1980.
KBS Technical Reports 80-01 – 80-25.
Summaries. Stockholm, March 1981.

1981
TR 81–17
The KBS Annual Report 1981.
KBS Technical Reports 81-01 – 81-16.
Summaries. Stockholm, April 1982.

1982
TR 82–28
The KBS Annual Report 1982.
KBS Technical Reports 82-01 – 82-27.
Summaries. Stockholm, July 1983.

1983
TR 83–77
The KBS Annual Report 1983.
KBS Technical Reports 83-01 – 83-76
Summaries. Stockholm, June 1984.

1984
TR 85–01
Annual Research and Development Report 1984
Including Summaries of Technical Reports Issued during 1984. (Technical Reports 84-01– 84-19)
Stockholm June 1985.

1985
TR 85-20
Annual Research and Development Report 1985
Including Summaries of Technical Reports Issued during 1985. (Technical Reports 85-01-85-19)
Stockholm May 1986.

Technical Reports

1986

TR 86-01
I: An analogue validation study of natural radionuclide migration in crystalline rock using uranium-series disequilibrium studies
II: A comparison of neutron activation and alpha spectroscopy analyses of thorium in crystalline rocks
J A T Smellie, Swedish Geological Co, A B MacKenzie and R D Scott, Scottish Universities Research Reactor Centre
February 1986

TR 86-02
Formation and transport of americium pseudocolloids in aqueous systems
U Olofsson
Chalmers University of Technology, Gothenburg, Sweden
B Allard
University of Linköping, Sweden
March 26, 1986

TR 86-03
Redox chemistry of deep groundwaters in Sweden
D Kirk Nordstrom
US Geological Survey, Menlo Park, USA
Ignasi Puigdomenech
Royal Institute of Technology, Stockholm, Sweden
April 1, 1986

TR 86-04
Hydrogen production in alpha-irradiated bentonite
Trygve Eriksen
Royal Institute of Technology, Stockholm, Sweden
Hilbert Christensen
Studsvik Energiteknik AB, Nyköping, Sweden
Erling Bjergbakke
Risö National Laboratory, Roskilde, Denmark
March 1986

TR 86-05
Preliminary investigations of fracture zones in the Brändan area, Finnsjön study site
Kaj Ahlbom, Peter Andersson, Lennart Ekman, Erik Gustafsson, John Smellie,
Swedish Geological Co, Uppsala
Eva-Lena Tullborg, Swedish Geological Co, Göteborg
February 1986

TR 86-06
Geological and tectonic description of the Klipperås study site
Andrzej Olkiewicz
Vladislav Stejskal
Swedish Geological Company
Uppsala, October, 1986

TR 86-07
Geophysical investigations at the Klipperås study site
Stefan Sehlstedt
Leif Stenberg
Swedish Geological Company
Luleå, July 1986

TR 86-08
Hydrogeological investigations at the Klipperås study site
Bengt Gentzschein
Swedish Geological Company
Uppsala, June 1986

TR 86-09
Geophysical laboratory investigations on core samples from the Klipperås study site
Leif Stenberg
Swedish Geological Company
Luleå, July 1986

TR 86-10
Fissure fillings from the Klipperås study site
Eva-Lena Tullborg
Swedish Geological Company
Göteborg, June 1986

TR 86-11
Hydraulic fracturing rock stress measurements in borehole Gi-1, Gideå Study Site, Sweden
Bjarni Bjarnason and Ove Stephansson
Division of Rock Mechanics,
Luleå University of Technology, Sweden
April 1986

TR 86-12
PLAN 86— Costs for management of the radioactive waste from nuclear power production
Swedish Nuclear Fuel and Waste Management Co
June 1986

TR 86-13
Radionuclide transport in fast channels in crystalline rock
Anders Rasmuson, Ivars Neretnieks
Department of Chemical Engineering
Royal Institute of Technology, Stockholm
March 1985

TR 86-14
Migration of fission products and actinides in compacted bentonite
Börje Torstenfelt
Department of Neclear Chemistry, Chalmers University of Technology, Göteborg
Bert Allard
Department of water in environment and society, Linköping university, Linköping
April 24, 1986

TR 86-15
Biosphere data base revision
Ulla Bergström, Karin Andersson, Björn Sundblad, Studsvik Energiteknik AB, Nyköping
December 1985

TR 86-16
Site investigation Equipment for geological, geophysical, hydrogeological and hydrochemical characterization
Karl-Erik Almén, SKB, Stockholm
Olle Andersson, IPA-Konsult AB, Oskarshamn
Bengt Fridh, Bengt-Erik Johansson, Mikael Sehlstedt, Swedish Geological Co, Malå
Erik Gustafsson, Kenth Hansson, Olle Olsson, Swedish Geological Co, Uppsala
Göran Nilsson, Swedish Geological Co, Luleå
Karin Axelsen, Peter Wikberg, Royal Institute of Technology, Stocholm
November 1986

TR 86-17
Analysis of groundwater from deep boreholes in Klipperås
Sif Laurent
IVL, Swedish Environmental Research Institute
Stockholm, 1986-09-22

TR 86-18
Technology and costs for decommissioning the Swedish nuclear power plants.
Swedish Nuclear Fuel and Waste Management Co
May 1986

TR 86-19
Correlation between tectonic lineaments and permeability values of crystalline bedrock in the Gideå area
Lars O Ericsson, Bo Ronge
VIAK AB, Vällingby
November 1986

TR 86-20
A Preliminary Structural Analysis of the Pattern of Post-Glacial Faults in Northern Sweden
Christopher Talbot, Uppsala University
October 1986

TR 86-21
Steady-State Flow in a Rock Mass Intersected by Permeable Fracture Zones. Calculations on Case 2 with the GWHRT-code within Level 1 of the HYDROCOIN Project.
Björn Lindbom, KEMAKTA Consultants Co, Stockholm
December 1986

TR 86-22
Description of Hydrogeological Data in SKBs Database Geotab
Bengt Gentzschein, Swedish Geological Co, Uppsala
December 1986

TR 86-23
Settlement of Canisters with Smectite Clay Envelopes in Deposition Holes
Roland Pusch
Swedish Geological Co
December 1986

TR 86-24
Migration of Thorium, Uranium, Radium and Cs—137 in till Soils and their Uptake in Organic Matter and Peat
Ove Landström, Björn Sundblad
Studsvik Energiteknik AB
October 1986

TR 86-25
Aspects of the Physical State of Smectite-adsorbed Water
Roland Pusch, Ola Karnland
Swedish Geological Co, Lund
Engineering Geology
December 1986

TR 86-26
Modern Shear Tests of Canisters with Smectite Clay Envelopes in Deposition Holes
Lennart Börgesson
Swedish Geological Co, Lund
December 1986